



Wroclaw University
of Economics and Business

Department of Financial Investments and
Risk Management

A Parsimonious Approach to Forecasting the Yield

Curve: The CIR# Model

by

Giuseppe Orlando

Doctoral thesis

Social Sciences, Economics and Finance

2021

Supervisor:

Prof. Krzysztof Jajuga

**OSZCZĘDNE PODEJŚCIE DO PROGNOZOWANIA
KRZYWEJ DOCHODOWOŚCI: MODEL CIR#**

GIUSEPPE ORLANDO
PRACA DOKTORSKA – EKONOMIA I FINANSE

Promotor

Prof. Dr Hab. Krzysztof Jajuga

Katedra Inwestycji Finansowych i Zarządzania Ryzykiem

Uniwersytet Ekonomiczny we Wrocławiu

2021

Acknowledgements

I would like to express my sincere gratitude and appreciation to my advisor, Prof. Krzysztof Jajuga, for the time and patience he showed when we were going through all the drafting stages.

Introduction

This Thesis is about interest rates forecasting which is introduced by an explanation of the basics concepts on interest rates characteristics and determinants. Then, after a review of existing tools developed so far in the literature, the CIR# [122, 123, 124, 125, 121] is introduced.

The idea to work on interest rates originates from our experience in finance. On the verge of the financial crisis and in the ensuing years, we were struck by the number of financial companies that still relied on CIR model developed by Cox, Ingersoll & Ross in far 1985 [46]. While the model (contrarily to many others developed in literature) is parsimonious, understandable and manageable, on other hand it is indubitably outdated and, by construction, prevents negative interest rates.

Then, the challenge for us was to deal with the additional limitations inherent to the CIR model such as the absence of jumps, volatility dumping when interest rates are low, linear risk premium, etc. This has to be done by preserving the market volatility structure as well as the analytical tractability of the original CIR model.

I Goal, original contribution and hypotheses

My original contribution to the specific literature is twofold: enhance the CIR model and turn it from a short-rate model into a forecasting tool for any yield curve.

The goal is to provide a new accessible methodology to forecast future interest rates which is quite powerful for the following reasons. First, all the improvements are obtained within the CIR framework in order to preserve the single-factor simplicity and the analytical tractability of the original model. This is achieved by a suitable partition of data where we calibrate the CIR parameters by replacing the Wiener process in the random term of the CIR model with normally distributed standardized residuals. Those are the proceeds of an “optimal” ARIMA model suitably chosen in our procedure aimed at ensuring that the assumptions on which the CIR model is built are fulfilled. That allows capturing all the statistically significant time changes in the volatility of interest rates, thus giving an account of jumps and related market dynamics.

For the reason that the illustrated methodology is not a complete departure from the CIR model but is an enhancement, we have called it CIR#.

The scientific hypothesis is that the CIR# is outperforming other single factor models and that the new approach proves particularly useful in describing the term structure of interest rates post 2007 financial crisis. In fact, the model overcomes the inability of modelling negative/near-to-zero values and the issue of the built-in mechanism of dampening volatility when rates are low. Moreover, it provides an alternative to Monte Carlo for deriving the expected value of interest rates as the suggested discretization scheme returns the same results without the need of simulating 100,000 paths.

The idea to write a Thesis come to us during the visiting period in the academic

year 2018-2019 at the Business Department of Financial Investments and Risk Management of the Wroclaw University of Economics and Business, directed by Prof. Krzysztof Jajuga. As the Thesis has been discussed and outlined in that period, all material published on interest rates forecasting from that time onwards, and particularly on the CIR#, is original and is the result of the advancements performed within the doctoral program.

II Structure of the Thesis

This Thesis is organized as follows: Chapter 1 introduces the basic concepts around interest rates such as the yield curve, the role played by central banks and the factors determining the fluctuation of interested rates. Chapter 2 provides the basic mathematical concepts related to interest rates modelling starting from the definition of a stochastic process to the risk neutral probability measure. The latter is of fundamental importance in pricing because it allows prescindig from both real-world probabilities and individual utility functions. A description of short rates and their key role in determining the entire yield curve is followed by a review of existing models around them. As the objective of this Thesis is to illustrate a parsimonious model which works in the current market environment, in Chapter 3 we introduce the Vasicek the CIR and the Hull-White models.

Having described the above mentioned (single factor) popular models, Chapter 4 provides a new methodology (which we called the CIR# model) that well fits the dynamic of interest rates as observed in real markets. To prove that point, we show a test on the EUR and USD term structure.

Chapter 5 illustrates how data partitioning allows the capture of statistically significant time changes in the volatility of interest rates, thus giving an account of

jumps in market dynamics. The performance of the new approach is carried out for different term structures and is tested for both the CIR and the Vasicek models. In there it is shown how the proposed methodology overcomes both the usual challenges (e.g. simulating regime switching, volatility clustering, skewed tails, etc.) as well as the new ones added by the current market environment characterized by low to negative interest rates.

The following Chapter 6 compares the CIR# versus real data, the EWMA and an improved version of the traditional CIR model that we called CIR_{adj} . The dataset is different from one used in the previous Chapter as data are monthly money market interest rates ranging from 1 day to 12 months over EUR, USD, JPY and CHF currencies which includes both turmoil and calm periods. Apart from that, the novelty is that we compute the predictive power in terms of the directionality of rates being that rather difficult to forecast. The Chapter concludes with a section dedicated to model validation where a purposely built dataset has been created to show the validity of our forecasts.

Chapter 7 compares the predictive power in the forecasting of the CIR# versus the so-called CIR_{adj} and the single factor Hull and White model applied to a dataset of interest rates in PLN. As shown through this Thesis, the CIR# anticipates future rates better than its peers consistently across sampling frequencies and periods.

The last Chapter draws some concluding remarks and highlights some points such as shortfalls of the present methodology, implications for hedging and next research.

Chapter 1

Interest rates and the role of central banks

In this Chapter we are illustrating the basics of interest rates starting from the yield curve, the role played by central banks and the factors determining interest rates while the next Chapter 2 will provide the basic mathematical concepts related to interest rates modelling.

1.1 The yield curve

The yield curve is a curve displaying several yields to maturity or interest rates across different contract lengths for a given debt contract (see 1-1). The curve relates interest rates with time to maturity and it is expressed as

$$Y(t) = P(t)^{-1/t} - 1$$

where $Y(t)$ is the yield and $P(t)$ denotes the present value of one unit of currency t years in the future (i.e. the discount factor). For example, a zero-coupon bond valued $P = 0.8$ and maturing in 3 years yields 7.7217%. The yield curve is obtained from money market interest rates (short end of the curve), futures on bonds (mid part) and interest rate swaps (long end). Usually, the yield curve is sloped upward because of expected inflation, counterparty risk, preference for both liquidity and current consumption. In case of deflation and positive unbalance between available liquidity and investment opportunities, the yield curve could be inverted (i.e. negatively sloped). A flat yield curve is when maturities have similar yield and a humped curve corresponds to similar short-term and long-term yields, both below medium-term yields. Fig. 1-1 displays several snapshots of the USA Treasury yield curves for different dates evidencing how the shape of the yield curve changed with time.

1.1.1 Par and zero-coupon yield curve

A zero-coupon bond is a type of bond that does not provide any cash flow until maturity (when its face value is paid). A bond with intermediate cash flows until maturity, when yields the same as its coupons, is said to trade at par. The related yield curve is called the par yield curve. The zero-coupon or spot yield curve corresponds either to the yield to maturity of actual zero-coupon or to those of a par bonds trading in the market.

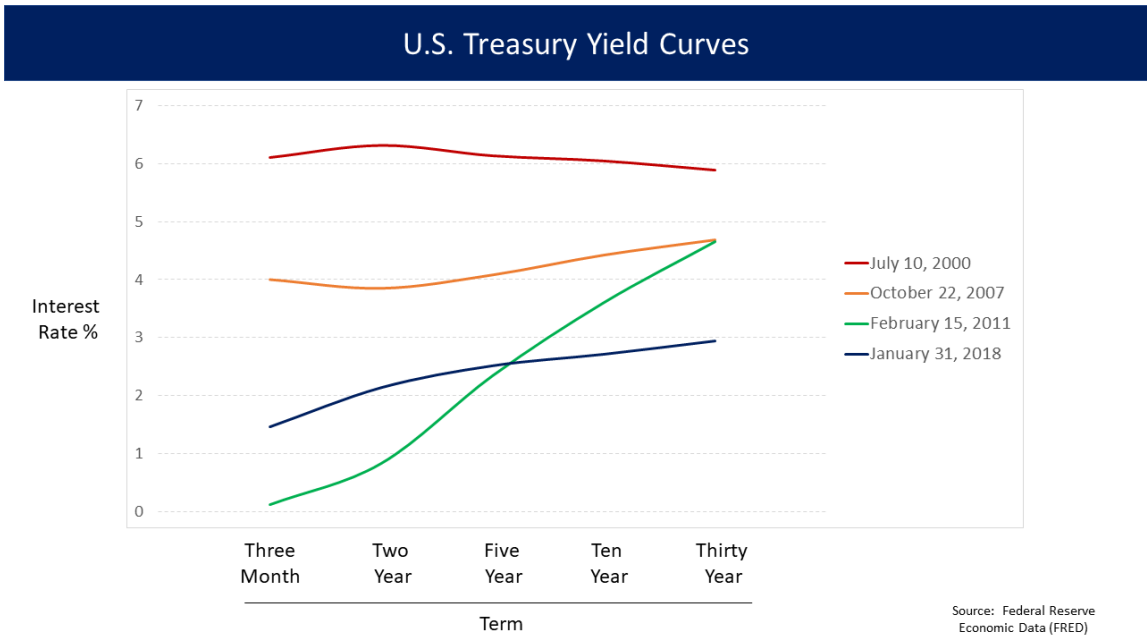


Figure 1-1: Snapshots of USA Treasury yield curves for different dates. Yield lines describe: red = flat and humped; orange = inverted at the short-end; blue = normal; green = steep. Sources FRED and [158].

1.1.2 Forward yield curve

Given a time interval from t_0 to t_2 divided in two subintervals $[t_0, t_1]$ and $[t_1, t_2]$, the following no arbitrage equality must hold

$$e^{(r_2 t_2)} = e^{(r_1 t_1)} e^{(r_{1,2} (t_2 - t_1))} \tag{1.1}$$

i.e. the proceeds of investing from $[t_0, t_2]$, at the rate r_2 is are the same of the proceeds of investing from $[t_0, t_1]$ at the rate r_1 and then reinvesting from $[t_1, t_2]$ at the rate $r_{1,2}$. Notice that r_1 and r_2 are spot rates while $r_{1,2}$ is the forward rate (which

generates the forward yield curve). Moreover Eq. 1.1 is equivalent to

$$r_{1,2} = \frac{(r_2 t_2) - (r_1 t_1)}{t_2 - t_1}. \quad (1.2)$$

1.1.3 Normal yield curve

When the slope of the yield curve is positive, it means that investors' expectation for the economy is to grow in the future. This, in turn, implies the expectation of higher inflation and, consequently, of tightening monetary policy by the central bank. Another consequence of inflation is the demand for a higher risk premium associated with uncertainty. Moreover, when the yield curve is positive, lenders profit from the so-called *rolldown* i.e. buying and selling because yields decrease as bonds get closer to maturity.

1.1.4 Flat and humped yield curve

The yield curve may flatten in case of uncertainty which leads to the so-called "flight to safety/quality". In fact, in case of turbulence investors sell other assets and buy T-bills because the latter are perceived as safe a proxy for cash. As demand increases for T-Bills, prices go up, thus driving yields down. This, when compounded with demand for long-term securities, flattens the yield curve and leaves a hump on the mid-term maturities.

1.1.5 Inverted yield curve

An inverted yield curve is when the yields on bonds with a shorter duration are higher than the yields on bonds with a longer duration thus implying that investors expect current economic growth to exceed future economic growth. That could be

an indicator of recessions [84] as illustrated by the yield curve spreads in Fig. 1-2. The rationale behind that is that, when interest rates go down, the demand for long term assets increases as investors want to lock-in the higher rates for a longer period. This drives up prices and lowers yields.

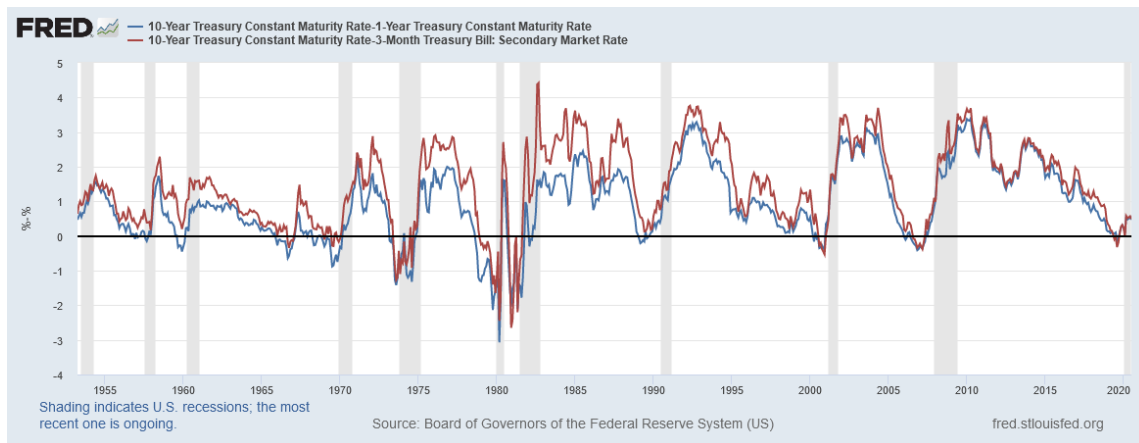


Figure 1-2: USA Treasury yield curve spreads. In blue 1 year T-bill versus 10 year T-bond. In red 3 month T-bill versus 10 year T-bond. Gray stripes indicate recessions. Sources [66, 64, 65].

As shown in the Fig. 1-2, the yield spread every is high (i.e. the yield curve is inverted) before or in conjunction with recessions. However, this relationship is not stable. For example, the lag is between 8 and 19 months and in some instances (e.g. between 1965 and 1970) the inverted yield curve did not anticipate any recession. Similarly, in the current situation (2020) the recession has not been accompanied nor anticipated by any interest rate inversion.

1.1.6 Relation between the yield curve and business cycle

Table 1.1 lists recessions following yield curve inversion. Mitchell (1913) [113], and much later Kessel (1965) [94], expressed their view on the behaviour of yields by

Table 1.1: Recessions following yield curve inversion (all values in months unless noted)

Recession	Inversion start date	Recession start date	Time between inversion start and beginning of recession	Duration of inversion	Time between start of recession and NBER announcement	Time between disinversion and end of recession	Recession duration	Time between end of recession and NBER announcement	Inversion maximum (basis points)
1970 recession	Dec-68	Jan-70	13	15	N/A	8	11	N/A	-52
1974 recession	Jun-73	Dec-73	6	18	N/A	3	16	N/A	-159
1980 recession	Nov-78	Feb-80	15	18	4	2	6	12	-328
1981-1982 recession	Oct-80	Aug-81	10	12	5	13	16	8	-351
1990 recession	Jun-89	Aug-90	14	7	8	14	8	21	-16
2001 recession	Jul-00	Apr-01	9	7	7	9	8	20	-70
2008-2009 recession	Aug-06	Jan-08	17	10	11	24	18	15	-51
Coronavirus recession	May-19	Mar-20	10	5	4	TBD	TBD	TBD	-52
Average since 1969			12	12	7	10	12	15	-147
Standard deviation since 1969			3.83	4.72	2.74	7.50	4.78	5.45	138.96

^a Sources FRED and [159].

pointing out that they tend to be low at the start of recessions (i.e. the business cycle peak) and high as expansions slow down after a cyclical trough.

Butler (1978) [32] explained the implications of declining short-term rates in terms of economic activity. However, research on the subject developed only a decade later with Harvey (1988) [85] who suggested a theoretical relationship between yields and consumptions, Furlong (1989) [70] that conceded some predictive power for recessions, but expressed his skepticism about the yield curve's reliability as a leading indicator. Estrella and Hardouvelis (1991) [57] who showed that yields may be used as a predictor of real economic activity and Laurent (1988, 1989) [100, 101] who used the yields to predict GNP growth. Based on the aforementioned research, the FED publishes an indicator of the probability of USA recession (Fig. 1-3).

In a comparison between a large number of alternative indicators, Estrella and Mishkin (1998) [58] found that yields are the best in tests of statistical significance. On the other hand, Stock and Watson (2003) [147], when examined a large number of competing indicators to forecasting the GNP, found that none of them was fit to the task. For that reason, by quoting Anna Karenina "happy families are all alike; every unhappy family is unhappy in its own way", they maintained that every decline in economic activity is peculiar. This is because each indicator measures "a

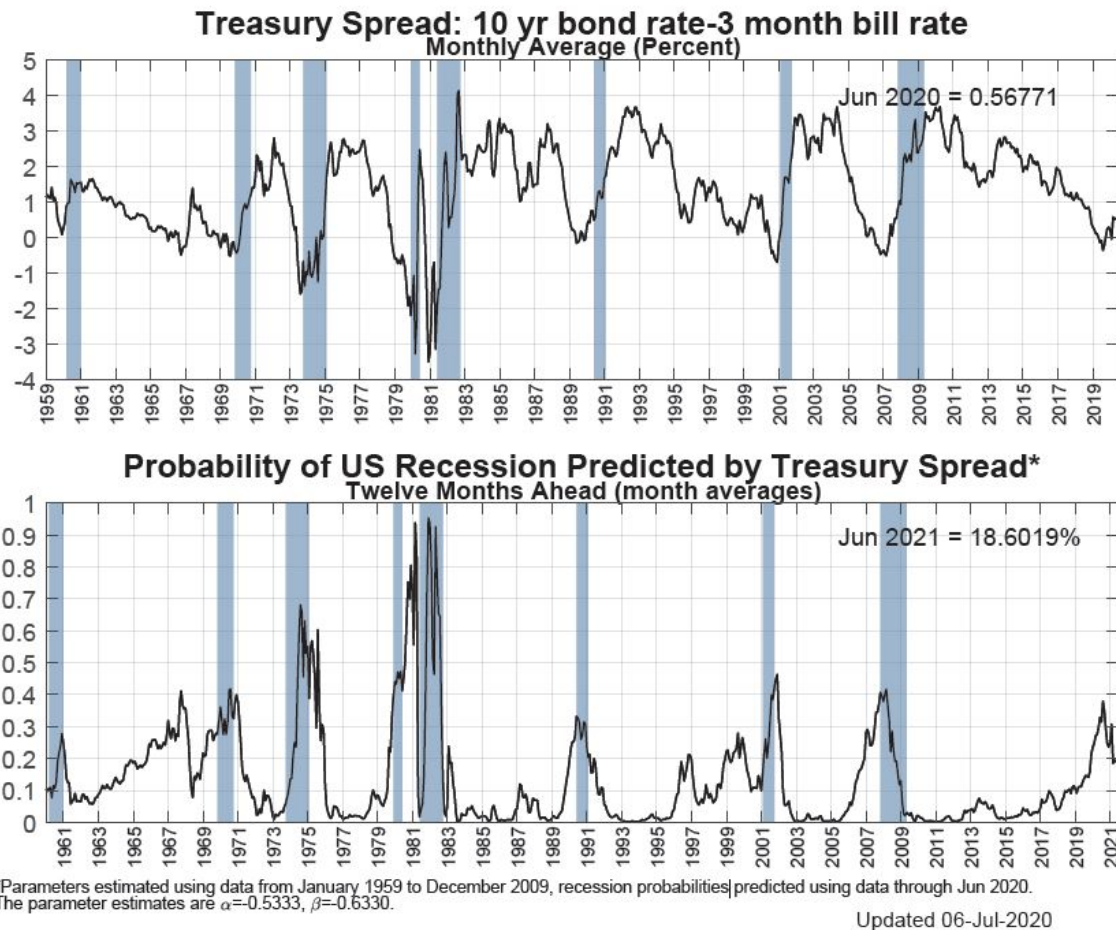


Figure 1-3: Percent (monthly average) probability of USA recession, twelve months ahead of the term spread [63]. Sources: Board of Governors of the Federal Reserve; National Bureau of Economic Research. The shaded areas indicate periods designated as recessions by the National Bureau of Economic Research (NBER).

different feature of economic activity, which in turn can play different roles in different recessions" [147]. Thus, a combination of forecasts of leading economic indicators (but excluding the monetary aggregates) is the best option in proving some warning of potential economic difficulties. The author of the present work agrees with that idea and, by using recurrence quantification analysis, Orlando et al. (2016, 2018)

[127, 128] have shown that economic downturns could be anticipated by looking at the hidden structure of the time series.

1.1.7 Estimation of yields: The Nelson-Siegel and Svensson models

Yield curves are not directly observable on the market: financial institutions and data provider compute their own. A standard model used for this purpose is the Nelson and Siegel model (1987) [119] which is a relatively parsimonious model because it has only four parameters. This is particularly useful when the number of available bond prices is limited so the model is not over-parametrized.

The Nelson-Siegel function takes the form

$$y(m) = \beta_1 + \beta_2 \frac{[1 - \exp(-m/\lambda_1)]}{m/\lambda_1} + \beta_3 \left(\frac{[1 - \exp(-m/\lambda_1)]}{m/\lambda_1} - \exp(-m/\lambda_1) \right)$$

where m is the maturity, and β_1 , β_2 , β_3 and λ_1 , are parameters to be fitted [19, 51].

The interpretation of the parameters is:

1. β_1 is the long run levels of interest rates
2. β_2 is the short-term component
3. β_3 is the medium-term component
4. λ_1 is the decay factor

Svensson (1994) [152] added a "second hump" term so, the resulting model, is called Nelson–Siegel–Svensson (NSS) model. The additional term is:

$$\beta_4 \left(\frac{[1 - \exp(-m/\lambda_2)]}{m/\lambda_2} - \exp(-m/\lambda_2) \right),$$

so that the Nelson–Siegel–Svensson (NSS) model is

$$y(m) = \beta_1 + \beta_2 \frac{[1 - \exp(-m/\lambda_1)]}{m/\lambda_1} + \beta_3 \left(\frac{[1 - \exp(-m/\lambda_1)]}{m/\lambda_1} - \exp(-m/\lambda_1) \right) + \beta_4 \left(\frac{[1 - \exp(-m/\lambda_2)]}{m/\lambda_2} - \exp(-m/\lambda_2) \right).$$

While the Nelson–Siegel–Svensson model is widely used for modelling the yield curve, it has some drawbacks. For example, the optimisation problem is not convex and there are multiple local stationary points. In addition, the model, for a certain range of the parameters, is badly conditioned. Thus they are unstable given small changes in the data (see Fig. 1-4).

Gilli et al. (2010) [74] have shown that non-standard optimisation heuristic such as differential evolution Gilli (2009) et al. [75], Storn et al. (1997) [148] can deal with the numerical issues while the instability of the parameters can be addressed with constrained optimization.

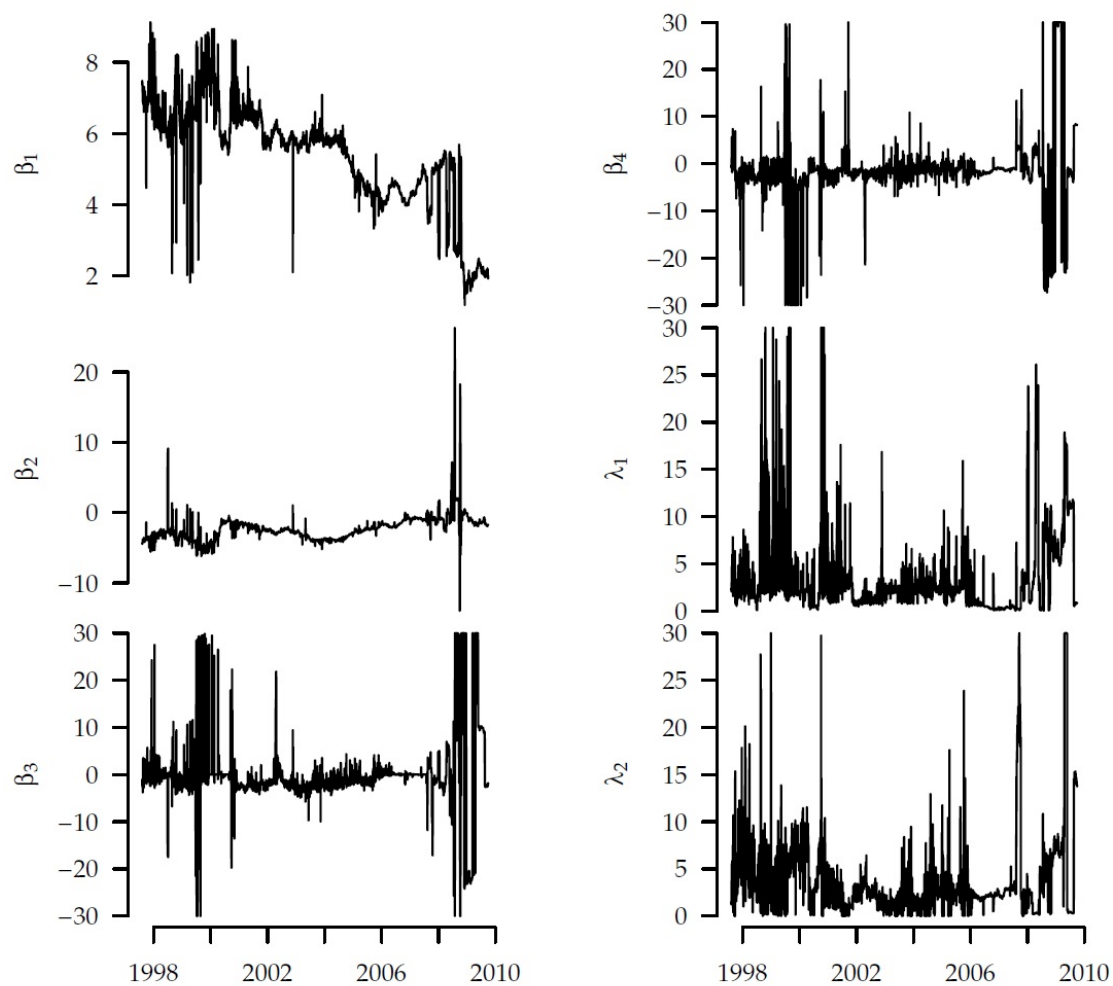


Figure 1-4: The Bundesbank's daily estimates for NSS parameters. Source Bundesbank and Gilli et al. (2010) [74]).

1.2 The role of central banks

The central bank is the bank of the banks in the sense that is a special type of bank acting as a banker to the commercial banks of a given country. The specific form, mandate and activities of a central bank vary from one country to another. In

some countries, the central bank is responsible for monetary policy, currency, fx and supervises commercial banks; in other countries, the central bank has a limited role and may not even be responsible for the issuance of the domestic currency. Topically the core functions of central banks are to act as a lender of last resort and to facilitate the operation of the country's payment system.

1.2.1 Operation of payment system

The payment is related to any form of payment used in a country; from debit cards to checks, from wire transfer to direct debits, etc. Those transactions involve a number of different and unrelated parties so that, for the transaction to be successful and completed, each of the parties involved needs some assurance on the ability of their counterparts to fulfil their obligations. The central bank provides the said assurance because it commits to step in and make good on the obligations in case one of the intermediary banks defaults. The required funds are taken from deposits (called reserve requirements) that commercial banks have to maintain with the central bank. As this amount may vary with time depending on a number of factors such as deposits, volume of transactions, relevance of the commercial bank in the payment system, etc., the actual amount of money that a bank has deposited at the central bank is greater than the minimum requirement and is called reserve.

The centralization of the reserve at the central bank provides assurance on the fulfilment of the obligations and it is an efficient way of moving money from one bank to another. This is because spares each bank from having to maintain an account with every other bank they deal with.

1.2.2 Lender of last resort

As lender of last resort, the central bank ensures the customers that, in the unlikely case they all want to withdraw, at the same time, the money they have on deposit, the central bank would step in by lending the bank whatever it needs to meet customer withdrawal requests and using the loans on the bank's balance sheet as collateral. Therefore, while a commercial bank could turn down the lending request of one of its peers, the central bank is always willing and able to perform this function. When the central bank is responsible for minting, it can issue whatever amount of cash is needed to support commercial banks as lender of last resort.

1.2.3 The USA Federal Reserve System (FRS)

Here we illustrate the USA Federal Reserve system as is a general benchmark for advanced economies and it is the most important central bank system in the world. The USA central bank consists of a Board of Governors, 12 regional reserve banks (for this reason is a system of banks denoted as Federal Reserve System), the so-called Federal Open Market Committee (FOMC) responsible to take decisions on the central bank's capital market activities such as sale or purchase of bonds issued by the USA Treasury. Moreover, the FOMC decides on the federal funds rate i.e. the interest rate at which banks with excess reserve funds at their District's Federal Reserve Bank can lend to other banks.

Additional responsibilities of the FED are the supervision of member banks and the issuance of the USA dollar.

1.2.4 The European Central Bank (ECB)

The European Central Bank (ECB) is the central bank of the Eurozone, which is a monetary union of 19 EU member states having the Euro as a common currency. Established by the Treaty of Amsterdam in 1997, the ECB is one the second most important central banks in the world after the FRS. The primary objective of the ECB, as stated in the second article of its Statute, is to maintain price stability within the Eurozone. Other responsibilities involve foreign exchange operations, control foreign reserves of the European System of Central Banks, manage the TARGET2 settlement system, issue of Euro banknotes, supervise directly the capital of "significant banks", etc.

While the Federal Reserve Act created a central bank for the United States consisting of 12 regional Federal Reserve Banks and a Board of Governors of the Federal Reserve System, the European System of Central Banks consists of 15 national central banks and a six member Executive Board.

1.2.5 The Bank of Japan (BOJ)

The Bank of Japan (BOJ) was established in 1882 and underwent two major changes, the first in 1949, after the defeat in World War II, and the second in 1998 because of the liberalization started in the USA by president Ronald Reagan (see Fig. 1-5). In 1949, the new act introduced a policy board modelled after the Federal Reserve System with the authority to decide on the discount and lending rate. However, the finance minister retained the authority to supervise the BOJ thus limiting its independence so that the central bank had to negotiate any adjustment to the official discount rate (see Shizume (2018) [145]). The BOJ act of 1998, fully reviewed the role of the BOJ by redefining it in terms of independence and transparency. Article

1, states that “the purposes of the BOJ are to issue banknotes, carry out currency and monetary control, and ensure smooth settlement of funds among banks and other institutions, thereby contributing to the stability of the financial system” [145], without any interference of the government. Moreover, article 2 stipulates that “the currency and monetary control of the BOJ shall aim to the achieve price stability, and thereby contribute to the sound development of the national economy" [145].

Year	BOJ	Year	Japanese economy
		1859	Opening of the treaty ports
		1868	Meiji Restoration
1882	BOJ established		
1885	First BOJ notes (silver standard)		
1897	Adoption of the gold standard	1894–1895	Sino-Japanese War
		1904–1905	Russo-Japanese War
1917	Suspension of the gold standard	1914–1918	WWI
		1927	Showa Financial Crisis
1930	Return to the gold standard		
1931	Departure from the gold standard		
1942	BOJ Act of 1942	1931–1945	Asia–Pacific War
1946	Emergency Financial Measures		
1949	Amendment of the BOJ Act		
		1960	National Income-Doubling Plan
1973	Move to flexible exchange rates	1973	First oil shock
		1985	Plaza Accord
		1987	Louvre Accord
1998	BOJ Act of 1998	1997–1998	Heisei Financial Crisis

Figure 1-5: Timeline of The Bank of Japan (BOJ). Source Shizume (2018) [145]).

1.2.6 The Schweizerische Nationalbank (SNB)

The Schweizerische Nationalbank (SNB), as stipulated in the National Bank Act (NBA) entered in force in May 2004, is responsible for the country’s monetary pol-

icy and its primary goal is to ensure price stability while taking due account of economic developments. This, with the ultimate objective to create an appropriate environment for economic growth [153]. The inflation target is less than 2% per annum, achieved by setting the SNB policy rate and related open market interventions. Other tasks of the SNB are note-issuing, oversight of the Swiss Interbank Clearing (SIC) payment system, managing the currency reserves, analysing sources of risk to the financial system, acting as banker to the Confederation, and compiling data and analysis on banks and financial markets [153].

1.2.7 Monetary policy

The primary goal of the Eurosystem is to “maintain price stability” and to “support the general economic policies”. Quantitatively, price stability is “a year-on-year increase in consumer prices of below 2%”. By contrast, the Federal Reserve System has three policy goals: “maximum employment, stable prices and moderate long-term interest rates”. To achieve those objectives the two central banks dispose of a set of tools listed in Table 1.2.

Table 1.2: Tools of Monetary Policy

Federal Reserve	ECB
Open market operations	Open market operations
Discount window	Standing facilities
Reserve requirements	Reserve requirements

Open market operations

The Federal funds rate is the interest rate that banks charge each other to borrow reserves overnight. The Federal Reserve exercises control over it through open market

operations that directly affect bank reserves. Similarly, the ECB controls the EMMI Euro Overnight Index Average (EONIA) that, from October 2019, has been replaced by the Euro short-term rate (€STR) [59].

The main differences between FED and ECB open market operations is they the first conducts them on daily basis by dealing exclusively in U.S. government securities, while the ECB mandates each central bank to conduct decentralized refinancing operations once a week. Moreover, the ECB accepts securities beyond those issued by member country governments.

Overnight loans

Overnight loans made to financial institutions are referred to as discount window loans by the Federal Reserve and marginal lending facilities by the ECB.

In the USA the discount rate is set below the federal funds rate target because the Federal Reserve discourages borrowing at the discount window. In the Euro area, the ECB provides overnight loans to financial institutions at a rate above the main refinancing rate. "In contrast to the constraints of the discount window, banks are allowed to freely borrow from this facility" Pollard (2003) [131]. In addition, both the FED and the ECB provide a deposit facility that allows banks to deposit funds overnight at their national central banks.

Reserve requirements

While reserve requirements are a standard monetary policy tool in central banking, some central banks do not have them at all (e.g. Australia, Canada and Sweden) [55]. Euro area and USA banks are required to hold a certain amount of funds as reserves in their current accounts at their national central bank. The ECB states the

bank's minimum reserve requirement is set over a maintenance period of six weeks. In order to provide some flexibility and to stabilise the interest rate banks charge each other for short-term funds, banks have to meet the minimum reserve requirement on average over the maintenance period.

Concluding remarks on the monetary policy

Monetary policy is believed to be mostly ineffective in the long run. In fact, while for large countries central bank manipulation of interest rates might be temporarily effective, for smaller open economies real interest rates are determined by world market conditions. Anyway, in both cases, in the long run, real interest rates will be determined by the perceived risk/reward of holding domestic assets. For example, *coeteris paribus*, a better risk/reward profile will cause an increase of domestic assets' values and a decrease in the domestic real interest rate.

Central banks, when trying to reduce (resp. increase) domestic interest rates, may cause capital outflows (resp. inflows). This will cause a deficit in the domestic balance of payments and, therefore, may force a reduction of imports. On the other hand, portfolio assets' reallocation due to interest rate differentials, involves the bid of foreign versus the sales of domestic assets. Unless countries apply tight control on capital flows, the result of portfolio rebalances is that domestic interest rates will rise again until when the equilibrium is reached again. Therefore, one may argue the monetary policy, in the long run, cannot change real interest rates as they are determined by real factors such as risk/reward profile and assets.

Similarly, when exchange rates are flexible, monetary shocks cannot affect the long-run output and employment. This is because an increase of, let say, money supply will cause both a rise in domestic prices and an imbalance in the portfolio's

assets. Domestic assets are sold and foreign are bought. This leads to an increase in nominal interest rates and a decrease in real rates. The equilibrium is reached when both domestic real interest rates and foreign exchanges will be back to their initial level.

Contrarily, when the money supply is increased sufficiently to keep up with growth in output, monetary policy is not neutral/ineffective.

1.2.8 Unconventional monetary policy

Because of the global financial crisis of 2008, central banks introduced new policy instruments such as negative interest rate policies (NIRP), new central bank lending operations (LO), asset purchase programs (APP), and forward guidance (FG) (for a review see Potter et al. (2019) [132]).

Negative interest rate policies

Negative interest rate policies were introduced by central banks to avert deflation and to provide some expansionary stimulus. The negative effect on the banking systems related to the compression of interest margins was offset from other sources of income "and the eventual recovery of bank portfolio values, including the declines in non-performing loans" [132].

Lending operations

As soon as it became evident that the interbank and money markets were impaired, central banks expanded their liquidity facilities. Among them the interventions were aimed at "extending the maturity of the typical lending operations, expanding the set of eligible collateral and the set of counterparties, changing the lending terms

(eg fixed rate full allotment) and imposing explicit conditions on loans to ensure the desired ultimate outcome (eg bank lending to non-financial private firms)" [132]. While lending operations proved helpful by providing credit to the private sector and stabilising interest rates, had the side effect of some inefficient allocation of credit and encouraging leverage.

Asset purchase programmes

Asset purchase programmes were aimed at lowering long-term yields and they have been responsible for a substantial expansion in central banks' balance sheets. While the objective has been largely achieved, some concerns were raised on "the risk of weakening the quality of central bank balance sheets, excessive suppression of premia in asset valuations, temporary scarcity effects in repo markets, spillovers in the form of boosting commodity prices and private sector leverage" [132].

In the USA, the Congress authorized \$475 billion for the so-called Troubled Assets Relief Program (TARP) by the Dodd-Frank Wall Street Reform and Consumer Protection Act (Dodd-Frank Act). The areas involved were: banking institutions (\$250 billion), credit markets (\$27 billion), automotive (\$82 billion), American International Group (AIG) (\$70 billion), foreclosure avoidance of struggling families (\$46 billion) [154].

Forward guidance

As unconventional monetary policy involved unprecedented operations, forward guidance has been instrumental to clarify central banks' strategic intentions. The challenge had been "balancing the trade-offs between clarity of message, the credibility of follow-up action and flexibility of future policy response to changing circumstances"

[132].

1.2.9 Importance of interest rates models for central banks

As central banks need to control interest rates for the effectiveness of inflation targeting, the ability to correctly model and predict them is essential. Basically, the models are used for economic projections and analysis with regard to changes in exogenous variables and/or assumptions. Then, models are used for evaluating the impact of a change in monetary or fiscal policy, in the labour market, social security, etc. Last but not least, models may be used for "counterfactual analysis where actual developments and government policies are compared with the outcome of alternative courses of action that could have been taken" Fagan et al. (2006) [61]. Fig. 1-6 lists the models adopted by European central banks in terms of number of equations and geographical coverage (single country or multi-country).

Central bank	Model name	Coverage	Number of equations	Number estimated
Belgium	NBB quarterly	Belgium	150	30
Germany	BbkM	Multi-country	691	292
Greece	Bank of Greece model	Greece	93	17
Spain	MTBE	Spain	150	23
France	MASCOTTE	France	280	60
Ireland	MCM block	Ireland	75	20
Italy	BIQM	Italy	886	96
Luxembourg	MCM block	Luxembourg	63	18
Netherlands	MORKMON	Netherlands	400	70
Netherlands	EUROMON ¹	Multi-country	1000	330
Austria	AQM	Austria	169	43
Portugal	AMM	Portugal	115	23
Finland	BOFMINI	Finland	240	40
Finland	EDGE	Euro area aggregate	40	11 (calibrated)
ECB	AWM	Euro area aggregate	84	15

Figure 1-6: Models adopted by European central banks. Source [61].

1.2.10 Supervision and regulation

Central banks have the role to ensure the stability of the financial system so it can withstand shocks without major disruption.

To achieve that objective macroprudential policies can be put in place such as set aside extra capital or place restrictions on financial institutions' e.g. on mortgage lending conditions.

This might especially be the case for institutions that are deemed systemically important, i.e. those which the failure would cause a significant ripple effect across the financial system.

Alternatively, macroprudential policies may place restrictions on financial institutions' activities by, for example, setting stricter mortgage lending conditions. This to face building-up of asset price bubbles, excessive risk-taking by banks, disproportional

tionate corporate or household debt.

Since 2014 the ECB has been tasked to directly supervise the biggest banks in the Euro area and to set guidelines for the European banking sector. The focus is on capital adequacy (capital ratios), asset quality and liquidity.

Similarly, the Federal Reserve plays a role in supervising and regulating banks in the USA by sharing the tasks with three federal agencies and with state agencies. "As a complement to this regulation, the Federal Reserve implements consumer protection laws in the area of credit and financial transactions" Pollard (2003) [131].

1.3 Factors determining real interest rates

In the last decade, advanced economies have experienced a falling trend in yields. For example, in the USA 10-year yields were around 6.7% percent in the 1990s and 4.5 % in the first decade of the 2000s which corresponds to a decline of the natural rate i.e. the level of the real short-term interest rate that defines a neutral monetary policy stance. Thus, the natural rate of interest r_t^* corresponds to a situation in which the economy is operating at potential and inflation is at its target value, so that there is no reason for the central bank to either inject or withdraw stimulus Lane (2019) [98]. Hence, the natural rate of interest "summarizes the real forces driving the movements in interest rates, abstracting from the influence of monetary policy decisions" Del Negro et al. (2017) [48].

The causes and the implications of this secular decline recall the Malthusian and Marxist view of diminishing returns the related chronic economic malaise characterized by low growth and low rates of return has been mentioned by Hansen (1939) [83] and, more recently, by Summers (2014) [149].

The main economic drivers of r_t^* are the potential growth rates, demographics and diverging developments in the returns on risky and safe financial assets [31]. Moreover, among the financial driver, we can mention the so-called "saving glut" made popular by Ben Bernanke (2011) [12, 13].

1.3.1 Natural and potential growth rates

The natural rate of interest r_t^* is closely connected to the potential growth rate of the economy: when the economy is booming, it needs a high volume of savings to sustain the required high investments. In turn, that requires a high level of interest to motivate people to save instead of consuming. According to Andersson (2018) [4]

r_t^* is estimated to be less than half of what it was 50 years ago (see Fig. 1-7).

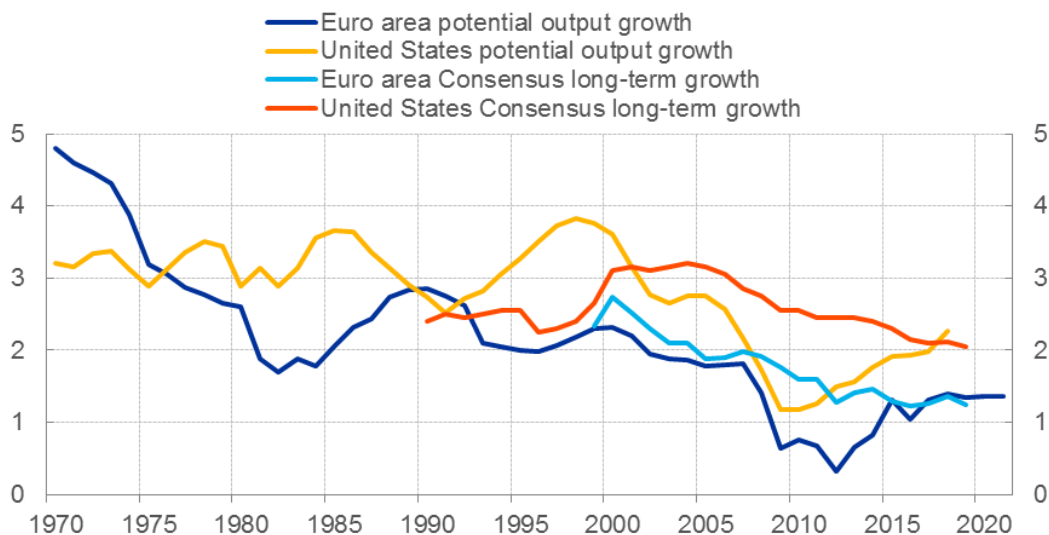


Figure 1-7: Potential output growth and long-term growth expectations. Sources: Bureau of Economic Analysis, European Commission and Consensus Economics [98].

This decline can be attributed to both a decline in total factor productivity growth and structural technological factors EIB (2019) [56]. In fact, especially in the services sector, there is an increasing gap between the labour productivity growth of firms operating at the technology frontier and other firms Camba-Mendez et al (2018) [33]. On the question of why technological diffusion has slowed down, there are several reasons. One explanation is "the fall in business dynamism as measured by business churn: the rate at which firms exiting the market are replaced by new ones has declined measurably over the last decade" Lane (2019) [98]. Another reason is a shift in economic activity from manufacturing to services that are more protected from the competition and, then, are less productive (see Fig. 1-8).

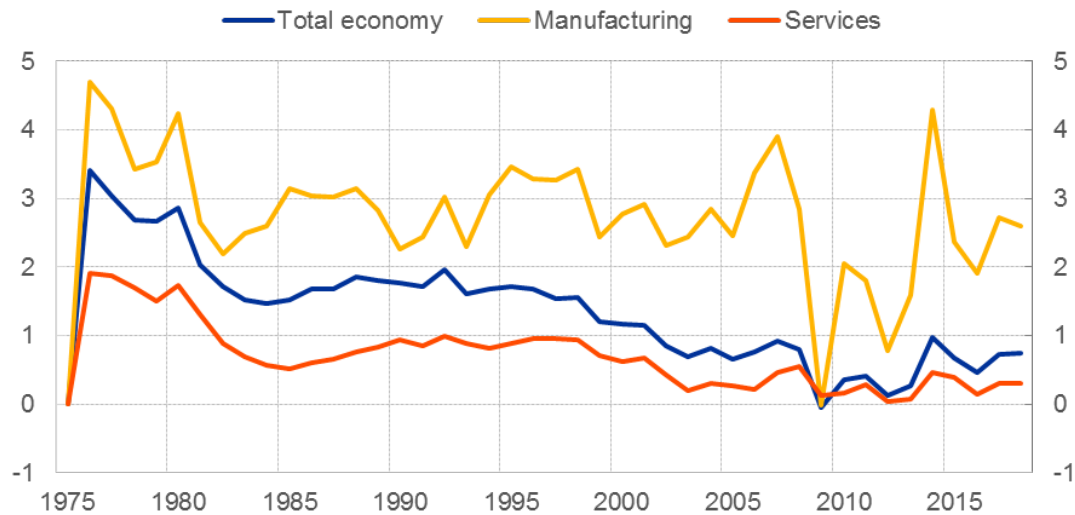


Figure 1-8: Euro area labour productivity by sector: real gross value added per person employed. Sources: European Commission AMECO database and ECB staff calculations [98].

1.3.2 Demographic factors

Demography is another important driving force for the real interest rate. Because of low fertility rates and rising life expectancy in advanced economies, the ratio of the elderly (aged 65 and over) to the working-age population (aged 15-64) is expected to rise from 20 percent to over 50 percent by 2050 (see Fig.1-9).

The ageing of the population reduces growth because the ratio of installed capital relative to the size of the workforce increases with the age. This lowers productivity growth and diminishes investment opportunities. Moreover, rising life expectancy implies a lower level of investment and a higher level of saving, thus affecting the level of real interest rates Lisack et al. (2017) [105].

Recent research [17, 129, 37, 71, 133] estimates that slowing population growth and rising life expectancy have an impact between 1% and 2% in the USA and the EURO area.

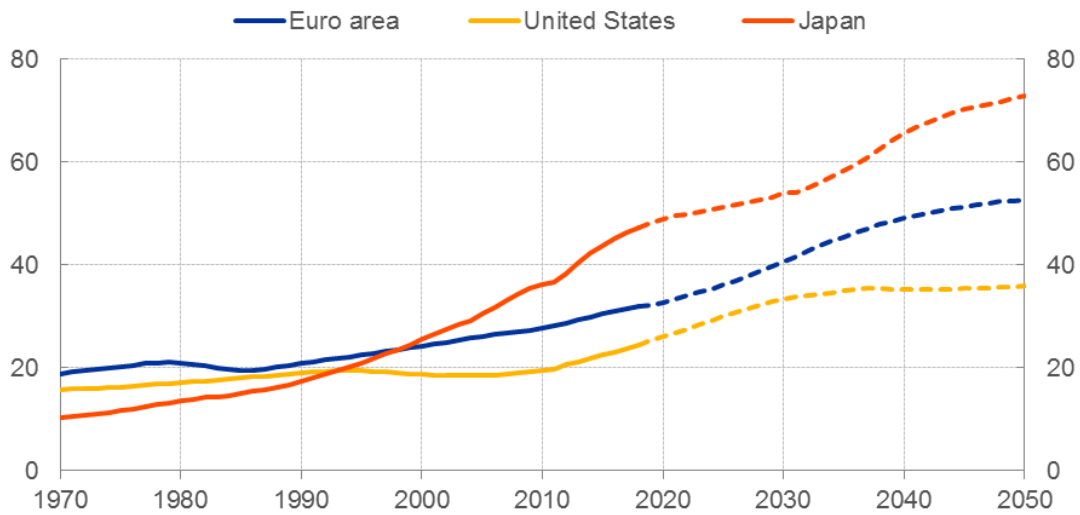


Figure 1-9: Old-age dependency ratios: historical data (solid line) and projections (dashed line). Sources: World Bank, Eurostat, OECD and ECB staff calculations [98].

Apart from ageing, inequality is a contributing factor in downward pressure on r_t^* Rannenberg (2019) [134]. Fig. 1-10 shows how inequality has increased considerably in developed countries since the 1980s. Rachel et al. (2015) [133] estimate that inequality contributes to a decline in equilibrium yields of about half a percentage point.

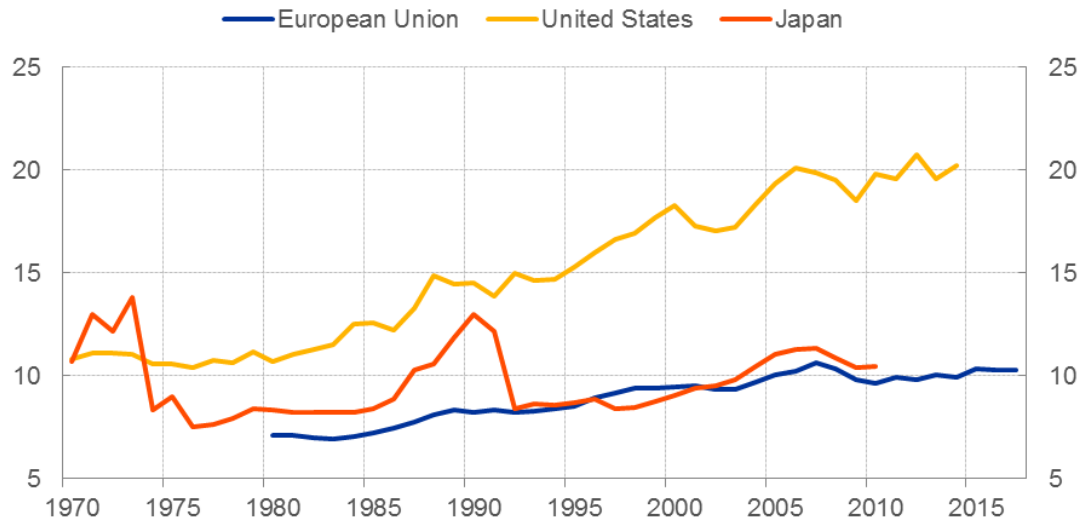


Figure 1-10: Share of national income earned by households in the top 1 percent income bracket. Sources: World Inequality Database [98].

1.3.3 Saving glut

The global saving glut (GSG) is also known as cash or liquidity hoarding [14, 143], a glut of excess intended saving [80], or shortfall of investment intentions [80], is when desired saving exceeds desired investment hypothesized by Ben Bernanke. In his view, "increased capital inflows to the United States from countries in which desired saving greatly exceeded desired investment—including Asian emerging markets and commodity exporters—were an important reason that U.S. longer-term interest rates" from 2003 to 2007 were lower than expected Bernanke (2012) [13].

Notably, in 1938 Alvin Hansen held a talk called "Economic Progress and Declining Population Growth", after an era of unprecedented expansion of the USA economy and the experience of the Great Depression, that induced Hansen to publicly question whether in future there would be sufficient demand of investment to sustain economic growth. The decline in interest rates poses important challenges

for both fiscal and monetary policy and it has become a matter of concern for many Baldwin et al. (2014) [8].

A definition of secular stagnation is that, in order to equate saving and investment with full employment, negative real interest rates are needed. In terms of monetary policy, this implies that is much harder to achieve full employment with low inflation and a zero lower bound (ZLB) on policy interest rates.

In fact, secular stagnation "undermines the most powerful and flexible tool we have for keeping growth near its potential rate – standard monetary policy. A workable definition for secular stagnation is that negative real interest rates are needed to equate saving and investment with full employment. As such, secular stagnation raises the likelihood that full employment cannot be achieved because low inflation and the ZLB on nominal interest rates keep real rates firmly positive" Baldwin et al. (2014) [8].

Berrospide (2012) [14] has found "supporting evidence for the precautionary motive hypothesis of liquidity hoarding in banks". Sanchez et al. (2013) [143] hold that "the rise in cash holdings of U.S. corporations to the increasing predominance of research and development (R&D). Since R&D is an activity intrinsically connected with uncertainty, the association of R&D and cash holdings is a natural one. The rising importance of R&D in the overall economy is a long-term phenomenon that is due to the rapid growth of information technology firms".

According to Summers (2014) [149] a decline in the full employment real interest rate (FERIR), coupled with low inflation, could indefinitely prevent the attainment of full employment thus arguing that "even if it were possible for the FERIR to be attained, this might involve substantial financial instability" [149].

1.3.4 Diverging trends of returns on risky and risk-free assets

In the last few years, the following phenomena on returns have been observed. The first is the decline in yields of safe assets and an increase in equity returns and returns on higher-risk debt instruments [78, 140, 41].

Notably, Del Negro et al. (2017-9) [48, 49] argue that the secular decline in the natural rate of interest in the USA is primarily due to the strong demand for safe and liquid assets. This holds for USA Treasuries and it is linked to financial crisis over the past 20 years. For that reason Treasuries are valued more for their safety and liquidity than for their financial returns. This lead to a steady decline in Treasury rates since the late 1990s and to an increase in the premium that investors are willing to pay for those characteristics.

By contrast, the returns on high quality corporate bonds, which are perceived as less liquid and less safe by the market, have declined much less. Their finding matches the saving glut hypothesis as a possible source of secular stagnation.

The premium on safe assets due to safety is coupled with ageing (as older savers seek safer portfolio allocations) and the lingering effects of the global financial crisis of 2007 and the ensuing Euro sovereign debt crisis (see Fig. 1-11). Those experiences, by revealing the cost of the crisis, have shifted asset allocation toward assets that preserve their value during bear times. Similarly, regulators acknowledged that the deregulation started in the USA left the financial system without sufficient capital and liquidity. This was coupled with the arbitrariness of business practices: from aggressive deals to purely formal risk and audit functions, from conflict of interest between rating agencies and issuers to investment banks that take market positions against their clients, and so on. New regulation had the effect to fuel demand for safe assets, and then, nowadays financial institutions have a reduced risk appetite

and are required to hold more liquid assets.

The side effect is that "banks subject to the Liquidity Coverage Ratio (LCR banks) create less liquidity per dollar of assets in the post-LCR period than non-LCR banks by, in part, lending less". On the other hand "LCR banks are more resilient as they contribute less to fire-sale risk, relative to non-LCR banks" Roberts et al. (2019) [138]. This poses a question on the trade-off between more liquidity available to the economy through banks and having a more resilient banking sector.

According to Neri et al. (2019) [120] risk premium shocks are, simply put, changes in agents' preference for safe assets. Those changes have been the main driver of interest rates dynamics in the Euro area. In the USA, shocks were more pertaining to the efficiency of investment.

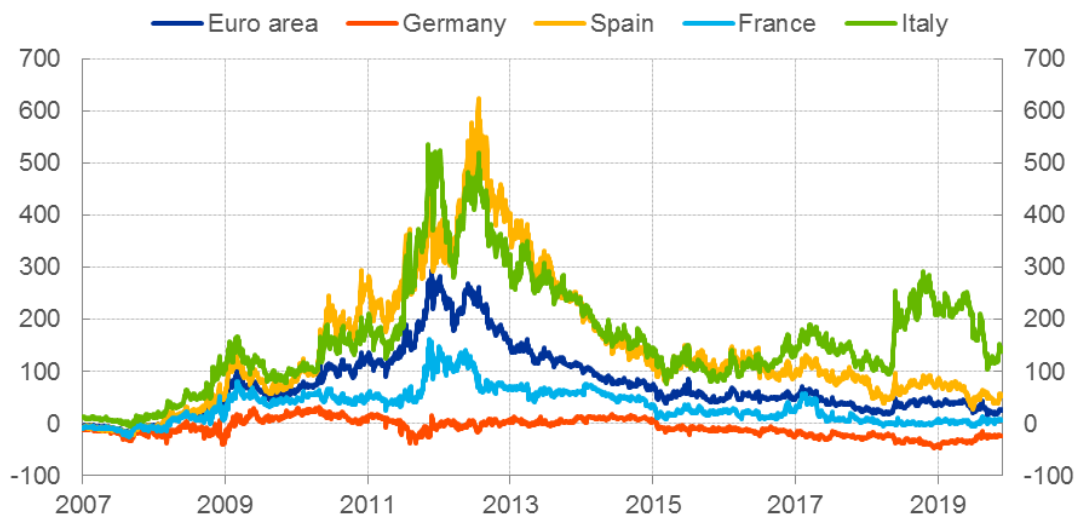


Figure 1-11: Ten-year Euro area sovereign bond yield to OIS spread. Sources: Bloomberg and ECB staff calculations [98].

From the demand-side there has been an increasing request for safe assets to the point that markets value considerably assets that offer protection against downside risks [120], on the supply side in the Eurozone availability has shrunk. This was

due to the interconnectedness between countries and banks that had a large part of their balance sheet invested in government bonds. The surge in public debt in the wake of the crisis ignited a doom loop effect between the risk profiles of banking systems and sovereigns. Government bonds in the Euro area with AAA-rating have collapsed since by two third. Moreover, in the Euro area the ratio of highly-rated short-term assets relative to GDP is very low compared to the USA (see Fig. 1-12). This is a problem as the scarcity of safe asset impair the possibility for European financial institutions to hedge against liquidity, interest rate, or default risk Brand et al. (2019) [21].

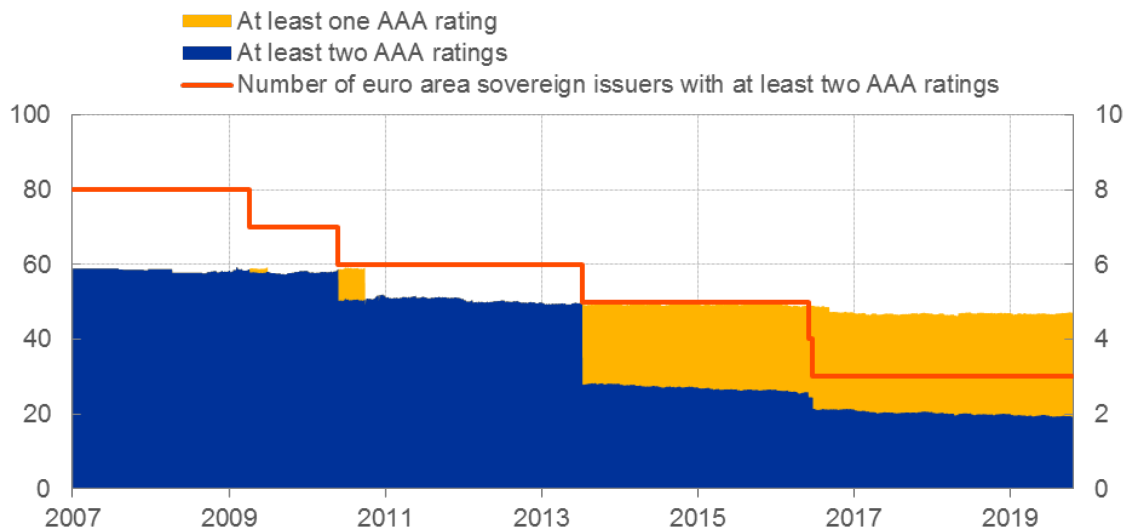


Figure 1-12: Share of short-term government debt with AAA rating relative to GDP. Source: ECB [98].

1.3.5 Implications of low rates and monetary policy issues

While the determinants of real rates are sometimes non-monetary in nature, central banks when the inflation rate falls short of the inflation target and the equilibrium

real rate is low (or negative) have to implement negative policy rate to increase inflation and to stabilise it to its medium-term target.

The problem is that when the policy rate is already close to the effective lower bound, alternative methods of providing monetary stimulus may be required to substitute for deeper rate cuts. Other available options to ease monetary policy include forward guidance about future policy rates; asset purchase programmes and targeted lending operations. The FED in 2008 and the ECB have been active in employing all of those instruments that have been proven highly effective in easing monetary and financial conditions Coenen et al. (2020) [42].

Quantitative easing and consequently raising central bank assets by several trillion is not something economists have been used to see as a healthy *modus operandi* of central banks. On the other hand, governments may have to provide a stimulus for years to offset the drag of prolonged private-sector balance-sheet repair because "any premature withdrawal of fiscal stimulus would unleash the deflationary forces as unborrowed savings are allowed to become a leakage in the economy's income stream. Indeed, in the US in 1937, Japan in 1997 and the UK and Eurozone in 2010 all experienced serious double-dip recessions when their governments pursued fiscal consolidation while their private sectors were still in the process of repairing balance sheets" Koo (2014) [96].

In order to leave room for central banks and to avoid them recurring too often to unconventional measures, it is necessary to have the inflation rate oscillating around its targeted medium level. This should be achieved by other policy dimensions that should enhance growth by implementing structural reforms and public investments. Furthermore, in case of negative shocks in the economy, fiscal policies should accompany monetary actions to achieve macroeconomic stabilisation.

To mitigate risk from extreme events, some measures have been taken to reinforce

risk management and capital adequacy in relation to the financial system. In the Eurozone the Single Supervisory Mechanism, the macroprudential policy framework and the European Stability Mechanism have become a source of stability in the sovereign debt market.

However, because of revolving doors between regulators and regulated firms [47], [23], dangerous mixing of commercial banking business with the investment banking business, relaxation of antitrust measures that have allowed the surge of the so-called too big to fail institutions and unresolved conflict of interests of any kind, the systemic risk is still untapped.

On the supply side, fiscal policy should be eased because "achievement of levels of deficits and government debt generally considered desirable especially if complemented by reductions in social insurance – would likely mean negative neutral real rates in the industrial world. Policymakers going forward will need to engage in some combination of greater tolerance of budget deficits, unconventional monetary policies and structural measures to promote private investment and absorb private saving if full employment is to be maintained and inflation targets are to be hit" Rachel et al. (2019) [133].

In the Euro area, it could be desirable a significant deepening of fiscal union to supply a common safe asset and to avoid kind of tax havens and fiscal dumping. This is particularly needed as the availability of high quality assets is particularly scarce compared to the USA.

As an intermediate solution, the supply of safe assets could be boosted through a range of innovations Leandro et al. (2018) [104]. In fact, as central banks target returns on short-term safe and liquid assets there is a need to link r_t^* with liquid and safe assets Del Negro et al. (2017) [48].

Chapter 2

Stochastic processes and short rate models

This Chapter provides the basic mathematical concepts related to interest rates modelling starting from the definition of a Wiener process. Then, we introduce the risk neutral probability measure which is a key concept in pricing because it allows ignoring both real-world probabilities and individual utility functions. The basic concepts aforementioned pave the way to the main subject of this Chapter i.e. short rates. As explained in the related Section 2.2 they are nonobservable instantaneous spot rates that, subject to some conditions, determine the entire yield curve. Being short rates so important, they have attracted much attention. The last Section 2.3 gives an inventory of the existing models. Then, after having walked through the reader on the basic mathematical concepts about interest rates modelling, in next Chapter 3 we will be in a position to illustrate the CIR, Vasicek and Hull and White models.

Definition 2.1 (Wiener process). Let us consider a probability space $(\Omega, \mathcal{F}, \mathbb{P})$ and

the \mathbb{R} -valued stochastic process $\{W_t : t \geq 0\}$. We denote W as a *Wiener process* if:

- $W_0 = 0$ almost surely
- Let $n \geq 1$ and $0 = t_0 < t_1 < \dots < t_n$. The increments $\delta W_{t_0 t_1}, \delta W_{t_1 t_2}, \dots, \delta W_{t_{n-1} t_n}$ are independent
- For $0 \leq s < t$ we have $\delta W_{st} \sim N(0, t - s)$
- W has continuous paths almost surely

Remark 2.1. From now onwards W_t , denotes a standard Brownian motion under a risk-neutral probability measure and dW_t , its differential.

Definition 2.2 (Existence of a Wiener process). There exists a probability space $(\Omega, \mathcal{F}, \mathbb{P})$ on which one can construct a Wiener process.

Definition 2.3 (Gaussian process). Let us consider a probability space $(\Omega, \mathcal{F}, \mathbb{P})$ and the \mathbb{R} -valued stochastic process $\{x_t : t \geq 0\}$. We denote W as a *Gaussian process* if for all $0 \leq t_1 < \dots < t_n$, the vector $(x_{t_1}, \dots, x_{t_n})$ is Gaussian.

Remark 2.2. Considered the Gaussian process x , the law of x is characterized by

$$\mu_t = E(x_t), \quad \text{and} \quad \rho_{s,t} = Cov(x_s, x_t).$$

Definition 2.4 (Brownian motion). The \mathbb{R} -valued Gaussian process W is called *Brownian motion* if the following properties hold

$$\mu_t = 0, \quad \text{and} \quad \rho_{s,t} = s \wedge t.$$

Definition 2.5 (Martingale). Let us consider a probability space $(\Omega, \mathcal{F}, \mathbb{P})$ and the \mathbb{R}^n -valued stochastic process $\{x_t : t \geq 0\}$. We say that x is a \mathcal{F}_t -*martingale* if

- $x_t \in L^1(\Omega)$ for all $t \geq 0$
- x is \mathcal{F}_t -adapted
- $E(\delta x_{st} | \mathcal{F}_s) = 0$ for all $0 \leq s < t$.

Remark 2.3. If W is a \mathcal{F}_t -Brownian motion then W is a \mathcal{F}_t -martingale.

Definition 2.6 (Ornstein–Uhlenbeck process). The *Ornstein–Uhlenbeck process* is the stochastic differential equation

$$dx_t = -\theta x_t dt + \sigma dW_t \quad (2.1)$$

where $\theta > 0$ and $\sigma > 0$ are the parameters and W_t is a Wiener process.

Definition 2.7 (Geometric Brownian motion (GBM)). The *geometric Brownian motion (GBM)* is the stochastic differential equation

$$dx_t = \mu x_t dt + \sigma x_t dW_t \quad (2.2)$$

where μ and σ are the parameters and W_t is a Wiener process.

2.1 No arbitrage and risk-neutral probability measure

Let assume that the current stock price is S_0 and that in next period from now the stock price can be either $S_0u = S_u$ if the price goes up by a factor u or $S_0d = S_d$ if the price goes down by a factor d . Then the *discrete single-period* price dynamics is

$$\begin{aligned}
S_0 &= \frac{S_0(u-d)}{(u-d)} = \\
&= \frac{1}{e^r} \frac{S_0(u-d)e^r}{(u-d)} = \\
&= \frac{1}{e^r} \frac{S_0(u-d)e^r + (S_0ud - S_0ud)}{(u-d)} = \\
&= \frac{1}{e^r} \left(\frac{S_0ue^r - S_0ud}{(u-d)} + \frac{-S_0de^r + S_0ud}{(u-d)} \right) = \\
&= \frac{1}{e^r} \left(S_0u \left(\frac{e^r - d}{u-d} \right) + S_0d \left(\frac{u - e^r}{u-d} \right) \right).
\end{aligned}$$

No arbitrage condition requires that $u \leq e^t \leq d$. In fact, it is immediate to see that, when for example $e^r > u$, one can short the stock S and invest in the risk-free asset. That means that in both future states one can buy back the stock for less than the proceeds from the risk free. Therefore no arbitrage condition results in the following bounds

$$\begin{aligned}
0 &\geq \frac{e^r - d}{u - d} \geq 1 \\
0 &\geq \frac{u - e^r}{u - d} \geq 1
\end{aligned}$$

and

$$\frac{e^r - d}{u - d} + \frac{u - e^r}{u - d} = 1.$$

If we denote

$$p_d := \frac{e^r - d}{u - d} \quad \text{and} \quad p_u := \frac{u - e^r}{u - d}$$

it can be observed that they qualify as probabilities as they represent mutually exclusive states of the world (the stock moves either up or down), their sum is 1 and

they are in $[0, 1]$ range.

Therefore the current price of the stock can be written in terms of probabilities as

$$S_0 = \frac{S_u p_u + S_d p_d}{e^r} = \frac{1}{e^r} E^Q(S_1).$$

which means that the market intended as the composition of all participants discounts, under the measure Q , at the same rate the probabilities of the stock going up or down as a consequence of no arbitrage condition.

Remark 2.4. Let us consider the Euler equation

$$S_0 = E_0(M_1 S_1)$$

where M is the stochastic discount factor that holds under the law of one price. By changing the probabilities associated with the expected value one can write

$$S_0 = \frac{1}{e^r} \frac{1}{e^r} E_0^Q(S_1)$$

which implies to price of the stock by discounting at the known risk free expectation with respect to the Q measure (to be determined). That allows pricing without having to take into consideration real-world probabilities nor the utility function. In this sense, the measure Q is said *risk-neutral probability measure*.

Remark 2.5. Arbitrage free models such as the Hull and White model are particularly straightforward to translate onto a tree or lattice, therefore, are used for pricing derivatives such as Bermudan swaptions.

2.2 Short rates process

Let us consider the stochastic state variable represented by the instantaneous spot rate r_t . In presence of a no-arbitrage condition and under risk-neutral measure Q the specification of the current short rate implies the specification of the entire yield curve. In fact, the price at time t of a zero-coupon bond maturing at time T with a terminal payoff of 1 is

$$P(t, T) = \mathbb{E}^Q \left[\exp \left(- \int_t^T r_s ds \right) \middle| \mathcal{F}_t \right],$$

where \mathcal{F} is the natural filtration for the process. The interest rates implied by the zero coupon bonds form the so-called zero curve (commonly known as yield curve). Thus, specifying a model for the short rate specifies future bond prices through the formula

$$f(t, T) = - \frac{\partial}{\partial T} \ln(P(t, T)).$$

When the stochastic state variable is the instantaneous forward rate we deal with short rates models i.e. model for which the stochastic differential equation describing the dynamics of r_t takes the form

$$r_t = A(t; r_t)dt + B(t; r_t)dW_t \tag{2.3}$$

W_t denotes a standard Brownian motion under a risk-neutral probability measure, A and B are, respectively, the drift and the diffusion term. Those models are also called one-factor models as there is only one stochastic driver.

Usually, the dynamics of interest rates is described by a stochastic differential

equation (SDE) in Eq. 2.3 as specified below

$$dr_t = \mu(t, r_t)dt + \sigma(t, r_t)dW_t, \quad r(0) = r_0, \quad (2.4)$$

with drift $\mu(\cdot, \cdot)$, diffusion term $\sigma(\cdot, \cdot)$ and $(W_t)_{t \geq 0}$ a standard Brownian motion. The unique solution to (2.4), say $r = (r_t)_{t \geq 0}$, in case it exists, is a diffusion process, i.e. a continuous Markov process defined on a given probability space $(\Omega, \mathcal{F}, \mathbb{P})$.

Remark 2.6. Eq. 2.4 basically assumes that dr_t/r_t is normally distributed with mean $\mu(t, r_t)\Delta t$, standard deviation $\sigma(t, r_t)\Delta t$ and that is independent over time (thus implying informational efficiency of markets). Therefore, Eq. 2.4 models interest rates dr_t/r_t as the sum of a deterministic component and of a random component (where the latter generates i.i.d. random increases/decreases) [76].

2.3 Term structure of interest rates models

2.3.1 Single factor interest rates models

As mentioned short rates models can describe the full default-free term structure. In his paper about a stochastic growth model, Merton (1973) [110] shows that the instantaneous risk-free interest rate can be modelled through a nonlinear diffusion process that is the basis for equilibrium term structure models. However, in that paper, Merton did not study the implications concerning the term structure. That, instead, was pursued years later by Sundaresan (1984) [150] who generalized the study and illustrated its consequences for the term structure. Among the most noticeable early contributions to the arbitrage-free models of term structure include Vasicek (1977) [155] and Brennan and Schwartz (1979) [22]. However, as pointed out

by Back (1997) [6], there is a difference between “traditional arbitrage-free approach” to term structure and the absence of arbitrage opportunities. In fact, just the latter implies the existence of a risk-neutral measure. Thus, only equilibrium models of term structure such as the later contribution by Cox, Ingersoll and Ross (1985) [46] are equivalent to risk-neutral pricing.

Unfortunately, while single-factor models are tractable from an analytical point of view and handy to implement, often they fail to model the default-free yield curve over time and across maturities [151]. Therefore, in several studies [30, 38, 73, 29], it has been shown they do not perform well in empirical tests. Notwithstanding, more recently Orlando et al. [122, 123, 124, 125, 121] turned out the CIR (1985) model into a forecasting tool (i.e. the CIR # model) and brought evidence on how to make work a single factor model. Table 2.1 lists a number of single factor models which differ because of alternative specifications of the parameters characterizing the spot interest rate process.

2.3.2 Multi factor interest rates models

Single-factor models do not perform well in empirical tests. For example, Brown and Dybvig (1986) [30] used USA Treasuries across different maturities and found that the term structure in the CIR model embodied the information available to the market about the future course of events. However, their paper does not address the linkage between the yield curve and the expectations [68]. This because does not allow a separate identification of term premiums i.e. of the difference between forward rates and expected value future spot rates. Along the same line, Gibbons and Ramaswamy (1993) tested the CIR model by using Hansen’s generalized method of moments. Their results demonstrated that the "CIR’s model for index bonds per-

Table 2.1: Alternative Specifications of the Spot Interest Rate Process of Single-Factor Models

#	Drift	Diffusion	Stationary	References
1	$k(\theta - r)$	σ	Yes	Vasicek (1977) [155]
2	$k(\theta - r)$	$\sigma r^{1/2}$	Yes	CIR (1985) [46]
3	$k(\theta - r)$	$\sigma r^{1/2}$	Yes	Brown & Dybvig (1986) [30]
4	$k(\theta - r)$	$\sigma r^{1/2}$	Yes	Gibbons and Ramaswamy (1993) [73]
5	$k(\theta - r)$	σr	Yes	Courtadon (1982) [44]
6	$k(\theta - r)$	σr^λ	Yes	Chan et. al (1992) [38]
7	$k(\theta - r)$	$\sqrt{\sigma\gamma r}$	Yes	Duffie and Kan (1996) [54]
8	$kr(\theta - \ln(r))$	σr	Yes	Brennan and Schwartz (1979) [22]
9	$kr + \theta r^{-(1-\delta)}$	$\sigma r^{\delta/2}$	Yes	Marsh and Rosenfeld (1983) [108]
10	$\theta - \alpha r$	σ	Yes	Hull and White (1990) [89]
11	$\theta + k + \gamma r^2$	$\sigma\gamma r$	Yes	Constantinides (1992) [43]
12	k	σ	No	Merton (1973) [110]
13	0	σr	No	Dothan (1978) [52]
14	0	$\sigma r^{3/2}$	No	CIR (1980) [45]

Source: Ait-Sahalia (1996) [2] and author's elaboration.

forms reasonably well when confronted with short-term Treasury-bill returns. The estimates indicate that term premiums are positive and that yield curves can take several shapes. However, the fitted model does poorly in explaining the serial correlation in real Treasury-bill returns" [73]. Ait-Sahalia (1996) [2], by using a nonparametric estimation on several single-factor models, concluded that every parametric single-factor model is rejected by the data. This was confirmed by Stanton (1997) [146] who found nonlinearities in the drift coefficient of single-factor models. As the reversion appears to play a strong role only at higher levels of short rates. To improve the accuracy as well as the explanatory power of the model, multi-factor models have been proposed. Among them, we mention **a**) Langetieg (1980) [99] who extended the Vasicek (1977) model by assuming that the short rate is the sum of n state variables,

each following the short rate process suggested by Vasicek; **b**) Brennan and Schwartz (1979) [22] who considered a two-factor model: one for the short rate and the other for the consol rate; **c**) Richard (1978) [136] that proposed the real rate as first factor and the expected inflation rate as the second factor; etc. (for a review see Rebonato (1996) [135]). Table 2.2 summarizes some well known multi-factor models in terms of the state variable, the relationship between state variables and their analytical tractability.

Table 2.2: Alternative Specifications of the Spot Interest Rate Process of Multi-Factor Models

#	State Variables	Relationship between State Variables	Analytical	Model
1	Multiple unobserved state variables	Short rate is the sum of all state variables	Yes	Langtieg (1980) [99]
2	Long rate and short rate	Both rates are correlated	No	Brennan and Schwartz (1979) [22]
3	Real rate and expected rate of inflation	Restricted	Yes	Richard (1978) [136]
4	Short rate and volatility	Correlated	Yes	Longstaff and Schwartz (1992) [107]
5	Unspecified	Correlated-flexible	Yes	Duffie and Kan (1996) [54]
6	Short rate and the drift of the short rate	Correlated	Yes	Hull and White (1990) [89]
7	Short rate, drift of short rate and the volatility	Restricted	Yes	Chen (1996) [40]
8	Short rate and volatility	Correlated	Yes	Fong and Vasicek (1992) [69]
9	Short rate and volatility	Correlated	No	Heston (1993) [87]
10	Short rate and volatility	Correlated	No	Bates (1996) [9]

Source: Sundaresan (2000) [151] and author's elaboration.

After the illustration of the basic concepts around stochastic processes and short rate models, as the objective of this Thesis is to illustrate a parsimonious approach to the problem, in the following Chapter , we are going to focus on the Vasicek (1977), Hull and White (1990) and CIR (1995) models as they are the most relevant for the remainder of this work.

Chapter 3

The CIR, Vasicek and the Hull-White models

As stated by the Nobel award Enrico Fermi *with more than four parameters one can fit an elephant into the car's trunk*. Whenever possible, we prefer parsimonious over complex models. For this reason, in our research, we focused on single factor models and on how to make them work. In the following, we describe the models which are relevant in the ensuing part of this Thesis.

3.1 The CIR model

The CIR process can be defined as the square of the norm of a d -dimensional Ornstein-Uhlenbeck (OU) process, with dimension $d = k\theta \in \mathcal{R}$, where k, θ are the parameters in the SDE (2.4), or, equivalently, by a space-time change, as a squared Bessel process with dimension $d = \frac{4k, \theta}{\sigma^2}$ [91].

The CIR model is an Ornstein-Uhlenbeck process that does not allow negative

interest rates with the following characteristics:

- 1) The variance is proportional to the short-rate which implies that the standard deviation is proportional to interest rates
- 2) The Euler discretization of CIR model is

$$r_V(t_{i+1}) = r_V(t_i) k (\theta - r_V(t_i)) \Delta t + \sqrt{\Delta t} \sigma Z_{i+1}$$

$$r_C(t_{i+1}) = r_C(t_i) k (\theta - r_C(t_i)) \Delta t + \sqrt{r_C(t_i)} \sqrt{\Delta t} \sigma Z_{i+1}$$

where δ^σ denotes a change in σ . Then the impact of δ^σ on r is

$$\Delta_C^\sigma r_C(t_{i+1}) = \delta^\sigma \sqrt{r_C(t_i)} \sqrt{\Delta t} Z_{i+1},$$

In other terms, in the CIR model the volatility contains the r_t term, which allows reducing the effect of a change in σ .

The CIR model in (2.4) can be described as

$$dr_t = \kappa(\theta - r_t)dt + \sigma(t, r_t)dW_t, \quad r(0) = r_0, \quad (3.1)$$

where the constant parameters κ and θ denote the reversion's speed and the long-term mean, respectively.

For the CIR model, $\kappa, \theta > 0$ and the volatility $\sigma(t, r_t) = \sigma\sqrt{r_t} > 0$ in (2.4), with $\theta\sigma^2/2\kappa$ the long-term variance. The process r is known as the *square-root process*. The conditional distribution of r is a non-central Chi-square distribution and the steady distribution is a Gamma. Therefore, the square-root process r is always non-negative; it is known that if the involved parameters satisfy the condition $2k\theta > \sigma^2$,

then r_t is strictly positive for any $t \geq 0$, and, for small r_t , the process rebounds as the random perturbation dampens with $r_t \rightarrow 0$.

The factor risk premium is the premium investors require for holding the risky security. In equilibrium, the factor risk premium should equal the excess expected return on that security above the risk free return (which is the instantaneous risk-free rate r). As in the CIR model, the risky security is the pure discount bond with price P , then the difference between the expected return on discount bond and rP is the risk premium [106].

Cox, Rubinstein and Ross [46] show that the risk premium is a linear function of r , $\lambda(t, r_t)rP(t, r_t)_r$ (where the latter denotes the partial derivative of P with respect to r). In equilibrium, a discount bond price $P(t, r_t)_r$ must satisfy the partial differential equation:

The relatively handy implementation and tractability of the CIR model, as well as the specific characteristic of precluding negative interest rates, an undesirable feature under 2008 pre-crisis assumptions, are two reasons that allowed the CIR model to become one of the most widely used short-term structure models in finance. Other applications include stochastic volatility modelling [126, 34]. However, there are a number of issues in describing interest rate dynamics within the CIR framework such as: **a)** interest rates can never reach negative values; **b)** the diffusion term $\sigma\sqrt{r_t}$ goes to zero when r_t is small, in contrast to actual experience; **c)** the volatility parameter σ is constant, whereas in reality σ changes continuously; **d)** as well as with the Vasicek model, there are no jumps (neglecting in this way events such as fiscal and monetary decisions, release of corporate financial results, changes in investors' expectations, etc.). **e)** the risk premium $\lambda(t, r_t)$ is linear with r_t (which is false if both credit worthiness of a counterparty and market volatility are considered); **f)** interest rates may vary according to the market risk only.

In fact, the current market environment with abrupt changes in volatility and negative interest rates has exacerbated the above-mentioned issues urging the need for more sophisticated frameworks, which could accommodate multiple sources of risks, as well as shocks and/or structural changes of the market. This has led to the development of several papers for pricing interest rate derivatives that are based on stochastic interest rate models generalizing the classical CIR and Vasicek paradigm [24]. More recently, Zhu (2014) [162] proposed a CIR variant with jumps modelled by a Hawkes process, and Moreno and Platania (2015) [115] presented a cyclical square-root model, where the long-run mean and the volatility parameters are driven by harmonic oscillators. Finally, Najafi and Mehrdoust (2017) [116] and Najafi et al. (2017) [117] proposed some extensions of the CIR framework where a mixed fractional Brownian motion is added to account for the random part of the model.

3.2 The Vasicek model

In the following, we explain the basic features of the Vasicek model versus the CIR model previously introduced. For a general overview on those models and on the yield curves, forward curves, term structures and their generalizations with increased state space dimension see Medvedev (2019) [109].

The Vasicek model is still an Ornstein-Uhlenbeck process and allows negative interest rates but is less commonly used by financial institutions for a number of reasons:

- 1) The variance is constant (while for the CIR the variance is proportional) to the short rate. The advantage for the CIR is that as the short-term interest rate increases, its standard deviation increases as well.

2) Let us take the Euler discretization of the Vasicek and CIR model

$$r_V(t_{i+1}) = r_V(t_i) k (\theta - r_V(t_i)) \Delta t + \sqrt{\Delta t} \sigma Z_{i+1}$$

$$r_C(t_{i+1}) = r_C(t_i) k (\theta - r_C(t_i)) \Delta t + \sqrt{r_C(t_i)} \sqrt{\Delta t} \sigma Z_{i+1}$$

and let us denote δ^σ a change in σ . Then the impact of δ^σ on r in the Vasicek model is higher than in the CIR model because

$$\Delta_V^\sigma r_V(t_{i+1}) = \delta^\sigma \sqrt{\Delta t} Z_{i+1}.$$

It can be shown that with low k and high σ values in the Vasicek model [50], it is possible to get bond prices bigger than 1 (which in most cases could appear illogical). Furthermore, the Vasicek model converges very fast to its long-run mean value and therefore oscillates around it. In reality, interest rates do not get pulled back to their long-term mean value immediately and they may stay above or beyond the equilibrium for some time.

The Vasicek and the CIR model in (2.4) has the form

$$dr_t = \kappa(\theta - r_t)dt + \sigma(t, r_t)dW_t, \quad r(0) = r_0, \quad (3.2)$$

where the constant parameters κ and θ denote the reversion's speed and the long-term mean, respectively. The rationale behind the mean reversion is that higher rates slow down the economy and reduce the demand for funds. When rates are low, the opposite happens. However, this has proved to be not always true as "you can take a horse to water, but you can't get it to drink".

For the Vasicek model, $\kappa, \theta > 0$, and the volatility $\sigma(t, r_t)$ is a constant parameter

$\sigma > 0$. r is an Orstein-Uhlenbeck process and has a steady normal distribution with mean θ and long-term variance $\sigma^2/2\kappa$. This allows the positive probability of getting negative interest rates, which was not expected before the massive injection of liquidity and credit facilities provided by central banks following 2008 credit squeeze. Among the drawbacks of this model are the poor fitting to the current term structure of interest rates (later addressed by Hull and White, 1990) [89] and the undesired property that the yields over all maturities are perfectly correlated. Moreover, the conditional volatility of changes in the interest rate is constant, independent on the level of r , which can unrealistically affect the prices of bonds (see Rogers, 1996) [139].

3.3 The one-factor Hull–White model

The one factor Hull and White model is described by the following stochastic equation:

$$dr_t = (\theta_t - \alpha_t r_t) dt + \sigma_t dW_t.$$

where θ is time dependent.

Remark 3.1. When θ and α are both time-dependent the model is called *extended Vasicek model*.

The Hull and White model belongs to the class of no-arbitrage models that are used to fit the term structure of interest rates. Moreover, this model easily translates onto lattice trees when discrete time computations are required. In fact, the same authors, for the simple case of constant volatility, show how their model work by using a trinomial lattice with upper and lower bounds on spot interest rates. The problem with that approach is that involves a numerical algorithm for the identification of

the expected value of the spot rate at each date. This may require Monte Carlo simulation and be computationally inefficient. To solve the said problem many solutions have been proposed to date such as the use of a specification where the volatility is proportional to the spot rate can mitigate substantially the concerns about negative interest rates [79]. This model is one of the benchmarks that we used versus the CIR#.

Having described what are in our view the three more important single factor models, in next Chapter 4 we provide a new methodology that we call the *CIR# model*.

Chapter 4

The CIR# model: a new approach to forecast market interest rates

4.1 Introduction

The aim of the present Chapter is to provide a new methodology within the CIR framework, which we call the *CIR# model*, that well fits the dynamic of interest rates as observed in real markets. Our approach is based on modelling the evolution of a given interest rate (rather the term structure at a given point in time) through some algorithm that we are going to explain in detail in the following pages. Here we only mention that we apply an appropriate partitioning of the data sample and, by doing so, we calibrate the CIR parameters by replacing the standard Brownian motion process in the random term of the CIR model with normally distributed standardized residuals of the “optimal” ARIMA model (suitably chosen from the above mentioned partition of the time series). In this Chapter, the efficiency of the new approach in forecasting future interest rates is tested for different yields for both

EUR and USD currencies. There are two reasons why we use this approach. First, we want to leverage a widespread model such as the CIR model and second because we want a forecasting tool to be able to overcome some major issues related to the original CIR model while preserving the market volatility structure as well as the analytical tractability of the mentioned model.

Cox, Ingersoll & Ross (1985)[46] proposed a stochastic model introduced by Feller (1951)[67] to describe the term structure of interest rates, well known in the financial literature as the CIR model. This model generalizes the Vasicek model [155] to the case of non-constant volatility and assumes that the evolution of the underlying interest rate is a diffusion process, i.e. a continuous Markov process unique solution to the following stochastic differential equation (SDE) under the real market probability measure \mathbb{P}

$$dr(t) = k(\theta - r(t)) dt + \sigma\sqrt{r(t)}dW(t), \quad (4.1)$$

with initial condition $r(0) = r_0 > 0$. $(W(t))_{t \geq 0}$ denotes a standard Brownian motion under the measure \mathbb{P} intended to model a random risk factor. The interest rate process $(r(t))_{t \geq 0}$ is usually known as the *CIR process* or *square root process*. The SDE (4.1) is classified as a one-factor time-homogeneous model, because the parameters k, θ and σ , are time-independent. Therefore the SDE (4.1) is composed of two parts: the “mean reverting” drift component $k[\theta - r(t)]$, which ensures the rate $r(t)$ is elastically pulled towards a long-run mean value $\theta > 0$ at a speed of adjustment $k > 0$, and the random component $W(t)$, which is scaled by the standard deviation $\sigma\sqrt{r(t)}$. The volatility of the instantaneous short-rate is denoted by $\sigma > 0$.

The remainder of the Chapter is organized as follows. Section 4.2 summarizes the existing literature on the CIR model and the related extensions. Section 4.3 describes the principal steps of the proposed *CIR# model*. Section 4.4 presents in more detail

the numerical procedure and tests the goodness-of-fit of the new methodology to market data. The efficiency of the new approach in forecasting future interest rates is shown in Section 4.5 for monthly observed interest rates in both money market and short-term to long-term datasets for both EUR and USD currencies. Finally, Section 4.6 concludes.

4.2 Literature

The CIR model became very popular in finance among practitioners because it was perceived as an improvement on the Vasicek model, not allowing for negative rates and introducing a rate dependent volatility, as well as for its relatively handy implementation and analytical tractability. Moreover, the Vasicek model [155] was quickly abandoned by practitioners because the conditional volatility of changes in the interest rate is constant, independent on the level of it, and this may unrealistically affect the prices of bonds that can grow exponentially (see Rogers [139]).

Other applications of the CIR model include stochastic volatility modelling in option pricing problems (see Orlando and Tagliatela (2017) [126], Canale et al. (2017) [35]), or default intensities in credit risk (see Duffie (2005)[53]).

Despite the rapid success, the CIR model fails as a satisfactory calibration to market data since it depends on a small number of constant parameters, k, θ and σ . As explained by Brigo & Mercurio (2001), Section 3.2 [26]: “the zero coupon curve is quite likely to be badly reproduced, also because some typical shapes, like that of an inverted yield curve, may not be reproduced by the model,..... no matter the values of the parameters in the dynamics that are chosen”. Cox, Ingersoll and Ross, instead, mentioned explicitly that the model can “produce only normal, inverse or humped shapes”[46]. The seeming contradiction lies in its practical implementation.

Thus the need for more sophisticated models for allowing a more precise fit to the currently-observed yield curve, which could take into account multiple correlated sources of risk [72] as well as shocks and/or structural changes of the market, led some years later to the development of extensions of the CIR model. Among the best known ones are: *a* the Hull-White (1990)[89] model based on the idea of considering time-dependent coefficients; *b* the Chen (1996)[39] three-factor model; *c* the CIR++ model by Brigo & Mercurio (2001)[26] that considers short-rates shifted by a deterministic function chosen to fit exactly the initial term structure of interest rates; *d* the jump diffusion JCIR model (see Brigo & Mercurio (2006) [27]); *e* the JCIR++ by Brigo & El-Bachir (2006)[24] where jumps are described by a time-homogeneous Poisson process; *f* the CIR2 and CIR2++ two-factor models (see Brigo & Mercurio (2006) [27]). Quite recently Zhu (2014)[162], in order to incorporate the default clustering effects, proposed a CIR process with jumps modelled by a Hawkes process (which is a point process that has self-exciting property and the desired clustering effect), Moreno et al. (2015)[115] presented a cyclical square-root model, and Najafi et al. (2017) ([116], [117]) proposed some extensions of the CIR model where a mixed fractional Brownian motion applies to display the random part of the model. Similarly, Mishura et al. (2018) [112] proved that the CIR process is a fractional Brownian motion with an arbitrary Hurst parameter. Fallah (2019) et al. [62] studied the existence and uniqueness of the solution of a fractional version of the CIR stochastic differential equation and “obtain the price of the double barrier option under transaction cost”.

Note that all the above cited extensions to CIR model preserve the positivity of interest rates, in some cases through reasonable restrictions on the parameters. But the financial crisis of 2008 [10], [114], [142] and the ensuing quantitative easing policies brought down interest rates, as a consequence of reduced growth of developed

economies, and accustomed markets to unprecedented negative interest regimes under the so-called “new normal” (that we are going to illustrate later in the remainder of this section). Therefore, the need for adjusting interest rate models for negative rates has become an additional characteristic that a “good” model should possess.

However, as mentioned in the introduction, in this Chapter instead of modelling short-term interest rates r_t as a stochastic process under a risk-neutral measure \mathbb{Q} we want to model real/observable interest rates r_t as a stochastic process under real probability distribution of the market prices under \mathbb{P} . Even though the \mathbb{Q} and \mathbb{P} associate different weights to the same possible outcomes for the same financial variables, it is possible transitioning from one set of probability weights to the other when the so-called risk-premia are determined. Thus models used under \mathbb{Q} by pricers and quant traders have been adopted as well by risk and portfolio managers.

4.3 The CIR# model

In the following, we will illustrate our original approach, but first let us recap what we believe to be the main issues that we want to address regarding the CIR model:

1. Negative interest rates are precluded;
2. The diffusion term in (4.1) goes to zero when $r(t)$ is small (in contrast with market data);
3. The instantaneous volatility σ is constant (in real life σ is calibrated continuously from market data);
4. There are no jumps (e.g. caused by government fiscal and monetary policies, by the release of corporate financial results, etc.);

The aim of the present work is to provide a new methodology that gives an answer to points **i.- iv.** by preserving the structure of the original CIR model (4.1) to describe the dynamics of spot interest rates observed in financial markets. For this purpose the first step is partitioning the available market data sample into sub-samples - not necessarily of the same size - in order to capture all the statistically significant changes of variance in real spot rates and consequently, to give an account of jumps. That represents the first novelty of our procedure because partitioning the data sample should allow overcoming the critical issue pointed out in **iv.**. After that, to overcome challenges **i.- ii.**, the real rates are properly translated to shift them away from zero or negative values and such that the diffusion term in (4.1) is not dampened by the proximity to zero but fully reflects the same level of volatility present on the market (see Section 4.4.1).

The second step consists in fitting an "optimal" - as explained in Sections 4.4.2 and 4.4.3 - ARIMA model to each sub-sample of market data. To ensure that the residuals of the chosen "optimal" ARIMA model in each sub-sample look like Gaussian white noise, the Johnson's transformation (Johnson (1949)[92]) is applied to the standardized residuals. This step will be useful in the sequel in order to obtain the best fitting to the observed rates.

As a third step, the parameters k, θ, σ in (4.1) are calibrated to the shifted market interest rates by estimating them for each sub-sample of available data, as explained in Section 4.4.3 (which allows overcoming the issue **iii.**). For this purpose, trajectories of the CIR process are simulated by a strong convergent discretization scheme. The second novelty in our procedure consists in using the standardized residuals of the "optimal" ARIMA model selected for each sub-sample in place of realizations of a standard Brownian motion into the simulation scheme. As a result, exact fitted values to real data following the CIR dynamics are calculated and the computational

cost of the numerical procedure is considerably reduced. Finally, the interest rates estimated by the CIR model are shifted back and compared to real data. As a measure of goodness-of-fit to the available market data, we compute:

- the statistics R^2 given by the following expression [97]

$$R^2 = 1 - \frac{\sum_{h=1}^m (e_h - \bar{e})^2}{\sum_{h=1}^m (r_h - \bar{r})^2}, \quad (4.2)$$

where $e_h = r_h - \hat{r}_h$ denotes the residual between the observed market interest rate r_h and the corresponding fitted value \hat{r}_h , evaluated on a data sample of size $m \geq 2$. Furthermore, \bar{e} and \bar{r} denote the sample mean of e_h and r_h , respectively;

- the square root of the mean square error (RMSE)

$$\varepsilon = \sqrt{\frac{1}{m} \sum_{h=1}^m e_h^2}. \quad (4.3)$$

4.4 Numerical implementation and empirical analysis

4.4.1 STEP 1: ANOVA test and market data translation

The Analysis of Variance (ANOVA) is a parametric statistical tool developed by R.A. Fisher in 1918 as an extension of the t and the z test (both used for analysing statistical differences between two groups). The idea is to compare means (and relative variance) between three or more independent groups in a sample using the F-distribution. ANOVA tests the non-specific null hypothesis that the population's

means are equal between groups (i.e. the "omnibus null hypothesis"). ANOVA is one-way (respectively two-way) when the number of independent variables is one (respectively two). The one-way ANOVA produces an F-statistic, obtained as a ratio of two estimates of population's variance. A higher ratio implies that the samples were drawn from populations with different mean values.

As explained in Section 4.3, our first objective is to overcome the issues pointed out in **i.**, **ii.** and **iv.** for the CIR model. Thus we start to partition the whole data sample into sub-samples, which we call *groups*, by a one-way ANOVA analysis to highlight statistically significant changes of variance in market spot rates and so to give an account of possible jumps. The main difficulty concerns the choice of the optimal partition into groups to apply the ANOVA test; we had to take into account both the size (the smaller the group, the more refined the analysis) and the ability to capture any jumps (the larger the group, the better in terms of statistical significance).

As an example, we consider the data sample consisted of $n=68$ interest rates with 1 day (overnight) maturity from Dataset I in EUR currency. After several tests, we decided to segment the whole sample into eight groups each of size $m = 8$ or a multiple thereof (except for the last group, obviously). The results of the one-way ANOVA test are reported in Table 4.1. The *p-value* ($\text{Prob}>F$) of $8.00796 \cdot 10^{-19}$ indicates a statistically significant difference between groups.

Furthermore, the boxplots (Figure 4-1.a)) and a multiple comparison test performed on the eight groups (Figure 4-1.b)) have suggested partitioning the data sample into the following four groups of observations 1–8, 9–16, 17–56, 57–68.

Table 4.1: The ANOVA Table shows the between-groups (Groups) and the within-groups (Error) variation. “SS” is the sum of squares and “df” means degrees of freedom associated to SS. MS indicates the mean squared error, i.e. the estimate of the error variance. The value of the F-statistic is given by the ratio of the mean squared errors.

Source	SS	df	MS	F	Prob>F
Groups	10.8783	7	1.55405	34.71	8.00796e-19
Error	2.6862	60	0.04477		
Total	13.5645	67			

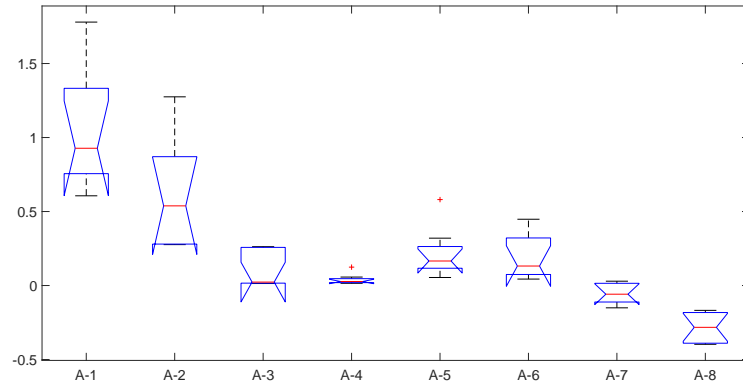
Moreover, since the CIR model (4.1) does not fit negative interest rates and normal/high volatility when the rate value is small, the following translation formula

$$r_{shift}(t) = r(t) + \alpha, \quad t \in [0, T], \quad (4.4)$$

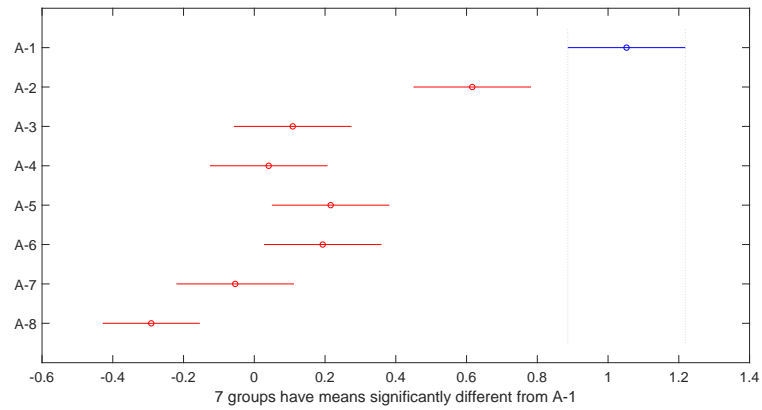
which leaves unchanged the stochastic dynamics of the interest rate process $r = (r(t))_{t \in [0, T]}$, is applied to the observed market data in the presence of near zero/negative values. The parameter $\alpha > 0$ is an arbitrary constant term. The most appropriate choice must take into account the empirical distribution of interest rates. For our purpose, we set α equal to the approximate value, calculated from the available market data, corresponding to the 99th-percentile of the conditional distribution of r . However, if further negative values are between the 99th- and the 100th-percentile, then α can be set equal to the approximate value corresponding to the 1st-percentile of the conditional distribution of interest rates. Hence the translation (4.4) becomes

$$r_{shift}(t) = r(t) - \alpha.$$

The translation is applied after carrying out a check on each group partitioning the



a)



b)

Figure 4-1: **a)**. Boxplots with notches around the median (red line). Notches of boxes A-1, A-2, A-8 do not overlap each other and with the other groups, this offers evidence of a statistically significant difference between the medians. Notches of boxes A-3, ..., A-7 overlap, indicating they may be from the same or similar populations. **b)**. Multiple comparison test of the means. The plot displays the mean estimates of each group with 95% intervals around them. The intervals of groups A-2, ..., A-8 are highlighted in red and the comparison interval of the group A-1 is in blue. The lack of intersection between intervals indicates that the corresponding group means are significantly different from each other.

original data sample. The check consists in calculating the harmonic mean, which is more robust than the arithmetic one in the presence of extreme values, and in verifying whether it is smaller than a constant value chosen arbitrarily small (e.g. 10^{-2}). If this happens in at least one group, then the whole sample is translated.

4.4.2 STEP 2. Sub-optimal ARIMA models

The second step of our procedure consists in deriving the best fitting ARIMA(p, i, q) model to each group of interest rates partitioning the observed market data sample.

In time series analysis, an ARIMA (autoregressive integrated moving average) model is a generalization of an ARMA (autoregressive moving average) model. Fixed $p, q \in \mathbb{N}^*$, the ARIMA(p, q) refers to the model with p autoregressive terms and q moving-average terms, i.e. a given process $X(t)$ is ARIMA(p, q) if

$$X(t) = m + \sum_{h=1}^p \phi(h)X(t-h) + \varepsilon(t) + \sum_{h=1}^q \theta(h)\varepsilon(t-h),$$

where m is a constant, $\phi(h)$, $\theta(h)$ are the parameters of the model and $\varepsilon(t)$ is white noise.

The process $X(t)$ is said to be *stationary* if the absolute value of any root of the polynomial $\phi(x) := 1 - \sum_{h=1}^p \phi(h)x^h$ is greater than 1. Analogously, $X(t)$ is said to be *invertible* if the absolute value of any root of the polynomial $\theta(x) := 1 + \sum_{h=1}^q \theta(h)x^h$ is greater than 1. Moreover, given $i \in \mathbb{N}$, let $\Delta^i X(t) = X(t) - X(t-i)$ the i^{th} -difference operator, then, an ARIMA(p, i, q) model is a process $X(t)$ where i^{th} -difference is a stationary and invertible ARMA(p, q) model (for more details see [20]).

We apply the ARIMA(p, i, q) on the interest rates time series $r(t)$ as a filter in

the sense that we take its residuals. In fact, a 'good' ARIMA has not autocorrelated, independent and normally distributed residuals. This conforms to the basic assumption in the CIR model (4.1) that the random term is governed by a Brownian motion. This strategy allows us to get an exact trajectory of CIR fitted values instead of a curve averaged over 100,000 simulated trajectories (i.e. the average of a Monte Carlo simulation), and so, the computational cost is considerably reduced. Moreover, our model depends implicitly on the updating parameters (p, i, q) and this provides a better calibration at each time step to market data. To recall how this objective is difficult we refer to Carmona and Tehranchi (2006) [36] who explained that: "tweaking the parameters can produce yield curves with one hump (a local maximum) or one dip (a local minimum), but it is very difficult (if not impossible) to calibrate the parameters so that the hump/dip sits where desired. There are not enough parameters to calibrate the models to account for observed features contained in the prices quoted on the markets".

Therefore, to keep working with a suitable CIR model, we choose the parameters (p, i, q) for the ARIMA such as the (standardized) residuals are like Gaussian white noise, as explained below.

First we start by selecting, for each group, a set of ARIMA (p, i, q) models, for $i \in \{0, 1, 2\}$ and $p, q \in \{1, 2, 3\}$, whose standardized residuals satisfy the following "sub-optimal" conditions:

1. Absence of both autocorrelation (AC) and partial autocorrelation (PAC) in the time series (if this condition is not verified, we can require just the absence of autocorrelation);
2. Absence of unit roots (stationarity of the time series);
3. To be normally distributed;

$$4. R_{ARIMA}^2 > 0.5,$$

where R_{ARIMA}^2 denotes the statistics R^2 defined in (4.2), computed for the ARIMA (p, i, q) model. Further, to ensure that the standardized residuals of the selected ARIMA (p, i, q) models satisfy the above condition 3, the Johnson's transformation system (Johnson (1949)[92]) is applied. The Johnson's method consists in transforming a non-normal random variable X to a standard normal variable Z as follows

$$Z = \gamma + \delta f\left(\frac{X - \xi}{\lambda}\right), \quad \lambda, \delta > 0 \quad (4.5)$$

where f is function of a simple form. In particular, $f((X - \xi)/\lambda)$ must be a monotonic function of X , and its range of values have to correspond to the actual range of possible values of $(X - \xi)/\lambda$. The parameters δ and γ reflect respectively the skewness and kurtosis of f , while ξ and λ are the mean and the standard deviation of X . The algorithm to estimate the four parameters γ, δ, λ and ξ , and perform the appropriate transformation is available as a Matlab Toolbox written by Jones (2014) [93]).

In the sequel, we will show how the normally distributed standardized ARIMA residuals apply to the diffusion term of the SDE (4.1) to simulate trajectories of the interest rate process and calibrate the corresponding parameters k, θ, σ to the shifted market interest rates.

4.4.3 STEP 3. Calibration of CIR parameters

Consider the j th-group partitioning the available market data sample, which we assume to be of length n_j . The calibration of the CIR parameters k, θ, σ in the group is performed as follows

- The volatility σ is estimated by the group standard deviation, namely $\hat{\sigma}_j$;

- The long-run mean parameter θ is estimated by the group mean, namely $\hat{\theta}_j$;
- The speed of mean reversion k is estimated by that value, say \hat{k}_j , solving the following minimization problem:

$$\min_{k>0} S_j(k) := \min_{k>0} \sqrt{\frac{\sum_{h=n_{j-1}+1}^{n_j} (u_h(k) - \bar{u}_j(k))^2}{n_j - 1}}. \quad (4.6)$$

For any $k > 0$, we define

$$u_h(k) := r_h(k) - r_{shift,h}, \quad h = n_{j-1} + 1, \dots, n_j, \quad (n_0 = 0) \quad (4.7)$$

being $r_{shift,h}$ the shifted market interest rate value in the j th-group, and $r_h(k)$ the corresponding simulated CIR interest rate value expressed as a function of the unknown parameter k . $\bar{u}_j(k)$ denotes the sample mean of $\{u_h(k), h = n_{j-1} + 1, \dots, n_j\}$. The $r_h(k)$ are calculated by applying the Milstein discretization scheme (1979)[111]¹ to the SDE (4.1).

Brigo & Mercurio (2006) [27, Section 22.7] showed that the Milstein scheme converges in a much better way than other numerical schemes for the CIR process. It reads as

$$r_{h+1}(k) = r_h(k) + k(\hat{\theta}_j - r_h(k)) \Delta + \hat{\sigma}_j \sqrt{r_h(k)} \Delta Z_{h+1} + \frac{(\hat{\sigma}_j)^2}{4} [(\sqrt{\Delta} Z_{h+1})^2 - \Delta], \quad (4.8)$$

where Δ is the time step - we set $\Delta = 1/30$ due to monthly observed data - and Z_{h+1} are the normally distributed standardized residuals of each ARIMA(p, i, q) model satisfying the "sub-optimal" conditions 1-4 for the j th-group.

¹A variant with polynomial convergence rates is described in [86]

After calculation of the estimates $\hat{k}_j, \hat{\theta}_j, \hat{\sigma}_j$, the CIR fitted values to the shifted observed interest rates in the j th-group are computed by the simulation scheme (4.8) as follows

$$\hat{r}_{h+1} = \hat{r}_h + \hat{k}_j(\hat{\theta}_j - \hat{r}_h) \Delta + \hat{\sigma}_j \sqrt{\hat{r}_h} \Delta Z_{h+1} + \frac{(\hat{\sigma}_j)^2}{4} [(\sqrt{\Delta} Z_{h+1})^2 - \Delta], \quad (4.9)$$

where Δ and Z_{h+1} are as before. We would emphasize that the partitioning of the available data sample in groups affects the estimation of the parameters k, θ, σ , which are so locally calibrated to each group. Moreover, it is worth noting that to simulate trajectories of the CIR process, the random terms in the simulation scheme (4.8) are generated by the standardized residuals Z_{h+1} in place of realizations of a standard Brownian motion, as usual. This strategy allows us to get an exact trajectory of CIR fitted values instead of a curve averaged over 100,000 simulated trajectories, with a considerably reduced computational cost.

To measure the goodness-of-fit, the statistics R^2 is computed. For sake of clarity, in the sequel we will denote by R_{CIR}^2 the statistics (4.2) when referring to the CIR model.

Optimal ARIMA model

For each group j , the "optimal" ARIMA(p, i, q) model providing the best CIR fitting to the observed market data will be chosen among the selected sub-optimal ARIMA(p, i, q) models, as described in Section 4.4.2, that satisfy the following additional conditions:

5. The ARIMA(p, i, q) minimizes the Bayesian Information Criterion (BIC) matrix whose rows and columns are the possible p and q lags, respectively (*BIC condition*);

6. $R_{CIR}^2 > 0.5$.

Therefore we define the following sets of candidate ARIMA models:

$$\mathcal{I}_{AC} = \{(p, i, q) \mid \text{ARIMA}(p, i, q) \text{ satisfies conditions 1-4 and 5}\}$$

and

$$\mathcal{I}_{ACB} = \{(p, i, q) \mid \text{ARIMA}(p, i, q) \text{ satisfies conditions 1-6.}\}.$$

Obviously, $\mathcal{I}_{ACB} \subset \mathcal{I}_{AC}$.

Last but not least, the “optimal” ARIMA model is chosen in the above defined classes as the model minimizing the RMSE ε_j

$$\min_{\hat{r}_j} \varepsilon_j := \min_{\hat{r}_j} \sqrt{\frac{1}{n_j} \sum_{h=n_{j-1}+1}^{n_j} (r_{shift,h} - \hat{r}_h)^2}, \quad (4.10)$$

where the minimum is computed with respect to all the CIR fitted values samples, $\hat{r}_j = \{\hat{r}_h; h = n_{j-1} + 1, \dots, n_j\}$, simulated for the j th-group.

For better understanding the *CIR#* methodology herein proposed, we implemented the algorithm described above to analyze the sample of $n = 68$ monthly observed EUR interest rates with 1 day (overnight) maturity, introduced in Chapter A). We recall that the ANOVA analysis suggested partitioning the data sample into four groups of observations: 1–8, 9–16, 17–56, 57–68 (see Section 4.4.1). Table 4.2 shows in detail the outputs for this sample. The group containing the observations 17–56 has been further segmented into three sub-groups of size $m = 8$ or a multiple thereof: 17–32, 33–48 and 49–56. The ARIMA(p, i, q) model identified by a rectangle in Table 4.2, indicates the “optimal” ARIMA model chosen for each group/sub-group with the smaller ε_j value. As can be seen, the bigger R_{CIR}^2 value

matches the “optimal” ARIMA model, except for the group of observations 57–68.

Nevertheless, none of these models fulfils the *BIC condition*.

Table 4.2: Outputs from the ARIMA-CIR algorithm for the 68 monthly EUR interest rates on overnight maturity

j	group/sub-groups	ARIMA model	$(R_{CIR}^2)_j$	ϵ_j	BIC cond.
1	1–8	(2,0,1)	0.8166	0.1643 ¹	
		(2,0,2)	0.5930	0.2414	
		(3,0,2)	0.780	0.1865	
		(1,1,1)	0.8166	0.1643	
		(1,2,1)	0.7309	0.2026	
		(1,2,2)	0.7805	0.1845	✓
		(3,2,1)	0.7023	0.2104	
2	9–16	(1,0,1)	0.6842	0.2090	
		(2,0,2)	0.7799	0.2588	
		(3,0,2)	0.6418	0.2661	✓
		(1,1,1)	0.7378	0.2043	
		(1,1,2)	0.8472	0.1554	
		(2,1,1)	0.6842	0.2169	
		(2,1,2)	0.7799	0.2012	
3	17–32	(3,1,2)	0.6418	0.2333	
		(1,0,3)	0.9174	0.0326	
4	33–48	(3,0,1)	0.5485	0.0646	
		(3,0,1)	0.6901	0.0833	
5	49–56	(3,1,2)	0.6332	0.1146	
		(3,2,1)	0.6332	0.1146	
		(1,0,1)	0.5076	0.0597	
		(1,0,2)	0.6030	0.0526	
		(2,0,1)	0.5702	0.0577	
		(3,0,1)	0.7648	0.0483	
		(3,0,2)	0.6240	0.0537	
		(1,1,1)	0.5702	0.0577	
		(2,1,1)	0.5393	0.0588	
		(3,1,2)	0.7715	0.0479	
5	49–56	(1,2,1)	0.5542	0.0582	
		(3,2,1)	0.6987	0.0479	
		(3,2,2)	0.6343	0.0536	✓

j	group/sub-groups	ARIMA model	$(R_{CIR}^2)_j$	ε_j	BIC cond.
6	57–68	(1,0,2)	0.5964	0.0752	
		(1,0,3)	0.8080	0.0570	
		(2,0,2)	0.8136	0.0559	
		(3,0,2)	0.7899	0.0577	
		(3,0,3)	0.6560	0.0704	
		(1,1,2)	0.8136	0.0559	
		(1,1,3)	0.8006	0.0614	
		(2,1,1)	0.8239	0.0486	
		(2,1,2)	0.8542	0.0525	
		(2,1,3)	0.8936	0.0551	
		(3,1,2)	0.9023	0.0511	
		(3,1,3)	0.8000	0.0580	

1 For a more exact comparison we use the numeric format long.

Figure 4-2 reports the qualitative statistical analysis carried out by applying the ARIMA(1, 1, 2) chosen as the “optimal” fitting model for the group 9–16 (similar plots for the other group/sub-groups are reported in the 4.5.2).

The total values of the statistics R^2 and the RMSE ε have been computed on the whole sample as a weighted mean of the $(R_{CIR}^2)_j$ and ε_j values corresponding to the “optimal” ARIMA model chosen for each group/sub-group, i.e.

$$R^2 = \sum_j \frac{n_j}{n} (R_{CIR}^2)_j,$$

$$\varepsilon = \sqrt{\sum_j \frac{n_j}{n} \sum_{h=n_{j-1}+1}^{n_j} (r_{shift,h} - \hat{r}_h)^2}. \quad (4.11)$$

Their values for the analysed data sample are: $R^2 = 0.8101$, $\varepsilon = 0.2922$. The 4.5.3 reports the CIR parameters estimates and the plots of the function $S_j(k)$, defined in (4.6), for all groups/sub-groups.

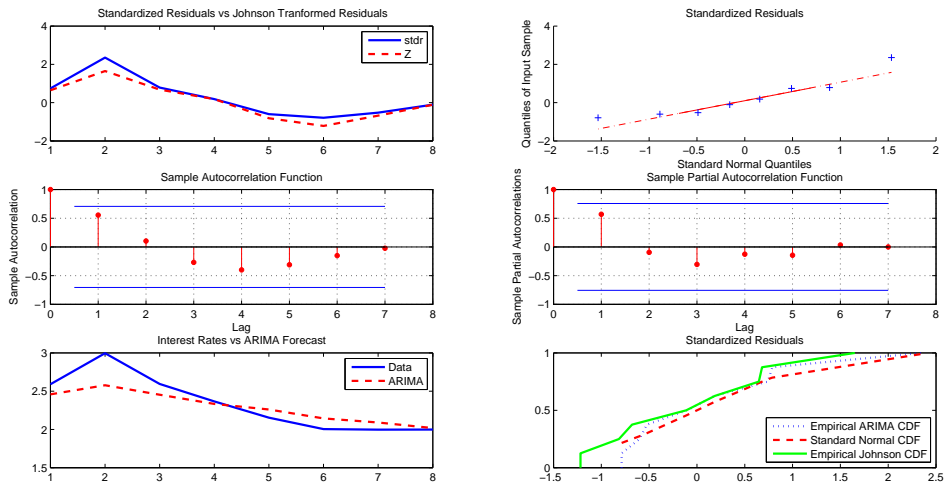


Figure 4-2: Qualitative statistical analysis related to the group 9–16. **Top line:** ARIMA (1, 1, 2) standardized residuals versus Johnson’s transformed residuals (*left*); Q-Q normal plot for the ARIMA(1, 1, 2) standardized residuals (*right*). **Middle line:** AC plot (*left*) and PAC plot(*right*). **Bottom line:** market interest rates versus ARIMA (1, 1, 2) fitted values (*left*); comparison between the empirical distribution function of the ARIMA (1, 1, 2) standardized residuals, before and after the Johnson’s transformation, and the cumulative distribution function (CDF) of the standard normal distribution (*right*).

The market interest rates have been shifted by using a translation of type (4.4), where α corresponds to the 99th-percentile of the conditional distribution of the interest rates process, as described in Section 4.4.1. Finally, the CIR fitted values have been shifted back.

Figure 4-3 compares the short-term interest rates structure of the analysed market data sample with the corresponding curve of CIR fitted values computed by the simulation scheme (4.9) for each group partitioning the whole data sample.

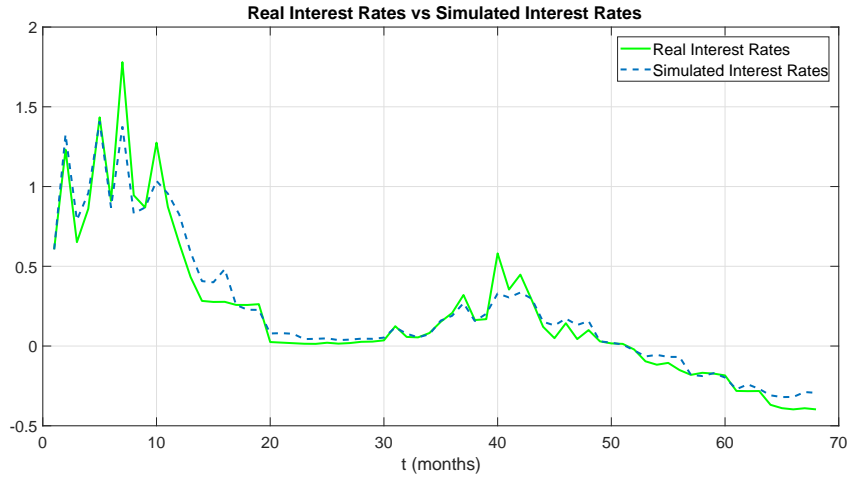


Figure 4-3: Monthly EUR interest rates with $T=1$ day (overnight) maturity vs CIR fitted rates

4.4.4 The change points detection problem

As explained in Section 4.4.1 the main difficulty concerns the choice of the optimal segmentation to detect abrupt changes in the variance of the interest rates dynamics. In the literature there exist several approaches for detecting multiple changes in the probability distribution of a stochastic process or a time series such as sequential analysis (i.e., “online” methods), clustering based on maximum likelihood estimation (i.e. “offline” methods), minimax change detection, etc. (see, for example, Bai and Perron (2003)[7], Lavielle (2005)[102] and (2006)[103], Hacker and Hatemi-J (2006)[82], Adams and MacKay (2007)[1], Arlot and Cénisse (2011)[5]).

We have chosen to implement the Matlab algorithm proposed by Lavielle (2005)[102] for the detection of changes in the variance, which allows partitioning the data sample analysed in the previous section into the following six groups of observations: 1–13, 14–19, 20–30, 31–39, 40–52, 53–68. However, the application of Step 2 and Step 3 of the proposed procedure to each group has not provided better results than

those previously illustrated.

4.5 Forecast of future interest rates

In this section we will address the CIR# model progress on future interest rate forecasts from a window of observed market data.

In this endeavour, we decided to impose the most challenging conditions by modelling first the overnight rate curve and using only a handful number of observations. As explained above, with monthly data we have found that $m = 8$ observations are sufficient for a good calibration. Thus we consider a fixed size window of 8 real interest rates that is rolled through time, each month adding the new rate and taking off the oldest one. The length of this window (8 months) is the historical period over which we forecast the next-month spot rate value. The numerical procedure described in Sections 4.4.1–4.4.3 has been applied to forecast future next-month interest rates. We would like to focus for a moment on some difficulties experienced in implementing the CIR# model to forecast future interest rate values:

- a. In case of low-frequency rates and with fixed "a priori" rolling windows of small length, as in our case, the partition of the data sample may not (always) be performed. When higher-frequency data are available (e.g. weekly interest rates), rolling windows of variable size can be determined by a segmentation of the historical data sample (Section 4.4.1) and a change point detection (Section 4.4.4).
- b. It is better to calibrate the long-run mean parameter θ to the historical data as an exponential moving average (EMA). Indeed, the EMA places a greater weight and significance on the most recent interest rate values. Thus, it reacts

more significantly to recent interest rate changes than the sample mean, which applies an equal weight to all observations in the historical period.

The predicted yield curve for monthly EUR and USD interest rates with overnight maturity is shown in Figure 4-4 and 4-5, respectively, and compared with the corresponding market observed data. It is evident that the predicted next-month spot rates computed by the CIR# model follow the market trend. Moreover, to measure the goodness-of-fit of forecast interest rates to the market data, we computed the values of the statistics R^2 and RMSE ε , which are respectively 0.8741 and 0.1120 for the EUR currency and 0.9216 and 0.0263 for the USD currency.

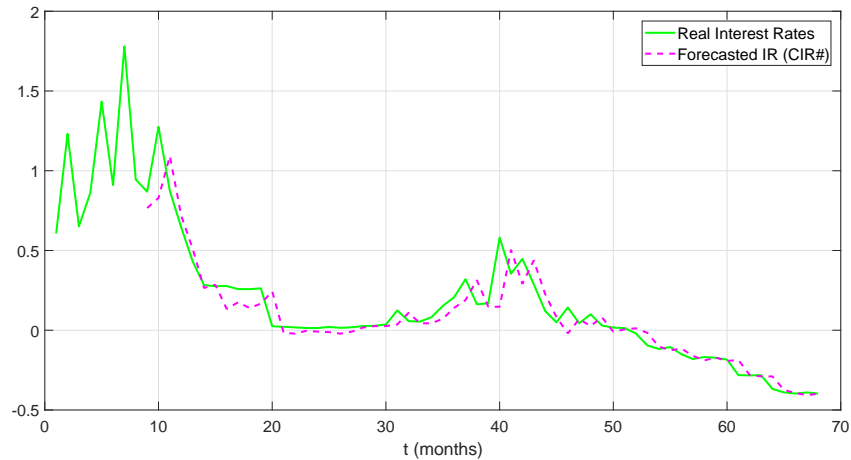


Figure 4-4: **Forecast of the next-month interest rate based on a historical rolling window of size $m = 8$ market data:** monthly EUR interest rates with maturity $T=1$ day (overnight) versus predicted next-month interest rates.

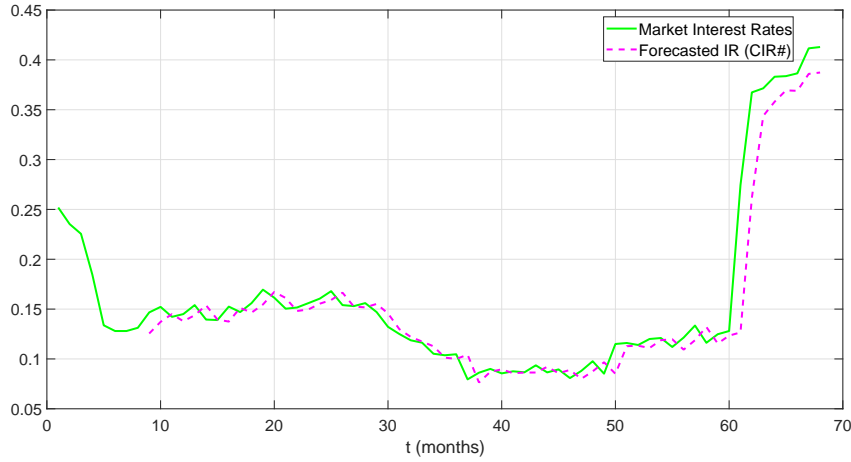


Figure 4-5: **Forecast of the next-month interest rate based on a historical rolling window of size $m = 8$ market data:** monthly USD interest rates with maturity $T=1$ day (overnight) versus predicted next-month interest rates.

4.5.1 CIR# forecasts versus CIR forecasts

In this Section, we would like to point out the CIR# improvements in the forecast as compared to the original CIR model. Note that future next-month interest rates are predicted by the CIR model using the expectation closed formula

$$E[r(t)|r(s)] = \theta + (r(s) - \theta)e^{-k(t-s)}, \quad 0 \leq s < t,$$

after the CIR parameters (k, θ, σ) have been calibrated to the market historical data. This is done by applying the martingale estimating function method for diffusion processes proposed by Bibby et al. (see [15, Example 5.4](2005) and [122, Section 4.3](2018)). In this case to ensure the existence of such estimates the length of a rolling window must be greater than the window size of $m = 8$ observations required by the CIR# model. Figures 4-6 and 4-7 below plot the future next-month values predicted by the CIR# methodology compared with the ones forecasted by the clas-

sical CIR model. A better fitting of the rate values predicted by the CIR# to the market available data is evident.

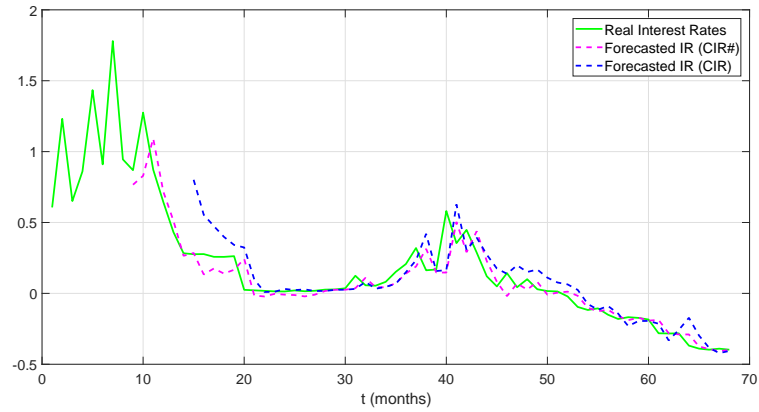


Figure 4-6: **CIR# versus CIR: forecast of future next-month interest rates.** Monthly EUR interest rates with overnight maturity (*green line*); future next-month interest rates predicted by the CIR# model based on a rolling window of $m = 8$ market data (*magenta dashed line*); future next-month interest rates predicted by the classical CIR model based on a rolling window of $m = 14$ market data (*blue dashed line*).

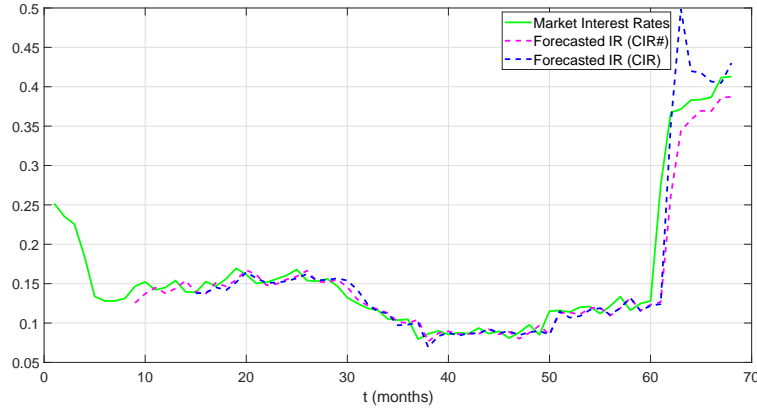


Figure 4-7: **CIR# versus CIR: forecast of future next-month interest rates.** Monthly USD interest rates with overnight maturity (*green line*); future next-month interest rates predicted by the CIR# model based on a rolling window of $m = 8$ market data (*magenta dashed line*); future next-month interest rates predicted by the classical CIR model based on a rolling window of $m = 14$ market data (*blue dashed line*).

Figures 4-8-4-9 and 4-10-4-11 report the error analysis carried out on all (63) market rate samples of both Dataset I and II respectively in EUR and USD currency. The analysis consists in comparing the statistics R^2 and $RMSE$ values computed for each future next-month interest rate sample predicted by the proposed CIR# and the original CIR model, respectively. The vertical black line separates Dataset I from Dataset II. The plotted results show globally a better performance (bigger R^2 value and smaller $RMSE$ value) of the CIR# model.

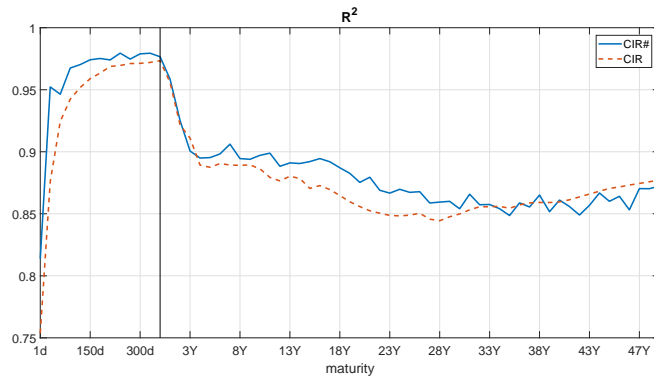


Figure 4-8: **Statistics for EUR dataset:** $R^2_{CIR\#}$ versus R^2_{CIR} , computed on a rolling window of size $m = 14$.

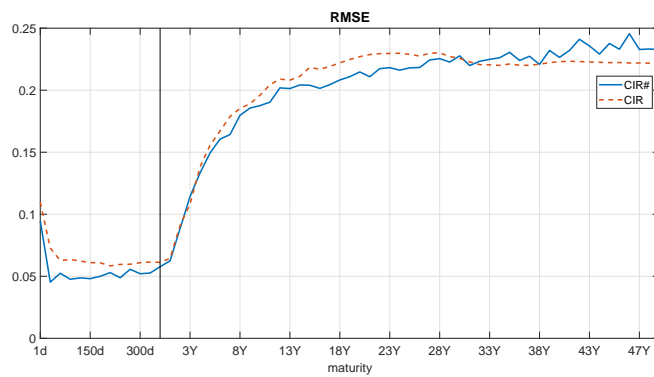


Figure 4-9: **Statistics for EUR dataset:** $RMSE_{CIR\#}$ versus $RMSE_{CIR}$, computed on a rolling window of size $m = 14$.

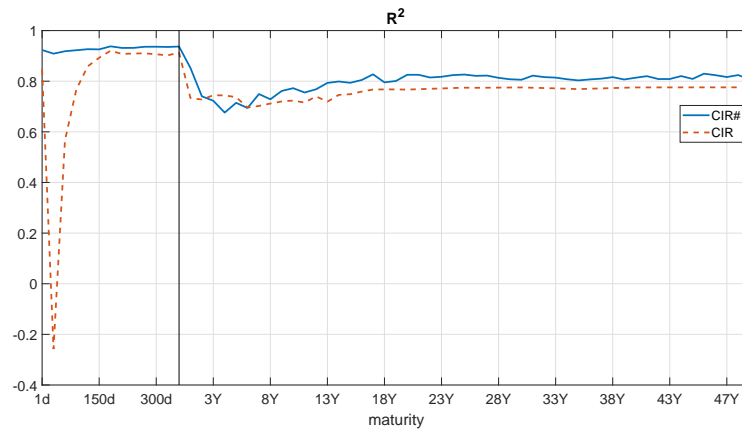


Figure 4-10: **Statistics for USD dataset:** $R^2_{CIR\#}$ versus R^2_{CIR} , computed on a rolling window of size $m = 14$.

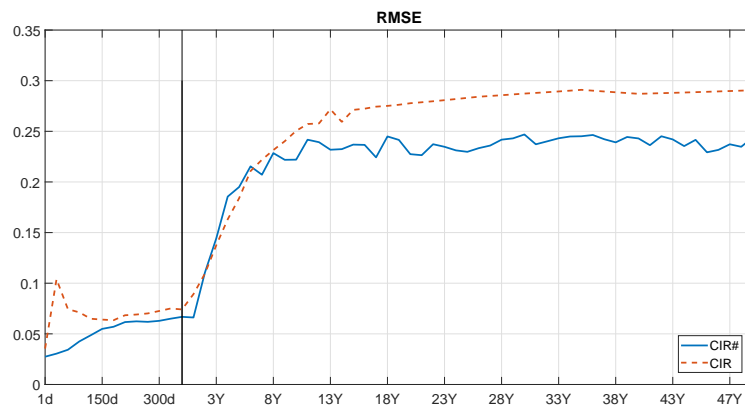


Figure 4-11: **Statistics for USD dataset:** $RMSE_{CIR\#}$ versus $RMSE_{CIR}$, computed on a rolling window of size $m = 14$.

4.5.2 Qualitative analysis related to Table 4.2

We report the qualitative statistical analysis carried out for each group/sub group according to the results reported in Table 4.2.

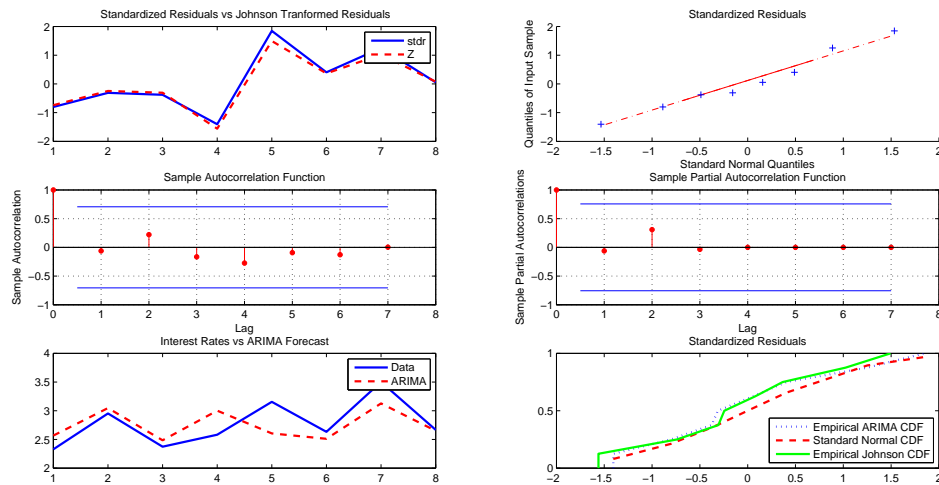


Figure 4-12: Qualitative statistical analysis related to the sub-group 1–8. **Top line:** ARIMA (2, 0, 1) standardized residuals versus Johnson’s transformed residuals (*left*); Q-Q normal plot for the ARIMA (2, 0, 1) standardized residuals (*right*). **Middle line:** AC (*left*) and PAC (*right*) plots. **Bottom line:** real interest rates versus ARIMA (2, 0, 1) fitted values (*left*); comparison of the standard normal cumulative distribution function (CDF) with the empirical CDF of ARIMA (2, 0, 1) standardized residuals and of Johnson’s transformed residuals (*right*).

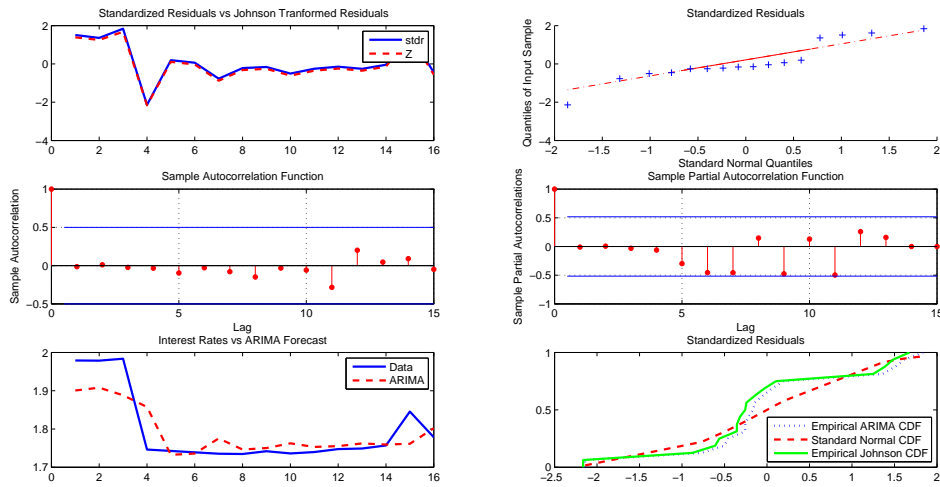


Figure 4-13: Qualitative statistical analysis related to the sub-group 17–32. **Top line:** ARIMA (1, 0, 3) standardized residuals versus Johnson’s transformed residuals (*left*); Q-Q normal plot for the ARIMA (1, 0, 3) standardized residuals (*right*). **Middle line:** AC (*left*) and PAC (*right*) plots. **Bottom line:** real interest rates versus ARIMA (1, 0, 3) fitted values (*left*); comparison of the standard normal cumulative distribution function (CDF) with the empirical CDF of ARIMA (1, 0, 3) standardized residuals and of Johnson’s transformed residuals (*right*).

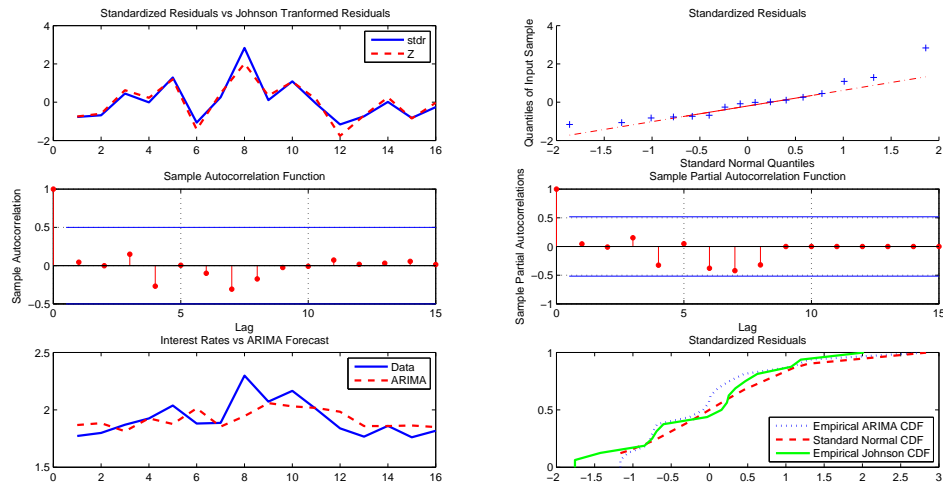


Figure 4-14: Qualitative statistical analysis related to the sub-group 33–48. **Top line:** ARIMA (3,0,1) standardized residuals versus Johnson’s transformed residuals (*left*); Q-Q normal plot for the ARIMA (3,0,1) standardized residuals (*right*). **Middle line:** AC (*left*) and PAC (*right*) plots. **Bottom line:** real interest rates versus ARIMA (3,0,1) fitted values (*left*); comparison of the standard normal cumulative distribution function (CDF) with the empirical CDF of ARIMA (3,0,1) standardized residuals and of Johnson’s transformed residuals (*right*).

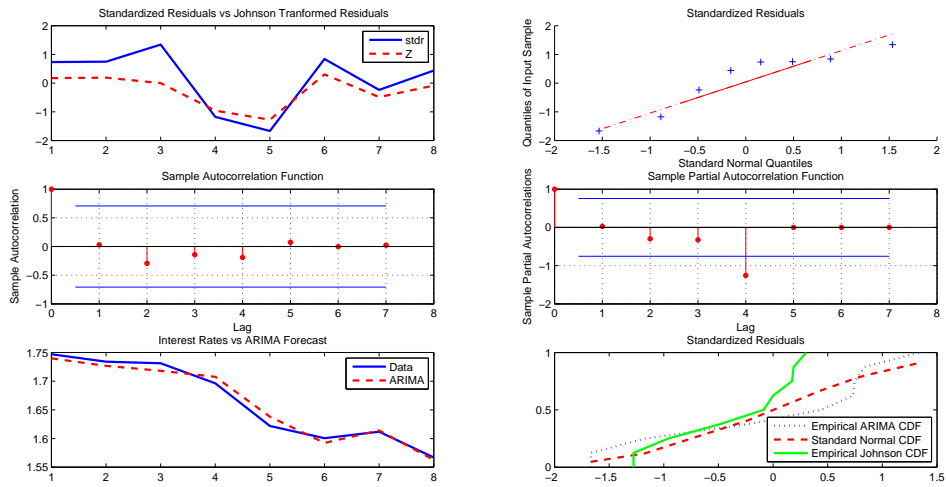


Figure 4-15: Qualitative statistical analysis related to the sub-group 49–56. **Top line:** ARIMA (3,1,2) standardized residuals versus Johnson’s transformed residuals (*left*); Q-Q normal plot for the ARIMA (3,1,2) standardized residuals (*right*). **Middle line:** AC (*left*) and PAC (*right*) plots. **Bottom line:** real interest rates versus ARIMA (3,1,2) fitted values (*left*); comparison of the standard normal cumulative function (CDF) with the empirical CDF of ARIMA (3,1,2) standardized residuals and of Johnson’s transformed residuals (*right*).

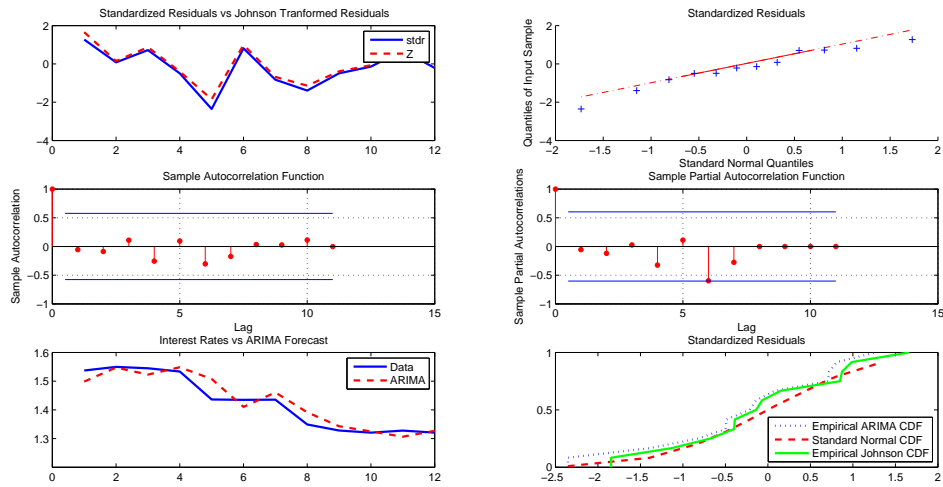


Figure 4-16: Qualitative statistical analysis related to the sub-group 57–68. **Top line:** ARIMA (2, 1, 1) standardized residuals versus Johnson’s transformed residuals (*left*); Q-Q normal plot for the ARIMA (2, 1, 1) standardized residuals (*right*). **Middle line:** AC (*left*) and PAC (*right*) plots. **Bottom line:** real interest rates versus ARIMA (2, 1, 1) fitted values (*left*); comparison of the standard normal cumulative distribution function (CDF) with the empirical CDF of ARIMA (2, 1, 1) standardized residuals and of Johnson’s transformed residuals (*right*).

4.5.3 CIR parameter estimates

We report the estimates of the CIR parameters k, θ, σ and, in particular, the plots of the function $S_j(k)$ defined in (4.6), corresponding to the selected "optimal" ARIMA models reported in Table 4.2.

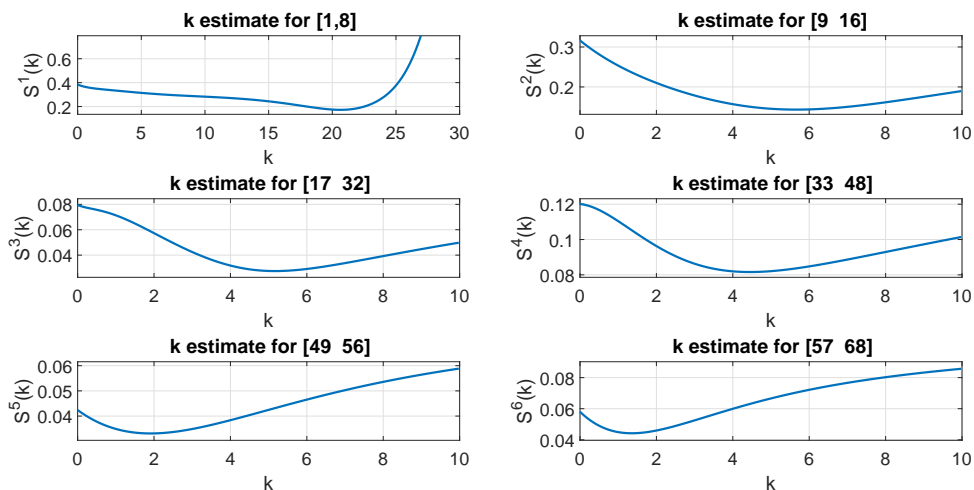


Figure 4-17: Plots of the functions $S_j(k)$ for each group/sub-group

Table 4.3: CIR parameter estimates based on 68 monthly observed 1-day (overnight) EUR interest rates

j	group/sub-group	\hat{k}_j	$\hat{\theta}_j$	$\hat{\sigma}_j$
1	1–8	20.6364	2.7699	0.4027
2	9–16	5.6621	2.3338	0.3663
3	17–32	5.1649	1.7924	0.0954
4	33–48	4.4462	1.9223	0.1546
5	49–56	1.9092	1.6637	0.0709
6	57–68	1.3555	1.4264	0.0958

4.6 Conclusions

The aim of the present Chapter is to propose a novel numerical methodology, the *CIR# model*, in order to forecast future interest rates that work when rates are negative and keep update the volatility with market conditions. The basic idea is to leverage the CIR model by maintaining the market volatility structure as well as the analytical tractability of the original model. Thus the suggested *CIR# model* is quite powerful for the following reasons. First of all, the historical market data sample is partitioned into sub-groups in order to capture all the statistically significant changes of variance in the interest rates. Also, we have included in the procedure an appropriate translation of market rates to positive values in order to overcome the issue of negative/near-to-zero values. Second, we have introduced a new way of calibrating the CIR model parameters to each sub-group partitioning the historical actual data. The standard Brownian motion process in the random part of the model is replaced with normally distributed standardized residuals of the “optimal” ARIMA model suitably chosen for each sub-group. As a result, exact CIR fitted values to the observed market data are calculated and the computational cost of the numerical procedure is considerably reduced. Third, we have shown that the *CIR# model* is efficient and able to follow very closely the structure of market interest rates (especially for short maturities that, notoriously, are very difficult to handle) and to predict future interest rates better than the original CIR model. As a measure of goodness-of-fit, we obtained high values of the statistics R^2 and small values of the RMSE ε for each sub-group and the entire data sample. Future research will show the predictive power of the model by extending the dataset in terms of frequency and size.

Next Chapter 5, will illustrate how to forecast, through Vasicek and CIR models,

future expected interest rates based on the methodology here outlined.

Chapter 5

Forecasting interest rates through Vasicek and CIR models: a partitioning approach

5.1 Introduction

The present Chapter has the objective of forecasting interest rates (by maturity) from observed financial market data through a new approach that preserves the analytical tractability of the stochastic models describing the dynamics of real market interest rates proposed by Vasicek (1977) [155] and Cox-Ingersoll-Ross (CIR) (1985) [46]. This is because of their popularity within the financial community given their simplicity (uni-factorial, mean reverting models) and their ability to provide closed form solutions for pricing interest rate derivatives (Zeytun and Gupta, 2007) [161]. The idea of this work is to overcome both the usual challenges imposed by regime switching, volatility clustering, skewed tails, etc., as well as the new ones added by

the current market environment (particularly the need to model a downward trend to negative interest rates). This is to be achieved by proposing a new methodology that allows forecasting of future expected interest rates by an appropriate partition of the dataset and assuming that the dynamic of each rate is represented by the Vasicek or CIR model. The effect of partitioning the available market data into sub-samples with an appropriately chosen probability distribution is twofold: (1) to improve the calibration of the Vasicek/CIR model's parameters in order to capture all the statistically significant changes of variance in market spot rates and so, to give an account of jumps; (2) to consider only the most relevant historical period. The distributions herein considered for the dataset partition are the Normal and non-central Chi-square distribution. These distributions have been chosen by analogy with the steady (resp. conditional) distribution of the interest rate process in the Vasicek (resp. CIR) model. The performance of the new approach, tested on weekly EUR data on bonds with different maturities, has been carried out for both Vasicek and CIR model, and compared with the Exponentially Weighted Moving Average (EWMA) model in terms of forecasting error. The error analysis highlighted a better performance of the proposed procedure with respect to the EWMA and better results in prediction when a partition with non-central Chi-square distribution (CIR model) is considered.

This Chapter is organized as follows: Section 5.2 presents the model in full detail. Section 5.3 shows the empirical results for weekly recorded EUR interest rates in both money market and short-term to long-term datasets. Section 5.4 contains the conclusions.

5.2 The Model: procedure and accuracy

Financial time series for interest rates frequently show an empirical distribution as a mixture of probability distributions with sudden changes in the magnitude of variations of the observed values. Thus, in order to capture all the statistically significant changes of variance in market spot rates and so, to give an account of jumps, the available market data sample is partitioned into sub-samples - not necessarily of the same size - with a Normal or a non-central Chi-square distribution by using an appropriate technique described in Section 5.2.1. Further, in case negative or close-to-zero market interest rates are present in the observed dataset, the procedure involves a shift to positive values by a suitable scalar parameter (Section 5.2.2). This to avoid that the diffusion term in (3.2) is not dampened when near to zero, as for the CIR model, but fully reflects the same level of volatility present on the market .

Finally, to deal with the crucial issue of a constant volatility parameter σ and the problem of an unsatisfactory calibration to market data for both CIR and Vasicek models, we calibrate, for each sub-sample, the model's parameters to the observed interest rates (Section 5.2.3).

The proposed procedure is first tested on some samples from the available dataset (Section 5.3) and then is applied to predict future expected next-week interest rates based on rolling windows, as described in Section 5.3.1.

5.2.1 Step 1- Dataset partition

As observed in the Introduction, the novelty in our procedure consists in partitioning the available market data into sub-samples with an appropriately chosen probability distribution. The effect of partitioning is twofold: (1) to improve the calibration of the Vasicek/CIR model's parameters to take account of multiple jumps in the dy-

namics of market interest rates and so, of time changes in volatility; (2) to determine only the latest historical period over which predicting expected future interest rates that closely follow market rates. The sub-samples are chosen according to the data empirical probability distribution, which is unknown.

Notice that in the literature there are several approaches for detecting multiple changes in the probability distribution of a stochastic process or a time series (see, for instance, for instance, Lavielle, 2005 [102]; Lavielle and Teyssiere, 2006 [103]; Bai and Perron 2003 [7]). We shall use these methodologies in an ongoing research work, but in this Chapter we adopt the numerical partition into sub-samples following a Normal or a non-central Chi-square distribution, as described in the next subsections.

Partition with Normal Distribution

In Orlando, Mininni and Bufalo, 2018 [122], we hypothesized the empirical distribution of the observed data sample to be a mixture of normal distributions for the presence of negative interest rate values. This hypothesis is appropriate because in the Vasicek model the interest rate process r has a steady normal distribution. Moreover, the dynamics of the form (3.2) for the square-root process in the CIR model is obtained from a squared Gaussian model (see, for example, Rogers, 1996). Our idea was, therefore, to divide the data sample into a number of sub-samples each coming from an appropriate normal distribution. The goodness-of-fit to a normal distribution is checked with the Lilliefors test at a 5% significance level. This is an improvement over the Kolmogorov-Smirnov test where the population mean and standard deviation are not known, but are estimated from data. In this Chapter we have implemented a *forward* procedure that starts by considering the first four data

of the original sample, say (r_1, \dots, r_4) , and performs the Lilliefors test until the first normally distributed sub-sample, say (r_1, \dots, r_{n_1}) , with $n_1 \geq 4$, is not rejected. Then, the procedure is applied to the remaining sequence $(r_{n_1+1}, \dots, r_{n_1+4})$ until the second normally distributed sub-sample $(r_{n_1+1}, \dots, r_{n_2})$, with $n_2 \geq n_1 + 4$, is not rejected and so on, up to partition the entire data sample into m normally distributed sub-samples, namely $(r_1, \dots, r_{n_1}), (r_{n_1+1}, \dots, r_{n_2}), \dots, (r_{n_{m-1}+1}, \dots, r_{n_m})$, $n_m \leq n$. Table 5.1 summarizes the *forward* segmentation procedure.

Table 5.1: “Forward” procedure

<ol style="list-style-type: none"> 1. Initialize $h=4$; 2. run the Lilliefors test on the interest rate vector $r(1:h)$; 3. while the null hypothesis is not rejected 4. $h=h+1$; 5. run the Lilliefors test on $r(1:h)$; 6. end 7. set $n(1)=h$; 8. initialize $i=1$; 9. while $n(i)<\text{length}(r)$ 10. $h=n(i)+4$; 10. repeat steps 2-6 for $r(n(i)+1:h)$ and find $n(i+1)$; 11. if $\text{length}(r)-n(i+1)<4$ 12. set $\text{resti}=r(n(i+1)+1:\text{length}(r))$; 13. break 14. else 15. set $i=i+1$; 16. end 17. end
--

Further, observe that in performing the Lilliefors test it could happen that the p-value is greater than the chosen significance level, but differs from it by no more than 10^{-2} . Thus, in this case, the Johnson transformation is applied to ensure that each sub-sample follows a normal distribution. The Johnson’s method consists in transforming a non-normal random variable X to a standard normal variable Z as

follows,

$$Z = \gamma + \delta f\left(\frac{X - \xi}{\lambda}\right), \quad \lambda, \delta > 0 \quad (5.1)$$

where f must be a monotonic function of X with the same range of values of the standardized random variable $(X - \xi)/\lambda$, where ξ and λ are respectively the mean and the standard deviation of X . The parameters δ and γ reflect respectively the skewness and kurtosis of f . The algorithm to estimate the four parameters γ , δ , λ and ξ , and to perform the appropriate transformation is available as a Matlab Toolbox written by Jones (2014) [93].

To apply the Johnson's method to our case, the market interest rates in each sub-sample have been first transformed by (5.1) to m sub-samples with standard normal distribution that is, for any $k = 1, \dots, m$,

$$z_h = \gamma + \delta f\left(\frac{r_h - \mu_k}{\sigma_k}\right), \quad h = n_{k-1} + 1, \dots, n_k \quad (n_0 = 0),$$

where μ_k , σ_k denote respectively the sample mean and standard deviation of the k -th sub-group. Then, they are transformed to m sub-samples with normal distribution $N(\mu_k, \sigma_k)$ as follows

$$r_h = \sigma_k z_h + \mu_k, \quad h = n_{k-1} + 1, \dots, n_k \quad (n_0 = 0).$$

Partition with non-central Chi-square Distribution

As an alternative to the previous hypothesis of a mixture of normal distributions, the empirical distribution of the analysed data sample may be assumed as mixture of non-central Chi-square distributions. This hypothesis is justified from the conditional distribution of the CIR process. Since the non-central Chi-square distribution admits

only positive values, the market observed interest rates have to be first shifted to positive values as described in the next subsection. The partitioning procedure is analogous to that described in Section 5.2.1 and the Kolmogorov-Smirnov test is performed (at a 5% significance level) to test the goodness-of-fit of the m sub-samples to a non-central Chi-square distribution.

5.2.2 Step 2 - Shift in interest rates

As mentioned above, a step of the procedure consists in translating market interest rates to positive values to eliminate negative/near-zero values and not to dampen the volatility in the CIR model. Herein we consider the following transformation

$$r_{shift}(t) = r(t) + \alpha, \quad t \in [0, T], \quad (5.2)$$

where α is a deterministic positive quantity. This translation leaves the stochastic dynamics of the interest rates unchanged, i. e. for any time t , $dr_{shift}(t) = dr(t)$. There are many values that could be assigned to α , but we believe that the most appropriate choice is the 99th percentile of the empirical interest rate probability distribution. If the translation (5.2) is not adequate to move negative interest rates to corresponding positive values, which means further negative values are between the 99th- and the 100th-percentile, we can set α equal to the 1st-percentile of the empirical distribution. In this case (5.2) becomes

$$r_{shift}(t) = r(t) - \alpha.$$

5.2.3 Step 3 - Calibration

In order to estimate interest rates from the Vasicek and CIR model, the involved parameters k, θ, σ need to be calibrated to the market interest rates. In the present work, among many approaches existing in the literature to estimate the parameters of a SDE (see, for instance, Poletti Laurini and Hotta, 2017 [130], and references therein), we applied the estimating function approach for ergodic diffusion models introduced in Bibby et al. (2010) [16], which turned out to be very useful in obtaining optimal estimators for the parameters of discretely-sampled ergodic Markov processes whose likelihood function is usually not explicitly known. In Orlando, Mininni and Bufalo, 2018a [122]; 2019 [123], a better performance of the latter method is shown by comparing its efficiency with the maximum likelihood estimation routine implemented in Matlab for the CIR process by Kladívko (2007) [95]. In Bibby, Jacobsen, and Sørensen (2010) [16] the authors constructed an approximately optimal estimating function for the CIR model, from which they derived the following explicit estimators of the three parameters κ, θ, σ based on a sample of n observed market spot rates (r_1, \dots, r_n) :

$$\begin{aligned}
 \hat{\kappa}_n &= -\ln \left(\frac{(n-1) \sum_{i=2}^n r_i / r_{i-1} - (\sum_{i=2}^n r_i)(\sum_{i=2}^n r_{i-1}^{-1})}{(n-1)^2 - (\sum_{i=2}^n r_{i-1})(\sum_{i=2}^n r_{i-1}^{-1})} \right), \\
 \hat{\theta}_n &= \frac{1}{(n-1)} \sum_{i=2}^n r_i + \frac{e^{-\hat{\kappa}_n}}{(n-1)(1 - e^{-\hat{\kappa}_n})} (r_n - r_1), \\
 \hat{\sigma}_n^2 &= \frac{\sum_{i=2}^n r_{i-1}^{-1} (r_i - r_{i-1} e^{-\hat{\kappa}_n} - \hat{\theta}_n (1 - e^{-\hat{\kappa}_n}))^2}{\sum_{i=2}^n r_{i-1}^{-1} ((\hat{\theta}_n / 2 - r_{i-1}) e^{-2\hat{\kappa}_n} - (\hat{\theta}_n - r_{i-1}) e^{-\hat{\kappa}_n} + \hat{\theta}_n / 2) / \hat{\kappa}_n}.
 \end{aligned} \tag{5.3}$$

Similar calculations allow to compute in closed-form the estimators of the three parameters κ, θ, σ for the Vasicek model:

$$\begin{aligned}\hat{\kappa}_n &= -\ln \left(\frac{\frac{1}{(n-1)} (\sum_{i=2}^n r_{i-1}) (\sum_{i=2}^n r_i) - \sum_{i=2}^n r_{i-1} r_i}{\frac{1}{(n-1)} (\sum_{i=2}^n r_{i-1})^2 - \sum_{i=2}^n r_{i-1}^2} \right), \\ \hat{\theta}_n &= \frac{1}{(1 - e^{-\hat{\kappa}_n})} \left(\frac{1}{(n-1)} \sum_{i=2}^n r_i - \frac{e^{-\hat{\kappa}_n}}{(n-1)} \sum_{i=2}^n r_{i-1} \right), \\ \hat{\sigma}_n^2 &= \frac{2\hat{\kappa}_n}{(1 - e^{-2\hat{\kappa}_n})} \cdot \frac{1}{(n-1)} \sum_{i=2}^n (r_i - r_{i-1} e^{-\hat{\kappa}_n} - \hat{\theta}_n (1 - e^{-\hat{\kappa}_n}))^2.\end{aligned}\tag{5.4}$$

Remark 5.1. Notice that the estimators given in (5.3) and (5.4) exist provided that the expression for $e^{-\hat{\kappa}_n}$ is strictly positive (Bibby, Jacobsen, and Sørensen observed that this happens with a probability tending to one as $n \rightarrow \infty$).

It is worth noting that in the presence of negative/near-zero interest rate values, as shown in Figure A-2, the calibration of the unknown parameters for the CIR model may be carried out only after shifting spot rates to positive values by using the transformation (5.2).

5.2.4 Step 4 - Forecasting

After calibration to the market data, the estimates of the parameter vector (k, θ, σ) have been used to forecast future expected interest rates by the following conditional expectation formula available in closed form for the interest rate process in both Vasicek and CIR model (3.2)

$$E[r(t)|r(s)] = \theta + (r(s) - \theta)e^{-k(t-s)}, \quad 0 \leq s < t.\tag{5.5}$$

5.2.5 Accuracy

In order to measure the accuracy of our approach, we compute the square-root of the mean square error (RMSE), say ε , defined as

$$\varepsilon = \sqrt{\frac{1}{n} \sum_{h=1}^n e_h^2}, \quad (5.6)$$

where $e_h = r_h - \hat{r}_h$ denotes the residual between the market interest rate r_h and the corresponding fitted value \hat{r}_h . In our case the fitted values are the expected interest rates estimated through the numerical procedure described in the following subsections and compared to market data in Section 5.3.

5.3 Empirical results

In order to test the performance of the methodology herein proposed, some empirical investigations have been done using two data samples of the dataset reported in Table A.2. We started to examine a market data sample from Dataset II. We considered a sample consisting of $n = 308$ weekly observed market interest rates on derivatives with maturity $T = 30Y$. Figure 5-1 shows that the observed interest rates are all positive with near-to-zero values in the tail (green line).

We begin to estimate the expected interest rates from the Vasicek and CIR models. To calibrate the parameter vector (k, θ, σ) in both models to the market data, we applied the optimal estimating function method mentioned in Section 5.2.3. Notice that for the CIR model, we first shifted the whole data sample away from zero by formula (5.2). Then the optimal parameter estimates have been used to calculate the estimated expected interest rates, say $(\hat{r}_{exp}(t))_{t \geq 0}$, by formula (5.5). The initial value

has been set equal to the first value in the observed data sample. Table 5.2 lists the parameter estimates $(\hat{k}_n, \hat{\theta}_n, \hat{\sigma}_n)$ and the corresponding RMSE ε for both models. In Figure 5-1 the original market data sample with the corresponding sequence of the estimated expected CIR/Vasicek interest rates are compared.

Table 5.2: Optimal parameter estimates and the corresponding RMSE ε for the Vasicek and CIR model. Data sample: $n = 68$ monthly observed interest rates with maturity $T = 30Y$ from Dataset II in Table A.2.

Parameter Estimates		
	Vasicek	CIR
\hat{k}_n	0.0087	0.0094
$\hat{\theta}_n$	5.1470	5.2037
$\hat{\sigma}_n$	0.0918	0.0379
ε	0.4411	0.4324

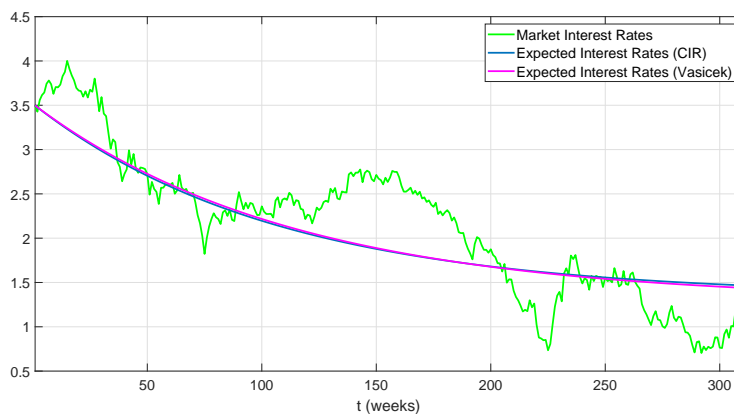


Figure 5-1: Estimated expected interest rates: CIR model (blue line) and Vasicek model (magenta line) versus $n = 308$ weekly observed EUR interest rates (green line) with maturity $T = 30Y$ from Dataset II in Table A.2.

To improve the results shown in Figure 5-1 in terms of fitting closely the market data, we implemented a numerical algorithm based on the following main steps

summarizing the model described in Sections 5.2.1-5.2.3 :

1. Shifting each sub-group to positive values by using the translation formula (5.2) (if needed);
2. Partitioning the whole sample into m Normal/non-central Chi-square distributed sub-groups;
3. Applying the Johnson's transformation (only in the case of normally distributed sub-samples);
4. Calibrating the parameters of the CIR/Vasicek interest rate process r to each sub-group by applying the optimal estimating function method described in Section 5.2.3;
5. Generating a sequence of estimated expected CIR/Vasicek interest rates by using the closed formula (5.5) for each sub-group.

Again, we considered the above mentioned weekly observed data sample on derivatives with long-term maturity ($T=30Y$). From Step 2 we obtained a partition of the sample into $m = 8$ normally distributed sub-groups (see Table 5.3), and into $m = 42$ sub-groups with non-central Chi-square distribution (see Table 5.4). Note that the values r_{308} , in the first case, and (r_{307}, r_{308}) , in the second case, were left out the partitioning. We then applied Steps 3-5 to each sub-group for both the partitions. Tables 5.3 and 5.4 list the RMSE computed for each sub-group, namely ε_k , with $k = 1, \dots, m$, and the total RMSE, say $\tilde{\varepsilon}$, computed over the whole sample as a weighted mean of the ε_k , that is

$$\tilde{\varepsilon} = \sqrt{\sum_{k=1}^m \frac{n_k}{n} \sum_{h=1}^{n_k} e_h^2}. \quad (5.7)$$

Table 5.3: Partition by a Normal distribution: error analysis of a sample of $n = 308$ weekly EUR interest rates with maturity $T = 30Y$ from the Dataset II in Table A.2.

	Normal distribution				
Sub-group	(r_1, \dots, r_{33})	(r_{34}, \dots, r_{49})	(r_{50}, \dots, r_{72})	(r_{73}, \dots, r_{202})	$(r_{203}, \dots, r_{245})$
ε_k	0.1686	0.1181	0.0916	0.2538	0.2879
Sub-group	$(r_{246}, \dots, r_{250})$	$(r_{251}, \dots, r_{267})$	$(r_{268}, \dots, r_{307})$		
ε_k	0.0575	0.1182	0.1355		
$\tilde{\varepsilon}$	0.8663				

Figures 5-2 and 5-3 below compare the plots of the estimated expected interest rates with the original market data sample. From them a better fitting to the market data is evident when we considered partitioning data through non-central Chi-square distributed sub-samples.

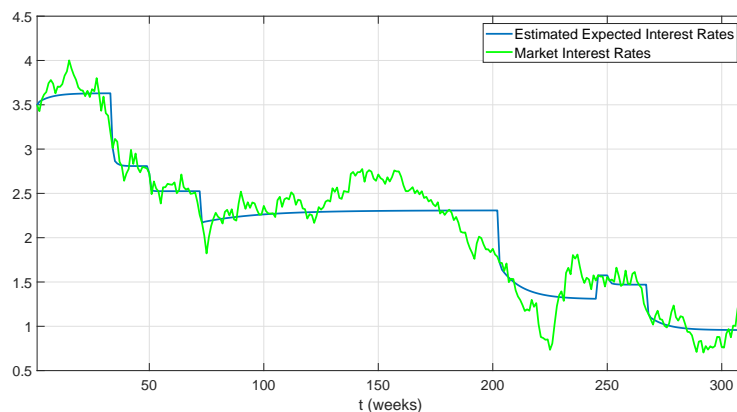


Figure 5-2: Estimated expected interest rates (blue line) versus market rates (green line) after segmentation with the Normal distribution for a data sample of $n = 308$ weekly EUR interest rates with maturity $T = 30Y$ from Dataset II in Table A.2.

Table 5.4: Partition by a non-central Chi-square distribution: error analysis of a sample of $n = 308$ weekly EUR interest rates with maturity $T = 30Y$ from Dataset II in Table A.2.

	Non-central Chi-square distribution				
Sub-group ε_k	(r_1, \dots, r_8) 0.0731	(r_9, \dots, r_{16}) 0.0701	(r_{17}, \dots, r_{23}) 0.0372	(r_{24}, \dots, r_{31}) 0.1208	(r_{32}, \dots, r_{40}) 0.1267
Sub-group ε_k	(r_{41}, \dots, r_{47}) 0.1079	(r_{48}, \dots, r_{55}) 0.1024	(r_{56}, \dots, r_{62}) 0.0396	(r_{63}, \dots, r_{69}) 0.0675	(r_{70}, \dots, r_{77}) 0.1241
Sub-group ε_k	(r_{78}, \dots, r_{84}) 0.0483	(r_{85}, \dots, r_{91}) 0.1045	(r_{92}, \dots, r_{98}) 0.0473	(r_{99}, \dots, r_{105}) 0.0415	$(r_{106}, \dots, r_{112})$ 0.0474
Sub-group ε_k	$(r_{113}, \dots, r_{119})$ 0.0671	$(r_{120}, \dots, r_{126})$ 0.0586	$(r_{127}, \dots, r_{133})$ 0.0579	$(r_{134}, \dots, r_{140})$ 0.0782	$(r_{141}, \dots, r_{147})$ 0.0439
Sub-group ε_k	$(r_{148}, \dots, r_{154})$ 0.0311	$(r_{155}, \dots, r_{161})$ 0.0557	$(r_{162}, \dots, r_{168})$ 0.0250	$(r_{169}, \dots, r_{175})$ 0.0312	$(r_{176}, \dots, r_{182})$ 0.1061
Sub-group ε_k	$(r_{183}, \dots, r_{189})$ 0.0767	$(r_{190}, \dots, r_{196})$ 0.0806	$(r_{197}, \dots, r_{203})$ 0.0820	$(r_{204}, \dots, r_{211})$ 0.0942	$(r_{212}, \dots, r_{218})$ 0.0848
Sub-group ε_k	$(r_{219}, \dots, r_{225})$ 0.0652	$(r_{226}, \dots, r_{235})$ 0.1457	$(r_{236}, \dots, r_{242})$ 0.0751	$(r_{243}, \dots, r_{249})$ 0.1203	$(r_{250}, \dots, r_{256})$ 0.0623
Sub-group ε_k	$(r_{257}, \dots, r_{263})$ 0.0886	$(r_{264}, \dots, r_{271})$ 0.0722	$(r_{272}, \dots, r_{278})$ 0.0524	$(r_{279}, \dots, r_{285})$ 0.0588	$(r_{286}, \dots, r_{292})$ 0.0626
Sub-group ε_k	$(r_{293}, \dots, r_{299})$ 0.0519	$(r_{300}, \dots, r_{306})$ 0.0700			
$\tilde{\varepsilon}$	0.0339				

The second tested data sample consists of $n = 308$ weekly EUR interest rates in a money market, on derivatives with maturity $T = 30/360A$ from Dataset I in Table A.2. From Step 2 of the above described numerical procedure, the entire sample has been partitioned into $m = 23$ normally distributed sub-groups (see Table 5.5) and into $m = 59$ non-central Chi-square distributed sub-groups (see Table 5.6). In this case, the observations $(r_{304}, r_{305}, r_{306}, r_{307}, r_{308})$ and r_{308} , respectively, were left out of the partitioning. The results listed in Tables 5.5 and 5.6 as well as the plots in

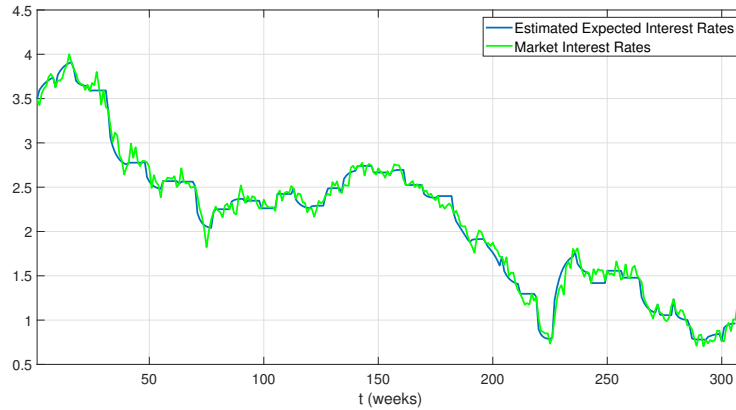


Figure 5-3: Estimated expected interest rates (blue line) versus market rates (green line) after segmentation with non-central Chi-square distribution for a data sample of $n = 308$ weekly EUR interest rates with maturity $T = 30Y$ from Dataset II in Table A.2.

Figures 5-4 and 5-5, show, also in this case, a better fitting to the observed money market interest rates when a partitioning into non-central Chi-square distributed sub-samples was considered.

Table 5.5: Partition by a Normal distribution: error analysis of a sample of $n = 308$ weekly EUR interest rates with maturity $T = 30/360A$ from Dataset I in Table A.2.

	Normal distribution				
Sub-group ε_k	(r_1, \dots, r_{10}) 0.0435	(r_{11}, \dots, r_{23}) 0.0933	(r_{24}, \dots, r_{38}) 0.0470	(r_{39}, \dots, r_{44}) 0.0028	(r_{45}, \dots, r_{73}) 0.2238
Sub-group ε_k	(r_{74}, \dots, r_{79}) 0.0038	(r_{80}, \dots, r_{89}) 0.0220	(r_{90}, \dots, r_{104}) 0.0019	$(r_{105}, \dots, r_{118})$ 0.0029	$(r_{119}, \dots, r_{126})$ 0.0016
Sub-group ε_k	$(r_{127}, \dots, r_{141})$ 0.0032	$(r_{142}, \dots, r_{146})$ 0.0007	$(r_{147}, \dots, r_{152})$ 0.0039	$(r_{153}, \dots, r_{163})$ 0.0143	$(r_{164}, \dots, r_{181})$ 0.0299
Sub-group ε_k	$(r_{182}, \dots, r_{192})$ 0.0097	$(r_{193}, \dots, r_{197})$ 0.0107	$(r_{198}, \dots, r_{225})$ 0.0143	$(r_{226}, \dots, r_{264})$ 0.0488	$(r_{265}, \dots, r_{279})$ 0.0315
Sub-group ε_k	$(r_{280}, \dots, r_{284})$ 0.0008	$(r_{285}, \dots, r_{298})$ 0.0031	$(r_{299}, \dots, r_{303})$ 0.0004		
$\tilde{\varepsilon}$	0.1700				

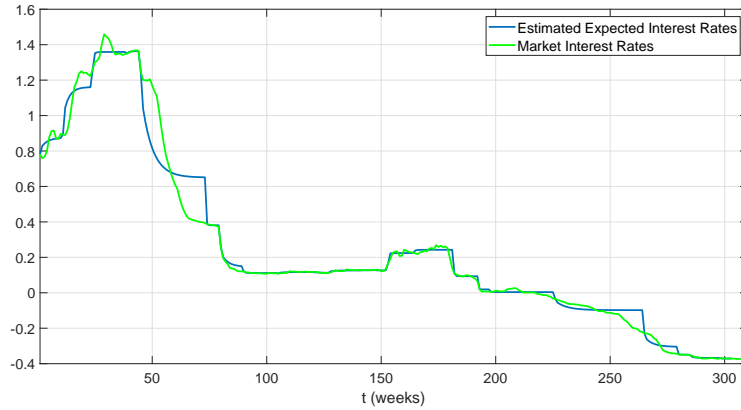


Figure 5-4: Estimated expected interest rates (blue line) versus market rates (green line) after segmentation with Normal distribution for a data sample of $n = 308$ weekly EUR interest rates with maturity $T = 30/360A$ from Dataset I in Table A.2.

Table 5.6: Partition by a non-central Chi-square distribution: error analysis of a sample of $n = 308$ weekly EUR interest rates with maturity $T = 30/360A$ from Dataset I in Table A.2.

	Non-central Chi-square distribution				
Sub-group ε_k	(r_1, \dots, r_6) 0.0886	(r_7, \dots, r_{11}) 0.0326	(r_{12}, \dots, r_{18}) 0.0586	(r_{19}, \dots, r_{24}) 0.0149	(r_{25}, \dots, r_{30}) 0.0382
Sub-group ε_k	(r_{31}, \dots, r_{36}) 0.0148	(r_{37}, \dots, r_{42}) 0.0046	(r_{43}, \dots, r_{48}) 0.0435	(r_{49}, \dots, r_{55}) 0.0854	(r_{56}, \dots, r_{61}) 0.0306
Sub-group ε_k	(r_{62}, \dots, r_{66}) 0.0195	(r_{67}, \dots, r_{71}) 0.0033	(r_{72}, \dots, r_{76}) 0.0029	(r_{77}, \dots, r_{82}) 0.0620	(r_{83}, \dots, r_{87}) 0.0052
Sub-group ε_k	(r_{88}, \dots, r_{92}) 0.0021	(r_{93}, \dots, r_{97}) 0.0003	(r_{98}, \dots, r_{102}) 0.0021	$(r_{103}, \dots, r_{107})$ 0.0006	$(r_{108}, \dots, r_{112})$ 0.0028
Sub-group ε_k	$(r_{113}, \dots, r_{117})$ 0.0011	$(r_{118}, \dots, r_{122})$ 0.0007	$(r_{123}, \dots, r_{127})$ 0.0007	$(r_{128}, \dots, r_{132})$ 0.0020	$(r_{133}, \dots, r_{137})$ 0.0028
Sub-group ε_k	$(r_{138}, \dots, r_{142})$ 0.0008	$(r_{143}, \dots, r_{147})$ 0.0004	$(r_{148}, \dots, r_{152})$ 0.0049	$(r_{153}, \dots, r_{157})$ 0.0122	$(r_{158}, \dots, r_{162})$ 0.0115
Sub-group ε_k	$(r_{163}, \dots, r_{167})$ 0.0059	$(r_{168}, \dots, r_{172})$ 0.0069	$(r_{173}, \dots, r_{177})$ 0.0154	$(r_{178}, \dots, r_{182})$ 0.0436	$(r_{183}, \dots, r_{187})$ 0.0056
Sub-group ε_k	$(r_{188}, \dots, r_{192})$ 0.0116	$(r_{193}, \dots, r_{197})$ 0.0107	$(r_{198}, \dots, r_{202})$ 0.0019	$(r_{203}, \dots, r_{207})$ 0.0040	$(r_{208}, \dots, r_{212})$ 0.0076
Sub-group ε_k	$(r_{213}, \dots, r_{217})$ 0.0004	$(r_{218}, \dots, r_{222})$ 0.0017	$(r_{223}, \dots, r_{227})$ 0.0050	$(r_{228}, \dots, r_{232})$ 0.0042	$(r_{233}, \dots, r_{237})$ 0.0053
Sub-group ε_k	$(r_{238}, \dots, r_{242})$ 0.0047	$(r_{243}, \dots, r_{247})$ 0.0019	$(r_{248}, \dots, r_{252})$ 0.0027	$(r_{253}, \dots, r_{257})$ 0.0108	$(r_{258}, \dots, r_{262})$ 0.0046
Sub-group ε_k	$(r_{263}, \dots, r_{267})$ 0.0038	$(r_{268}, \dots, r_{272})$ 0.0163	$(r_{273}, \dots, r_{277})$ 0.0031	$(r_{278}, \dots, r_{282})$ 0.0014	$(r_{283}, \dots, r_{287})$ 0.0043
Sub-group ε_k	$(r_{288}, \dots, r_{292})$ 0.0013	$(r_{293}, \dots, r_{297})$ 0.0020	$(r_{298}, \dots, r_{302})$ 0.0016	$(r_{303}, \dots, r_{307})$ 0.0006	
$\tilde{\varepsilon}$	0.0323				

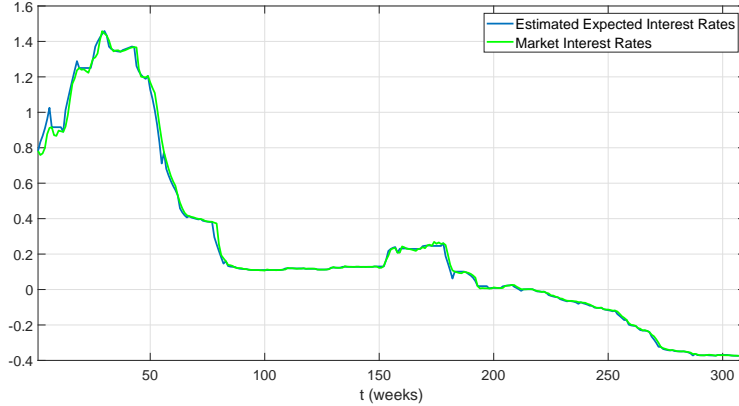


Figure 5-5: Estimated expected interest rates (blue line) vs market rates (green line) after segmentation with non-central Chi-square distribution for a data sample of $n = 308$ weekly EUR interest rates with maturity $T = 30/360A$ from Dataset I in Table A.2.

5.3.1 Forecasting expected interest rates

In this section we apply the proposed numerical procedure to forecast future expected values of market interest rates. We first consider a window of fixed size m of market interest rates that is rolled through time, each time adding a new rate and taking off the oldest one. The length of this window is the historical period over which we forecast the next expected spot rate value. It is worth noting that in case of large datasets, as with weekly observations, the methodology herein proposed necessarily requires that rolling windows of variable size should be used. Thus, the step of the procedure relative to the dataset partition, described in Sections 5.2.1, is modified as follows. Fixed the initial length m of the historical data sample, say $(r_{1+h}, \dots, r_{m+h})$, $h = 0, 1, 2, \dots$, the Lilliefors or the Kolmogorov-Smirnov test is carried out starting from the last observed rate r_{m+h} and then moving backward in the sample up to detect the smaller interest rate value r_{m+h-s} ($s = 1, \dots, m - 1$), such that the sub-goup $(r_{m+h-s}, \dots, r_{m+h})$ has Normal or non-central Chi-square distribu-

tion. The value r_{m+h-s} denotes the *change point* setting the window of latest interest rates, say $(r_{m+h-s}, \dots, r_{m+h})$, which is taken into account to calibrate the parameters of the Vasicek/CIR model and forecast the next expected interest rate value r_{m+h+1} (the past interest rate values $(r_{1+h}, \dots, r_{m+h-s-1})$ are disregarded). Clearly, when the historical period is rolled through time, the size of the window over which to forecast a future rate may be variable since it depends on the detected change point.

We applied the modified numerical procedure to forecast expected future next-week interest rates. To explain our idea we refer to the first data sample considered in the previous section ($n = 308$ weekly observed EUR interest rates with maturity $T = 30Y$). The initial size of the historical data sample was fixed to $m = 52$ weeks. Steps 1-5 of the numerical procedure were applied to the historical market interest rates. Note that the calibration of the Vasicek/CIR model parameters with sub-groups of size smaller than 12 is not always possible when the optimal estimating function method mentioned in Section 5.2.3 is applied (see Remark 5.1). In this case two adjacent sub-groups are joined together. The sequence of forecast next-week expected values computed by formula (5.5) for both Vasicek and CIR models, has been compared with the sequence of future rates computed by the Exponentially Weighted Moving Average (EWMA) by considering a rolling window of fixed size $m = 52$ weeks. The EWMA is a weighting scheme to estimate future values averaging on historical data with weights that decrease exponentially at a rate λ throughout as the observations are far in the past (the reader can refer, for example, to Hull (Hull, 2012, Ch.II). The EWMA has been shown to be powerful for prediction over a short horizon and track closely the volatility as it changes. Indeed recent interest rates movement is the best predictor of future movement as it is not conditioned on a mean level of volatility. The forecasted sequences are plotted in Figure 5-6. The proposed numerical procedure clearly shows a better performance with respect to

the EWMA model.

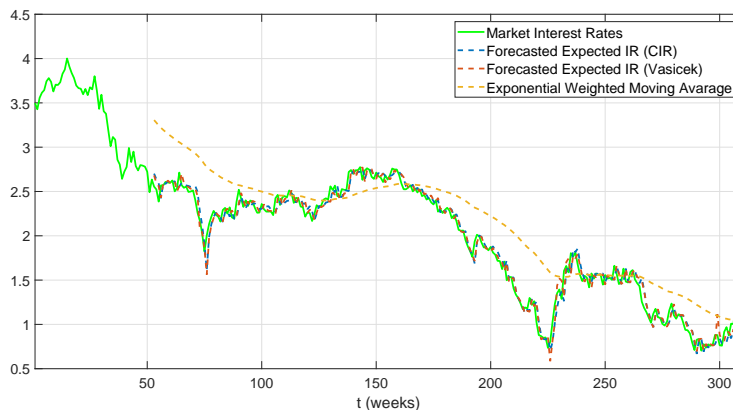


Figure 5-6: Forecast of expected next-week interest rates based on a rolling window of variable size: sequence of $n = 308$ weekly EUR interest rates with maturity $T=30Y$ (green line); CIR forecasted expected interest rates (blue dashed line); Vasicek forecasted expected interest rates (red dashed line); EWMA predicted values (yellow dashed line).

Moreover, an error analysis to all data samples (63 maturities) available from Dataset I and II in Table A.2 has been carried out. Figure 5-7 compares the corresponding RMSE values computed by applying our numerical algorithm to the Vasicek and CIR model with the ones computed by the EWMA model. The initial size of the historical data sample was fixed to $m = 52$ weeks (the vertical black line differentiates samples of Dataset I from samples of Dataset II). In this case, too, a better performance of our procedure with respect to the EWMA model is confirmed. Further, the modified procedure to make predictions based on rolling windows of variable size highlights an improvement in forecast when a partition with non-central Chi-square distribution (CIR model) is considered.

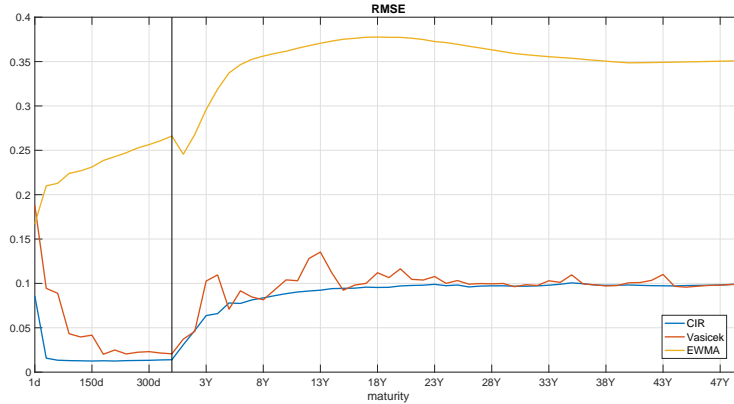


Figure 5-7: Error analysis in the forecast procedure of future next-week expected interest rates across 63 maturities. RMSE values computed by the proposed numerical procedure based on a rolling window of variable size: CIR model (blu line), Vasicek model (red line). RMSE values computed by the EWMA model (yellow line) based on a rolling window of fixed size $m = 52$ weeks. The vertical black line differentiates samples of Dataset I from samples of Dataset II in Table A.2.

5.4 Conclusions

In this Chapter, we have presented a new methodology for using both the Vasicek and the CIR model in order to forecast interest rates that works even when interest rates are negative. To achieve that objective, we have proposed a numerical procedure partitioning the selected data sample according to the best fitting of a Normal or a non-central Chi-square distribution. These distributions were chosen by analogy with the steady (resp. conditional) distribution of the interest rate process in the Vasicek (resp. CIR) model. Where the first was taken when the steady distribution of the interest rate process is modelled with Vasicek and the second when the conditional distribution of the said process is represented by the CIR model. After having partitioned the sample of observed market data, the Vasicek/CIR model's parameters are calibrated to each sub-sample of market spot rates and the corresponding

expected interest rates are estimated by the conditional expectation closed formula of both models. We have, also, included in the procedure a step concerning an appropriate translation of market interest rates to positive values in order to overcome the issue of negative/near-to-zero values which are not compatible with the CIR model. Finally, we have analyzed the empirical performance of the proposed methodology for two different weekly recorded EUR data samples in a money market and a long-term dataset, respectively. Better results are shown in terms of the RMSE when a segmentation of the data sample in non-central Chi-square distributed sub-samples is considered. After assessing the accuracy of our procedure, we have applied the implemented algorithm to forecast future expected interest rates over rolling windows of historical data with variable size. The performance of the new approach, tested on weekly rates with different maturities, has been carried out for both Vasicek and CIR model, and compared with the EWMA model in terms of forecasting error. The error analysis highlighted a better performance of the proposed procedure with respect to EWMA model and better results in prediction when a partition of the historical data sample in non-central Chi-square distributed sub-samples (CIR model) is considered.

In next Chapter 6 we will present our findings of the CIR# by considering a dataset composed of money market interest rates during turmoil and calmer periods, we show how the CIR# performs in terms of directionality of rates and forecasting error. Testing and validation is performed on *had hoc* data with different metrics and clustering criteria to confirm the analysis.

Chapter 6

The CIR# model: real data versus test data

6.1 Introduction

This Chapter expands on previous research [122, 123, 124] where we have provided a new accessible methodology to forecast future interest rates that we have called CIR#. In this introduction we are not going to mention all details of the CIR# model but we will recall the most important characteristics. Above all we mention that, in order to preserve its analytical tractability and simplicity of single-factor model, the CIR# has been designed in a way that the improvements are obtained within the original CIR framework. Apart from turning a short rate model model used for pricing into a forecasting tool, the novelty consists in an appropriate partitioning of the dataset into sub-groups. Besides the papers already mentioned [122, 123, 124], in Orlando et al. [125], we have shown that an appropriate partitioning of data enables us to capture statistically significant time changes in volatility of interest

rates. This, in turn, implies modelling sudden changes/jumps in data. To solve the issue of negative/near-to-zero interest rates, as others did [25], we contemplate an opportune shift of interest rates to positive values. Another feature of the CIR# model is the calibration of parameters to actual data. With regard to the latter, in our framework the random part of the numerical simulation scheme is driven not by a standard Brownian motion but by the Gaussian residuals of an “optimal” ARIMA model appropriately chosen. Thanks to that we get an exact trajectory of CIR fitted values which replaces the usual Monte Carlo averaged over 100,000 simulated trajectories, thus reducing considerably the computational cost of the estimating procedure.

For the reasons above-mentioned we are not considering other models available in literature for the simple reason that they belong to different classes (e.g. multi-factor models). In this Chapter we compare the CIR# model versus real data, the EWMA and an improved version traditional CIR model that we call CIR_{adj}. To level the playing field, the latter comparison is performed by using the same data (in terms of shifting and partitioning). The performance of both models has been tested on monthly money market interest rates ranging from 1 day to 12 months over EUR, USD, JPY and CHF currencies. The dataset includes both turmoil and calm periods on which we compute the predictive power in terms of directionality of rates and error.

The remainder of the Chapter is organized as follows. Section 6.2 presents the numerical procedure in full detail and tests the goodness-of-fit of the new methodology to real market data. Section 6.3 describes how forecasts can be tested and validated. Finally, Section 6.4 concludes.

6.2 Results

In this section firstly we are going to show the results over the full dataset reported in Appendix A.2 and, secondly, we will focus on turbulent periods where volatility is above the median.

6.2.1 Forecasting accuracy

In order to check whether our forecasts are closely matching the data, we use a measure of the amplitude of the error and an indicator of the direction of the interest rate dynamics. The first is quantified by the root mean squared error (RMSE) and its related normalized version (NRMSE), while the second is given by the so-called directional “success” criterion.

Root mean square error

The root mean squared error (RMSE) is a measure of the closeness between the observed data and the predicted values from a given model. Hence, it represents the accuracy of the model in terms of goodness of fit. It is defined as follows

$$RMSE = \sqrt{\frac{1}{n} \sum_{h=1}^n e_h^2}, \quad (6.1)$$

where e_h denote the residuals between the observed data and their predictions, over n times. Hence, a value of 0 (almost never achieved in practice) indicates a perfect fit to the data, and a value lower than 1 represents a good result. We note that the RMSE depends on the scale of observed data, thus it is sensitive to the outliers; however, larger errors have a disproportionately large effect. For that reason, and

to facilitate the comparison between data, we adopt the so-called normalized root mean squared error (NRMSE):

$$NRMSE = \frac{RMSE}{r_{\max} - r_{\min}}, \quad (6.2)$$

where r_{\max} denotes the maximum value and r_{\min} the minimum value of the observed sample data.

Directionality of forecasting

In order to understand whether the forecast predicts correctly a rise or a drop of interest rates, we introduce the index of directionality (IDX). Let us denote r_t as the interest rate at time t and the corresponding forecast as r_t^f . We define the variable $\alpha_{t+1} := r_{t+1} - r_t$ as the difference between two consecutive interest rates, and the variable $\beta_{t+1} := r_{t+1}^f - r_t$ as the difference between the forecast at time $t + 1$ and the actual interest rates at time t . Further, we consider the indicator variable $H(t + 1)$ assuming only the values 0, 1 as follows

$$\begin{cases} H(t + 1) = 1 & \text{if } \text{sgn}(\alpha_{t+1}) = \text{sgn}(\beta_{t+1}) \\ H(t + 1) = 0 & \text{if } \text{sgn}(\alpha_{t+1}) \neq \text{sgn}(\beta_{t+1}). \end{cases}$$

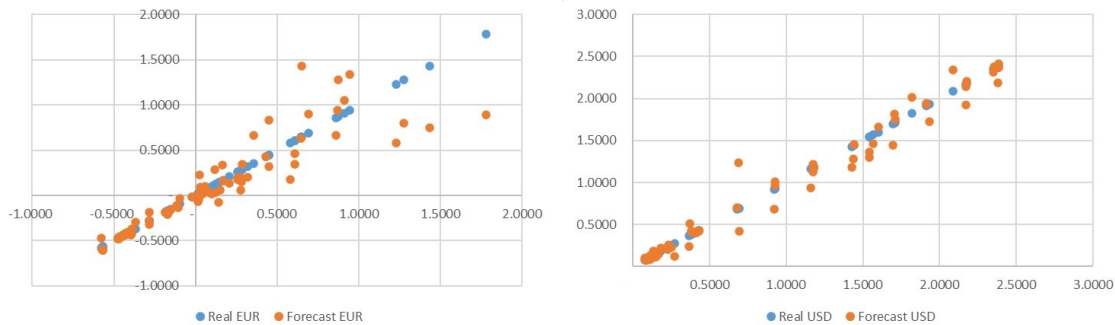
We attribute the term of forecast "success" (in sign) when $H(t + 1) = 1$. Therefore the index IDX is defined as an average of the $H(t + 1)$ values on the number of forecasts over a time series of length T that is,

$$IDX = \frac{1}{T - 1} \sum_{t=1}^{T-1} H(t + 1). \quad (6.3)$$

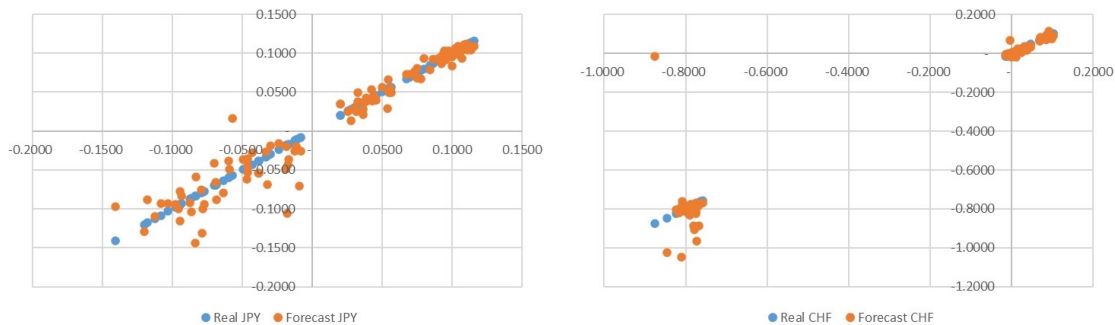
IDX indicates the percentage of correct predictions of interest rate directionality.

6.2.2 Forecasting results over the whole dataset

Let us start by plotting the performances versus the forecasts for all the four considered currencies. In Figure 6-1 we show that the forecasts closely follow the occurrences and they are not spread out.



(a) EUR overnight. Plot of the realized interest rate occurrence versus the forecasted value. (b) USD overnight. Plot of the realized interest rate occurrence versus the forecasted value.



(c) JPY overnight. Plot of the realized interest rate occurrence versus the forecasted value. (d) CHF overnight. Plot of the realized interest rate occurrence versus the forecasted value.

Figure 6-1: Multiple comparisons for the overnight interest rate occurrences across currencies versus their corresponding forecasts.

We supplement this visual analysis by considering the Bland–Altman plot (also called difference plot) which is a very popular tool in medicine and chemistry to analyse the agreement between two different methods [3], [18]. What inspired Bland and Altman was the need to know how much the outcomes of a method differ from another to be considered equivalent ¹. In our case, as the real data overlap with forecasts, we want to investigate the said agreement more clearly. Figure 6-2 [137] shows the agreement between real data and forecasts. Based on this analysis it is possible to confirm the good agreement between data and forecasts as the maximum number of outliers is 0.885% (=9/113).

After having concluded the graphical analysis, we introduce the results based on the more traditional analysis consisting of the results obtained with the Normalized Root Mean Square Error (NRMSE). In Tables 6.2, 6.3, 6.4 we compare the forecasting error (NRMSE) and the directionality of forecasting (IDX) for the EWMA, CIR_{adj}, CIR#. We have included the EWMA because it is a basic version of the Autoregressive Conditional Heteroscedasticity (ARCH) model, which is a common tool for forecasting time-varying financial data and a simple benchmark whenever no structure in data is assumed. The results show that, generally, the CIR# performs better over the whole dataset.

¹In this instance we prefer the Bland-Altman plot to the well-known Tukey mean difference for a number of reasons: **a)** The first is based on the data while the second is based on its quantiles; **b)** In our case we have paired data as assumed by the Bland-Altman plot, the Tukey mean difference plot, instead, applies to either paired or unpaired data; **c)** While the Tukey mean difference plot answers the question of whether the variables have the same underlying distribution, the Bland-Altman answers the question on the differences between the pairs (which is more relevant as we want to know whether there is a systematic bias between real data and CIR# forecasts)

Table 6.1: Averaged NRMSE and IDX for the dataset in Table A.3.

	EUR			USD			JPY		
	CIR#	CIR _{adj}	EWMA	CIR#	CIR _{adj}	EWMA	CIR#	CIR _{adj}	EWMA
NRMSE	3.47%	5.57%	11.41%	9.15%	13.60%	14.86%	5.31%	10.56%	9.41%
IDX	71.11%	65.60%	28.85%	62.77%	63.93%	38.55%	75.62%	70.39%	41.54%

Table 6.2: Averaged NRMSE and IDX for the dataset in Table A.3.

	EUR			USD			JPY			CHF		
	CIR#	CIR _{adj}	EWMA	CIR#	CIR _{adj}	EWMA	CIR#	CIR _{adj}	EWMA	CIR#	CIR _{adj}	EWMA
	Averages											
NRMSE	3.47%	5.57%	11.41%	9.15%	13.60%	14.86%	5.31%	10.56%	9.41%	8.26%	24.06%	11.54%
IDX	71.11%	65.60%	28.85%	62.77%	63.93%	38.55%	75.62%	70.39%	41.54%	53.38%	63.12%	57.51%

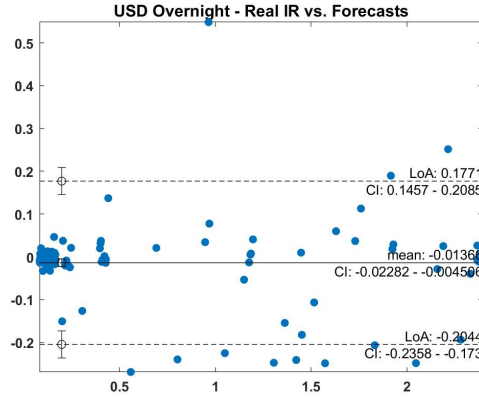
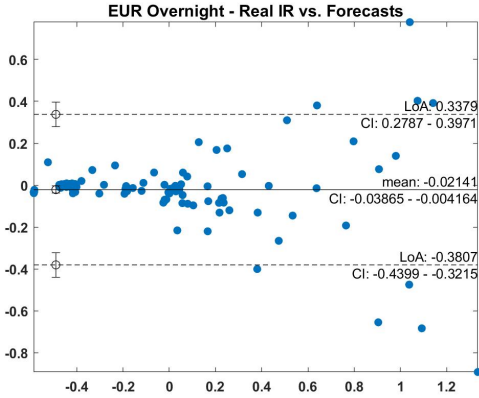
Results averaged over the six maturities .

Table 6.3: NRMSE for different models, tenors and currencies

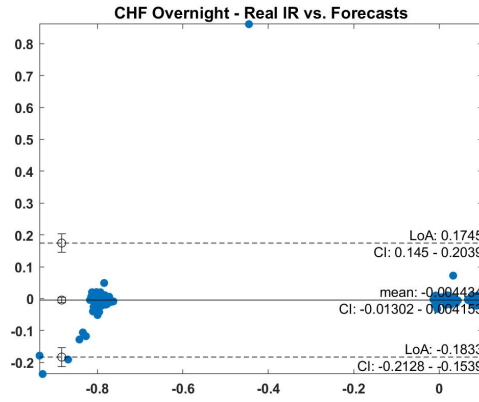
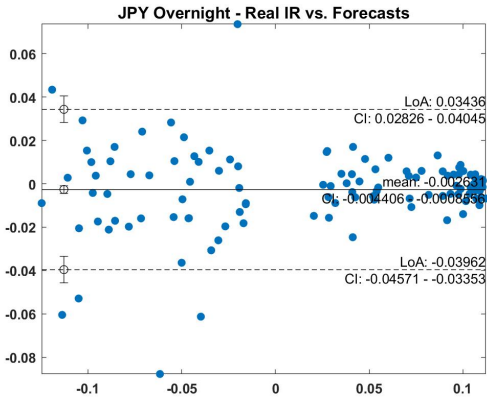
	EUR					
	EE000/N	EE0001M	EE0002M	EE0003M	EE0006M	EE0012M
CIR #	5.14%	3.63%	3.56%	3.05%	2.71%	2.77%
CIR_{adj}	10.94%	5.39%	4.87%	4.39%	4.18%	3.64%
EWMA	11.54%	11.77%	11.61%	11.50%	11.11%	10.95%
	USD					
	US000/N	US0001M	US0002M	US0003M	US0006M	US0012M
CIR#	7.88%	8.71%	8.53%	14.06%	7.83%	7.90%
CIR_{adj}	10.98%	28.15%	16.48%	10.98%	7.60%	7.75%
EWMA	15.69%	14.85%	15.07%	15.69%	14.32%	13.55%
	JPY					
	JY00S/N	JY0001M	JY0002M	JY0003M	JY0006M	JY0012M
CIR#	8.66%	5.20%	5.37%	4.85%	3.92%	3.88%
CIR_{adj}	13.55%	11.65%	9.26%	16.64%	6.82%	5.47%
EWMA	9.46%	9.82%	9.91%	9.60%	9.11%	8.56%
	CHF					
	CH00S/N	CH0001M	CH0002M	CH0003M	CH0006M	CH0012M
CIR#	9.29%	9.19%	8.53%	8.51%	7.51%	6.56%
CIR_{adj}	8.96%	16.80%	14.15%	12.59%	65.21%	26.73%
EWMA	12.47%	12.23%	12.11%	12.00%	10.95%	9.52%

Table 6.4: IDX for different models, tenors and currencies

	EUR					
	EE00O/N	EE0001M	EE0002M	EE0003M	EE0006M	EE0012M
CIR #	66.67%	71.67%	75.00%	75.00%	68.33%	70.00%
CIR_{adj}	53.73%	68.65%	65.67%	68.65%	65.67%	71.64%
EWMA	38.80%	28.35%	25.37%	29.85%	25.37%	25.37%
	USD					
	US00O/N	US0001M	US0002M	US0003M	US0006M	US0012M
CIR #	60.00%	58.33%	58.33%	66.67%	60.00%	73.33%
CIR_{adj}	73.13%	49.25%	50.74%	73.13%	71.64%	65.67%
EWMA	47.76%	40.29%	32.83%	47.76%	26.86%	35.82%
	JPY					
	JY00S/N	JY0001M	JY0002M	JY0003M	JY0006M	JY0012M
CIR #	67.16%	71.64%	74.62%	70.14%	86.56%	83.58%
CIR_{adj}	64.17%	77.61%	65.67%	65.67%	77.61%	71.64%
EWMA	56.71%	38.80%	47.76%	47.76%	26.86%	31.34%
	CHF					
	CH00S/N	CH0001M	JY0002M	CH0003M	CH0006M	CH0012M
CIR #	53.09%	53.09%	57.52%	52.21%	51.32%	53.09%
CIR_{adj}	69.02%	66.37%	61.06%	67.25%	59.29%	55.75%
EWMA	61.06%	56.63%	61.06%	61.06%	52.21%	53.09%



(a) EUR overnight. Over 113 data points outliers are 9 (out of which only 5 outside LoA confidence level). (b) USD overnight. Over 113 data points outliers are 9 (out of which only 6 outside LoA confidence level).



(c) JPY overnight. Over 113 data points outliers are 5 (all of them outside LoA confidence level). (d) CHF overnight. Over 113 data points outliers are 2 (none of them outside LoA confidence level).

Figure 6-2: Bland-Altman plot. Multiple comparisons for the overnight interest rates occurrences across currencies versus their corresponding forecasts. Maximum number of outliers are 0.885%.

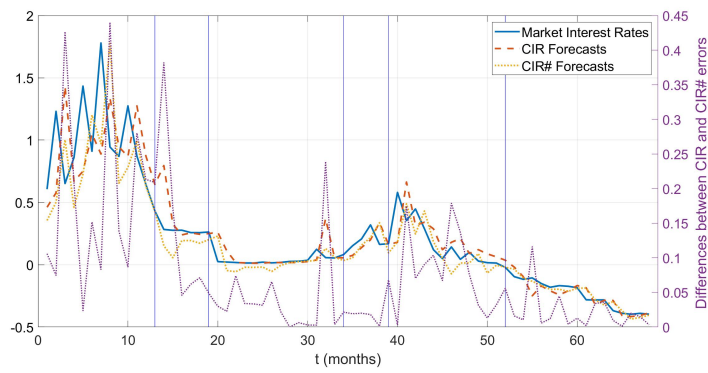
6.2.3 Forecasting results in turbulent periods

As mentioned, through our procedure we can identify clusters of volatility. In Section 6.2.2 we have shown the averaged performance over the whole dataset (Table 6.2) and for each currency (Tables 6.3, 6.4). In this Section we illustrate how the CIR# model

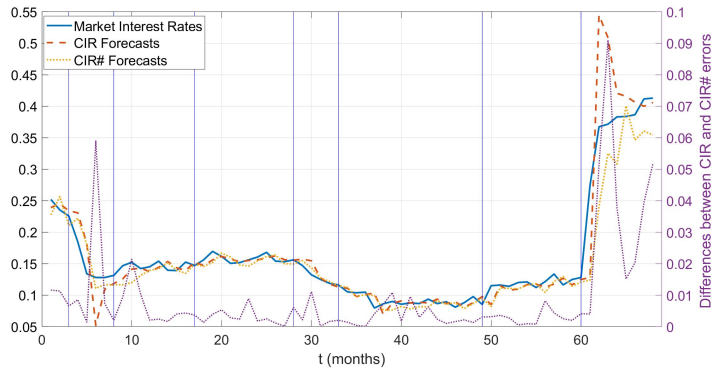
performs when volatility is high and forecasts are more challenging. This corresponds to considering the overnight (as it is the most exposed to market sentiment), which we have partitioned into clusters of volatility. Then, for each currency, we have selected the two clusters with higher volatility. Table 6.5 compares the forecasting error and the index of directionality for the EWMA, CIR_{adj} , $CIR_{\#}$. Note that the volatility ratio shows the volatility of the cluster over the median volatility recorded on the whole dataset for the selected currency. As displayed the $CIR_{\#}$ performs better in any situation. To understand how the $CIR_{\#}$ fits the overnight, for each currency, in Fig. 6-3 we display the evolution of market interest rates, the partitioning into clusters (vertical bars) and the CIR_{adj} taken as a benchmark. The difference in absolute value between the prediction errors of $CIR_{\#}$ and CIR_{adj} is also shown.

Table 6.5: NRMSE and IDX in turbulent periods for the $CIR_{\#}$, CIR_{adj} and EWMA over overnight maturities and different currencies

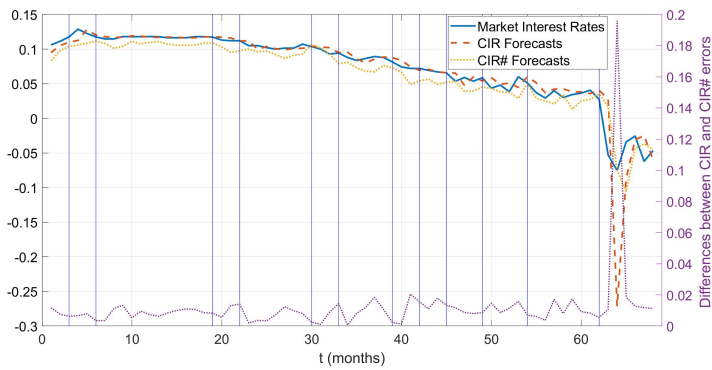
	EUR		USD		JPY		CHF	
Cluster	1-13	39-52	3-8	28-33	49-54	62-68	12-19	29-60
Volatility ratio	7.63%	18.33%	4.07%	1.60%	0.83%	3.35%	3.5%	23.63%
	10.00%	10.00%	1.26%	1.26%	0.49%	0.49%	1.22%	1.22%
NRMSE $CIR_{\#}$	72.70%	24.80%	27.90%	16.10%	50.00%	38.46%	54.31%	16.73%
NRMSE CIR_{adj}	72.70%	26.50%	43.50%	25.50%	67.10%	81.00%	67.46%	27.80%
NRMSE EWMA	54.50%	27.32%	61.40%	49.2%	56.30%	52.80%	98.12%	26.78%
IDX $CIR_{\#}$	36.30%	76.9%	100.00%	100.00%	80.00%	83.30%	66.67%	66.57%
IDX CIR_{adj}	35.30%	53.84%	80.00%	80.00%	60.00%	83.30%	66.65%	64.28%
IDX EWMA	36.60%	30.70%	40.00%	20.00%	60.00%	66.66%	64.28%	51.42%



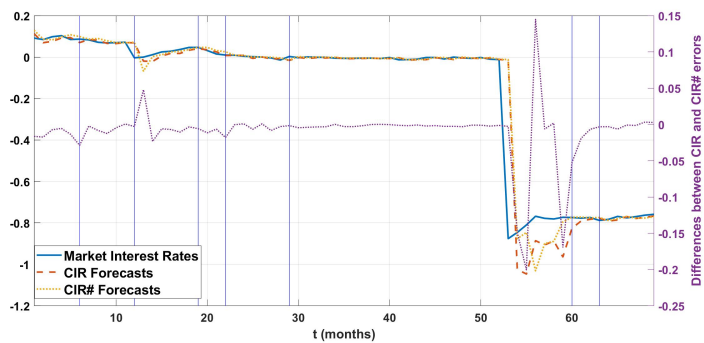
(a) EUR overnight. On the left y-axis EUR interest rates. On the right y-axis the difference in absolute value between the prediction errors of CIR_{adj} and $CIR\#$.



(b) USD overnight. On the left y-axis USD interest rates. On the right y-axis the difference in absolute value between the prediction errors of CIR_{adj} and $CIR\#$.



(c) JPY overnight. On the left y-axis JPY interest rates. On the right y-axis the difference in absolute value between the prediction errors of CIR_{adj} and $CIR\#$.



(d) CHF overnight. On the left y-axis CHF interest rates. On the right y-axis the difference in absolute value between the prediction errors of CIR_{adj} and $CIR\#$.

Figure 6-3: Multiple comparisons for the overnight interest rates across currencies. Vertical lines identify cluster of volatilities partitioning the sample data in subgroups.

6.2.4 Correlations between forecasts and real data

In this Section, in Tables 6.6, 6.8, 6.10 and 6.12, we report the correlation results obtained with Kendall rank correlation ² between real data and forecasts. The alternative hypothesis, against which p-values are computed, is of no correlation (see Tables 6.7, 6.9, 6.11 and 6.13).

Notice that we obtained similar results with Spearman's rank correlation but for reason of space we do not report them.

Table 6.6: EUR Kendall correlations

		Real time series					
		EUR1	EUR2	EUR3	EUR4	EUR5	EUR6
Forecasts	ForEUR1	0.898198	0.864369	0.840025	0.828644	0.847929	0.847613
	ForEUR2	0.876561	0.888257	0.881618	0.882883	0.889521	0.884780
	ForEUR3	0.830896	0.862203	0.915962	0.925449	0.914064	0.910902
	ForEUR4	0.812871	0.844494	0.909321	0.927979	0.912167	0.908689
	ForEUR5	0.840341	0.858046	0.887765	0.896617	0.932343	0.942144
	ForEUR6	0.816817	0.842105	0.885096	0.891102	0.930299	0.945788

Table 6.7: EUR Kendall p-values

		Real time series					
		EUR1	EUR2	EUR3	EUR4	EUR5	EUR6
Forecasts	ForEUR1	3.99E-45	6.41E-42	1.09E-39	1.15E-38	2.09E-40	2.24E-40
	ForEUR2	4.50E-43	3.49E-44	1.50E-43	1.13E-43	2.64E-44	7.49E-44
	ForEUR3	7.52E-39	1.06E-41	7.74E-47	8.92E-48	1.19E-46	2.43E-46
	ForEUR4	2.95E-37	4.48E-40	3.47E-46	5.00E-48	1.83E-46	4.00E-46
	ForEUR5	1.02E-39	2.47E-41	4.01E-44	5.67E-45	1.74E-48	1.79E-49
	ForEUR6	1.25E-37	6.90E-40	6.99E-44	1.86E-44	2.70E-48	7.41E-50

²The choice is because rank correlation assesses monotonic relationships, whilst Pearson's correlation is sensitive only to linear relationships.

Table 6.8: USD Kendall correlations

		Real time series					
		USD1	USD2	USD3	USD4	USD5	USD6
Forecasts	ForUSD1	0.888994	0.876977	0.832068	0.733397	0.807084	0.794434
	ForUSD2	0.870514	0.913202	0.886957	0.745613	0.859447	0.843320
	ForUSD3	0.835151	0.886992	0.915758	0.761814	0.891418	0.880354
	ForUSD4	0.797123	0.849917	0.893543	0.762981	0.901446	0.894491
	ForUSD5	0.797724	0.853034	0.892541	0.764855	0.916245	0.914981
	ForUSD6	0.787515	0.839984	0.879494	0.750849	0.909522	0.922797

Table 6.9: USD Kendall p-values

		Real time series					
		USD1	USD2	USD3	USD4	USD5	USD6
Forecasts	ForUSD1	3.24E-44	4.48E-43	5.98E-39	1.23E-30	9.54E-37	1.17E-35
	ForUSD2	1.76E-42	1.42E-46	4.93E-44	1.28E-31	1.89E-41	5.65E-40
	ForUSD3	2.93E-39	4.61E-44	7.50E-47	5.93E-33	1.74E-44	1.97E-43
	ForUSD4	6.51E-36	1.36E-40	1.10E-44	4.81E-33	1.91E-45	8.94E-45
	ForUSD5	5.57E-36	6.77E-41	1.32E-44	3.26E-33	6.50E-47	8.66E-47
	ForUSD6	4.20E-35	1.06E-39	2.34E-43	4.59E-32	3.02E-46	1.49E-47

Table 6.10: JPY Kendall correlations

		Real time series					
		JPY1	JPY2	JPY3	JPY4	JPY5	JPY6
Forecasts	ForJPY1	0.850634	0.837342	0.823735	0.810033	0.781963	0.772469
	ForJPY2	0.858410	0.863476	0.872340	0.859270	0.811873	0.784963
	ForJPY3	0.859633	0.838415	0.865016	0.861759	0.809597	0.786796
	ForJPY4	0.850535	0.861313	0.872725	0.885000	0.828978	0.796960
	ForJPY5	0.776996	0.783958	0.785540	0.797469	0.861483	0.862749
	ForJPY6	0.782279	0.772785	0.785760	0.788829	0.864241	0.886393

Table 6.11: JPY Kendall p-values

		Real time series					
		JPY1	JPY2	JPY3	JPY4	JPY5	JPY6
Forecasts	ForJPY1	1.40E-40	2.24E-39	3.66E-38	5.91E-37	1.47E-34	9.13E-34
	ForJPY2	2.87E-41	9.78E-42	1.46E-42	2.43E-41	4.27E-37	8.66E-35
	ForJPY3	2.35E-41	2.01E-39	7.48E-42	1.52E-41	7.10E-37	6.38E-35
	ForJPY4	1.88E-40	1.94E-41	1.69E-42	1.20E-43	1.63E-38	1.00E-35
	ForJPY5	3.79E-34	9.86E-35	7.25E-35	7.09E-36	1.38E-41	1.06E-41
	ForJPY6	1.38E-34	8.57E-34	7.02E-35	3.90E-35	7.77E-42	6.44E-44

Table 6.12: CHF Kendall correlations

		Real time series					
		CHF1	CHF2	CHF3	CHF4	CHF5	CHF6
Forecasts	ForCHF1	0.659276	0.604152	0.549661	0.551562	0.569303	0.591796
	ForCHF2	0.691701	0.673323	0.667619	0.668887	0.660965	0.692017
	ForCHF3	0.690049	0.668470	0.744631	0.735111	0.721783	0.726226
	ForCHF4	0.650816	0.650182	0.725014	0.758942	0.705037	0.757356
	ForCHF5	0.695040	0.673840	0.700103	0.723203	0.744087	0.743771
	ForCHF6	0.644845	0.675838	0.689121	0.732764	0.716003	0.814042

Table 6.13: CHF Kendall p-values

		Real time series					
		CHF1	CHF2	CHF3	CHF4	CHF5	CHF6
Forecasts	ForCHF1	5.38E-25	3.01E-21	7.39E-18	5.70E-18	4.82E-19	1.88E-20
	ForCHF2	2.42E-27	5.38E-26	1.39E-25	1.12E-25	4.14E-25	2.29E-27
	ForCHF3	3.77E-27	1.40E-25	2.42E-31	1.37E-30	1.50E-29	6.80E-30
	ForCHF4	2.31E-24	2.55E-24	7.70E-30	1.54E-32	2.62E-28	2.08E-32
	ForCHF5	1.17E-27	4.28E-26	4.88E-28	8.29E-30	1.86E-31	1.97E-31
	ForCHF6	4.66E-24	2.89E-26	3.04E-27	1.38E-30	2.80E-29	2.36E-37

6.3 Testing and validation

In this Section, the basic question we want to answer is how our forecasts differ from original time series, purely random data and noise? For the reason of space, we show the analysis on the EUR Overnight but we got similar results for all considered time series.

6.3.1 Results on test data

This analysis is carried out with R on data described in Section A.2 and the purpose of creating that data is the following: is the analysis we intend to run valid and consistent? If yes, time series 1 (EUR1) a 5 (a copy of EUR1) should be identical while time series 1 and 2 (random) should be unrelated. After having passed that check, the next question is: does time series 6 (EUR1 forecast) look similar to time series 1 or it does resemble more 2 or 3 (EUR1 + noise)?

Apart from the classical instruments described in Section 6.2.1 for testing the goodness of fit, and the correlation in Section 6.2.4, we measure the distance between data with several metrics. We start with the default Euclidean distance and complete clustering [157]. Figure 6-4 shows that there is no difference between EUR1 and its copy and that the next similarity is with the forecasts. Noise and random series are correctly grouped together and the EUR1 changed of the sign is left alone.

Now we want to understand whether the metric or the clustering criterion may influence the results. In particular, we adopt the Manhattan distance and we complement our clustering analysis with Ward's criterion (also known as Ward's minimum variance method) [156] [60]. As expected Figure 6-5 shows that the EUR1 times series and its copy are identical (which confirms that the analysis is able to correctly identify this feature). The forecasts follow immediately after. Noise and random are

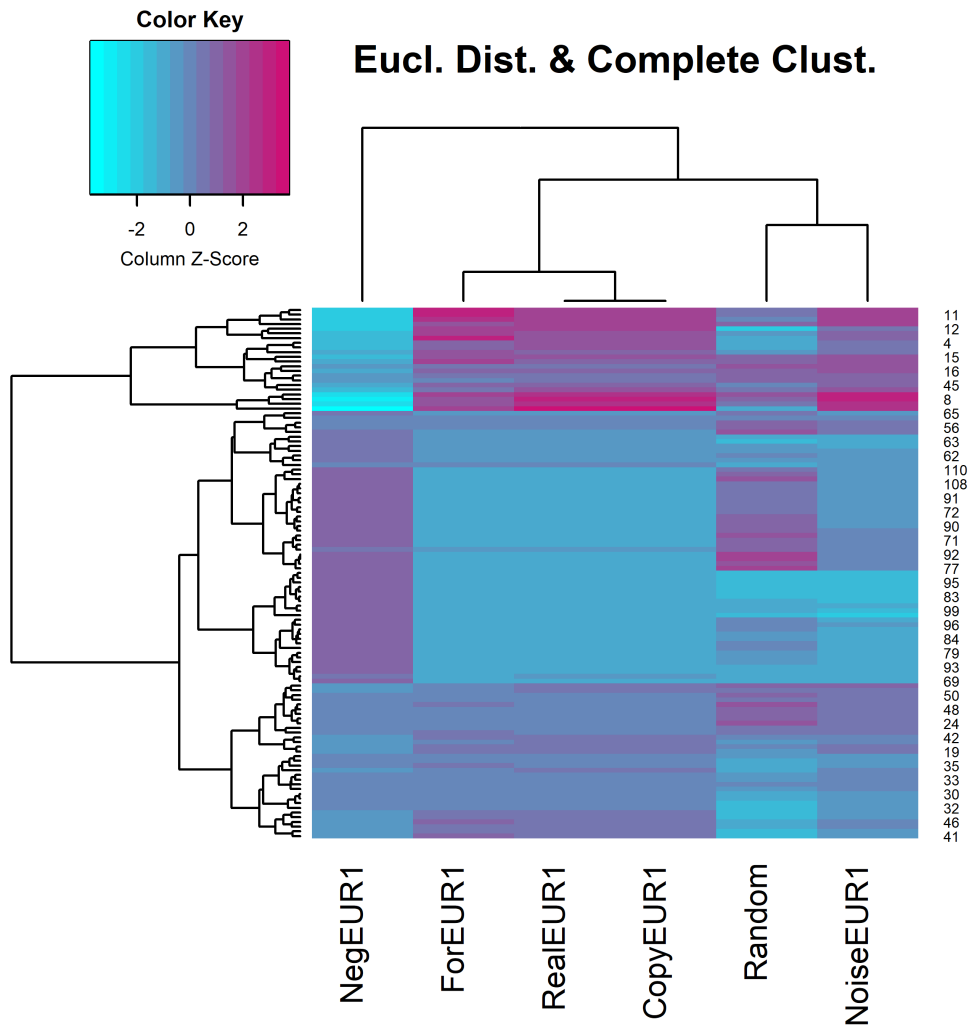


Figure 6-4: EUR overnight and test data. Euclidean distance and dendrogram based on complete clustering criterion.

recognized as similar and they group with the EUR1 changed sign time series.

A generalization of both the Euclidean and the Manhattan distance is the Minkowski distance [77], [11], [144]. Fig. 6-6 shows similar results to those already presented.

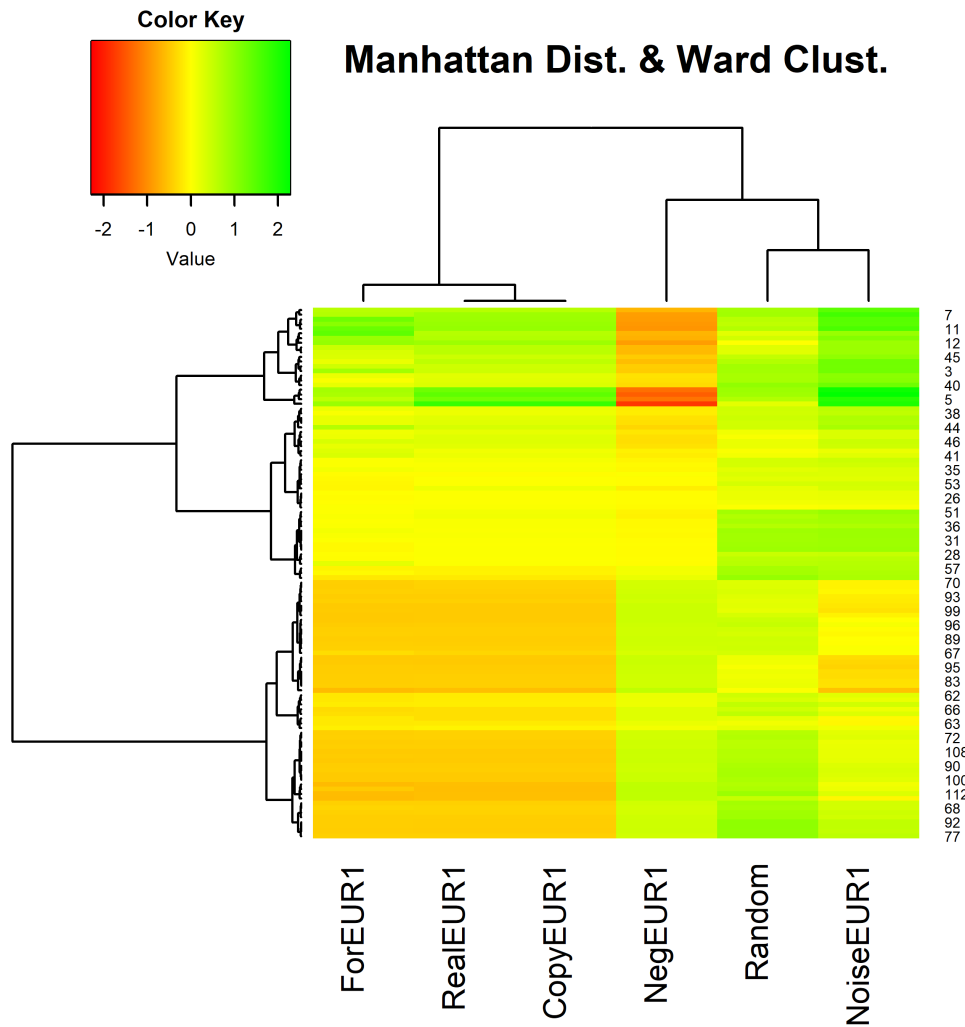


Figure 6-5: EUR overnight and test data. Manhattan distance and dendrogram based on Ward's criterion.

Hence, we can conclude that our model both spatially and hierarchy is very close to reality and, so, fits well with the intended purposes.

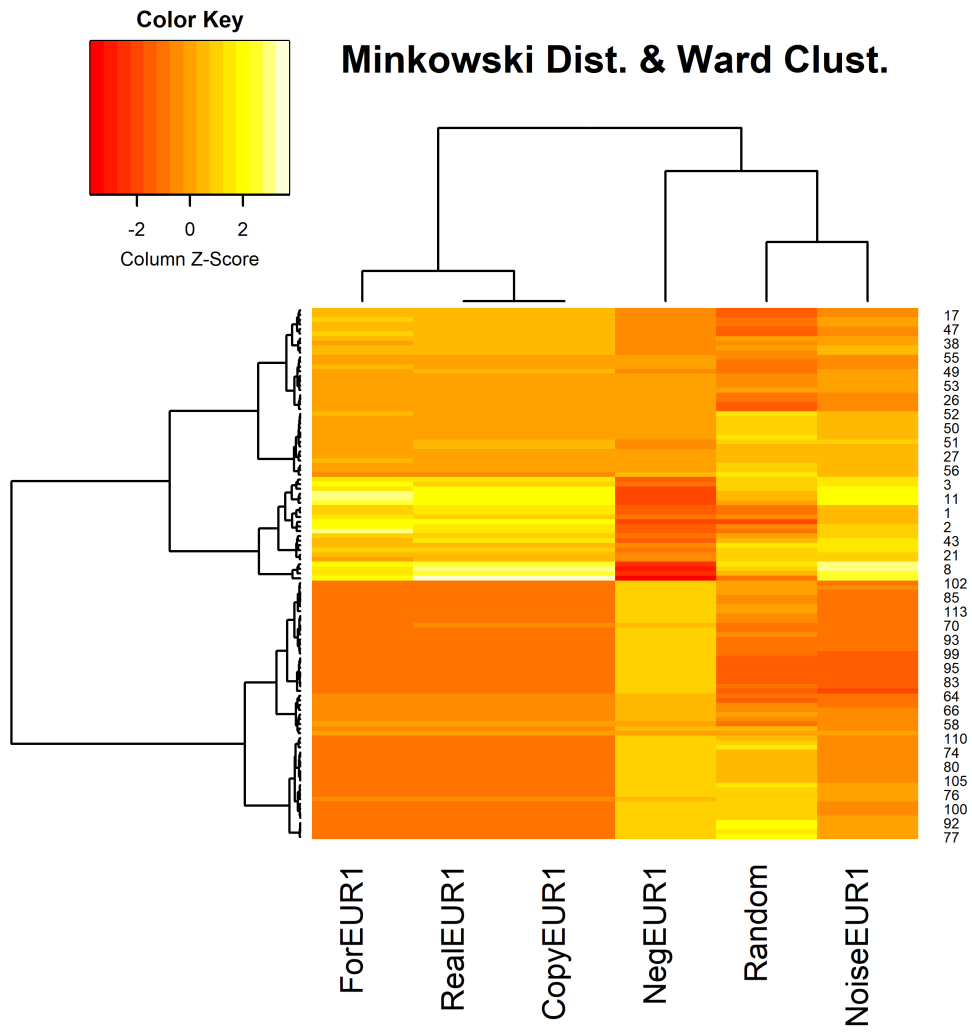


Figure 6-6: EUR overnight and test data. Minkowski distance and dendrogram based on Ward's criterion.

6.4 Conclusions

Several different extensions of the original model have been proposed to date, with the aim of overcoming the limitations of the CIR model: from one-factor models including time-varying coefficients or jump diffusions to multi-factor models. All these extensions preserve the positivity of interest rates but, in some cases, the analytical tractability of the basic model is violated. Moreover, often, those extensions are not suited for modelling both periods of high volatility and negative rates. In this work, we have shown that the CIR# model, instead, while preserving those features, is capable of coping with negative interest rates, cluster volatility and jumps. This has been tested on money market interest rates during turmoil and calmer periods, by measuring the directionality of rates as well as the forecasting error. Rank correlation and related p-values witness a link between real data and out-of-sample forecasts. Besides that, we have shown how the results of the model could be tested and validated with several metrics and clustering criteria.

Being this a Thesis carried out at the Wrocław University of Economics and Business, to complete the analysis, in next Chapter 7 we compare the predictive power in the forecasting of the CIR# versus the so-called CIR_{adj} , the single factor Hull and White model and the EWMA which is often considered when no model is assumed.

Chapter 7

The predictive power of the CIR_# model: An empirical analysis on Polish Zloty interest rates

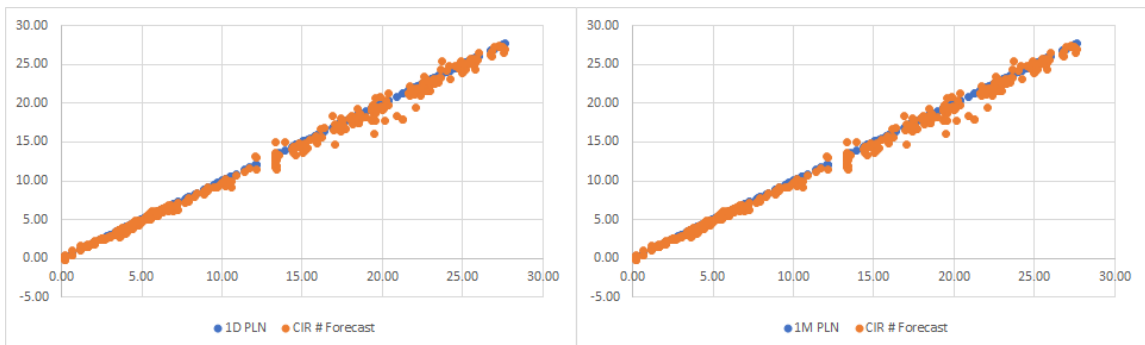
The present Chapter has the objective of comparing the predictive power in the forecasting of the CIR_# versus the so-called CIR_{adj} , the single factor Hull and White model and the EWMA which is often considered when no model is assumed. To this end, we retrieved several time series with different tenors (from overnight to 1 year) and frequency (daily and weekly data) and applied a number of analyses (NRMSE, MAPE, directionality of forecasting and Tukey's Honestly Significant Difference).

7.1 Results on Polish interest rates (all tenors)

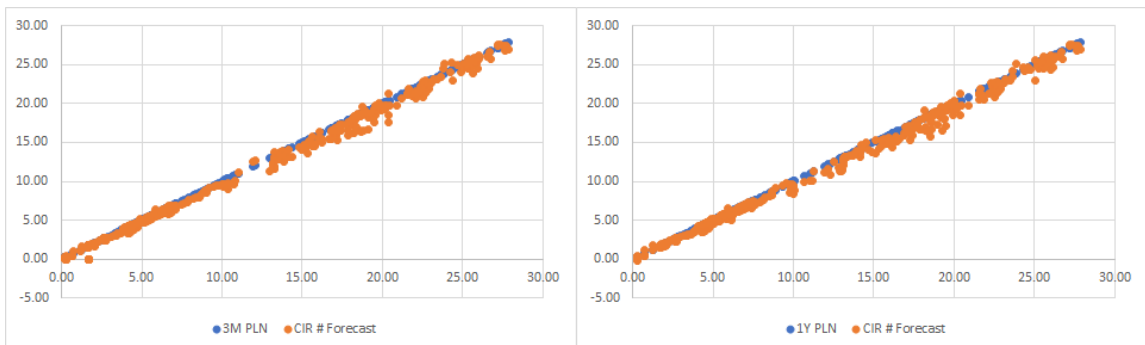
Real market data consists of Polish Zloty (PLN) interest rates from 1995-01-02 to 2021-02-05, weekly sampled, for the following tenors: Overnight, 1 Week, 1 Month,

3 Months, 6 Months, 1 Year.

Let us start by plotting the yields versus the forecasts for the overnight, 1 month, 3 months and 1 year tenor. In Figure 7-1 we show that the forecasts closely follow the realizations and they are not spread out.



(a) PLN overnight. Plot of the realized interest rate occurrence versus the forecasted value (b) 1 month PLN interest rate. Plot of the realized interest rate occurrence versus the forecasted value



(c) 3 months PLN interest rate. Plot of the realized interest rate occurrence versus the forecasted value. (d) 1 year PLN interest rate. Plot of the realized interest rate occurrence versus the forecasted value.

Figure 7-1: Multiple comparisons for the Polish interest rates occurrences tenors versus their corresponding forecasts.

Next, Fig. 7-2 displays market data while compares the Fig. 7-3 the CIR# forecasts versus the CIR_{adj} , EWMA and Hull and White (HW). As shown, the CIR# is the most accurate. To confirm that, Table 7.1 compares the CIR# versus the baseline models i.e. CIR_{adj} , EWMA and Hull and White (HW). As discussed, we are

interested in forecasting error (MAPE), accuracy error (NRMSE), and directionality error (IDX). For all tenors and from every point of view, the CIR# performs way better than the considered benchmarks.

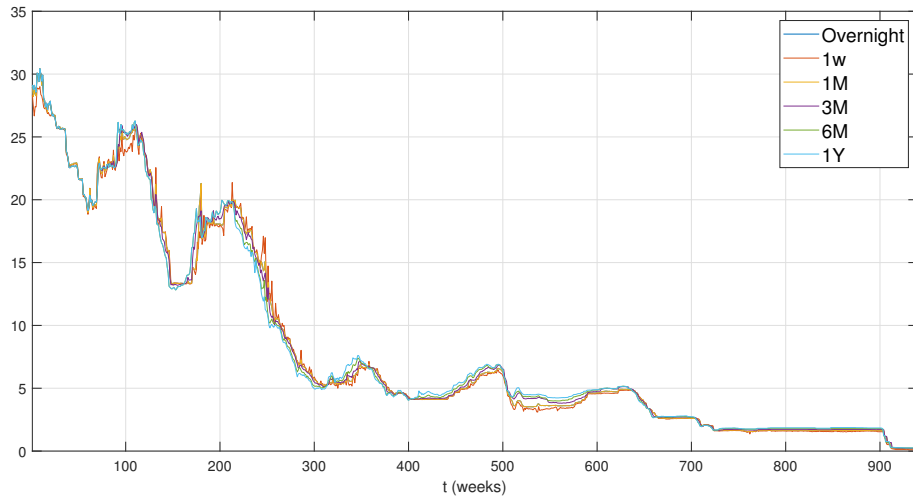


Figure 7-2: Real market data - Polish Zloty (PLN) interest rates.

Last but not least, we performed Tukey’s honestly significant difference procedure which is optimal when samples are of the same size and for balanced one-way ANOVA. When samples are of different sizes it is a conservative one-way ANOVA. According to the unproven Tukey-Kramer conjecture, it is also accurate for problems where the quantities being compared are correlated [88]. Table 7.2 reports the p-values obtained by comparing the models under consideration with the real data. As shown, while there is no evidence that the mean responses for the CIR# and CIR_{adj} are different from real data, one cannot say the same for the Hull and White model.

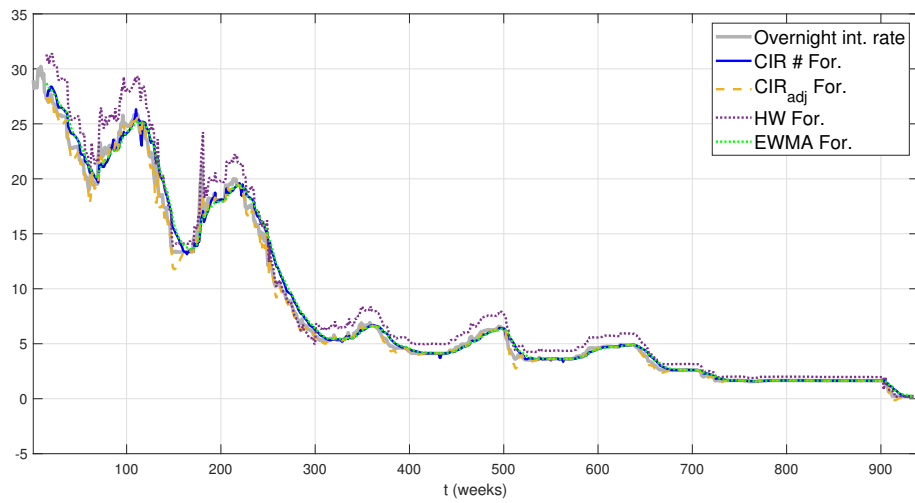


Figure 7-3: CIR# forecasts for the Overnight - Polish Zloty (PLN)- versus the baseline models.

Table 7.1: Forecasting accuracy: CIR# vs. CIR_{adj}, EWMA and HW

Err. Measure	Tenor	CIR#	CIR _{adj}	EWMA	HW
MAPE	Overnight	0.0409	0.0757	0.2172	0.0856
NRMSE		0.0168	0.0266	0.0856	0.0281
IDX		72.14%	56.95%	54.69%	59.63%
MAPE	1 Week	0.0519	0.0920	0.2187	0.1053
NRMSE		0.0205	0.0280	0.0872	0.0284
IDX		67.68%	58.97%	55.93%	57.01%
MAPE	1 Month	0.0409	0.0757	0.2172	0.0856
NRMSE		0.0168	0.0266	0.0856	0.0281
IDX		72.14%	59.63%	54.95%	56.69%
MAPE	3 Months	0.0401	0.0777	0.2139	0.0820
NRMSE		0.0288	0.0331	0.0847	0.0275
IDX		73.99%	59.63%	57.12%	58.10%
MAPE	6 Months	0.0405	0.0700	0.2140	0.0801
NRMSE		0.0169	0.0254	0.0843	0.0279
IDX		79.32%	67.57%	56.58%	59.84%
MAPE	1 Year	0.0415	0.0708	0.2143	0.0812
NRMSE		0.0172	0.0256	0.0843	0.0281
IDX		78.99%	68.00%	56.47%	59.95%

Table 7.2: Tukey's Honestly Significant Difference: CIR# CIR_{adj}, and HW vs. real data

p-values			
Tenor	CIR#	CIR _{adj}	HW
Overnight	0.60432	0.62882	0.00003
1 Week	0.70499	0.62817	0.00003
1 Month	0.60432	0.62882	0.00003
3 Months	0.90816	0.57571	0.00002
6 Months	0.50936	0.61708	0.00002
1 Year	0.49922	0.62167	0.00002

7.2 Results on 3-month Polish Zloty

In this Section we take a closer look at the 3-month Polish Zloty depicted in Fig. 7-4 and we compare the results obtained with the $CIR_{\#}$ versus the CIR_{adj} and the single factor Hull and White model.



Figure 7-4: Polish Zloty 3-month daily interest rates

7.2.1 Results on daily data

Out of sample forecasts are displayed in and Fig. 7-5 and Fig. 7-6. As shown, the $CIR_{\#}$ anticipates future rates much better than its peers and, as demonstrated through the present work, this is consistent across currencies, sampling frequencies and periods.

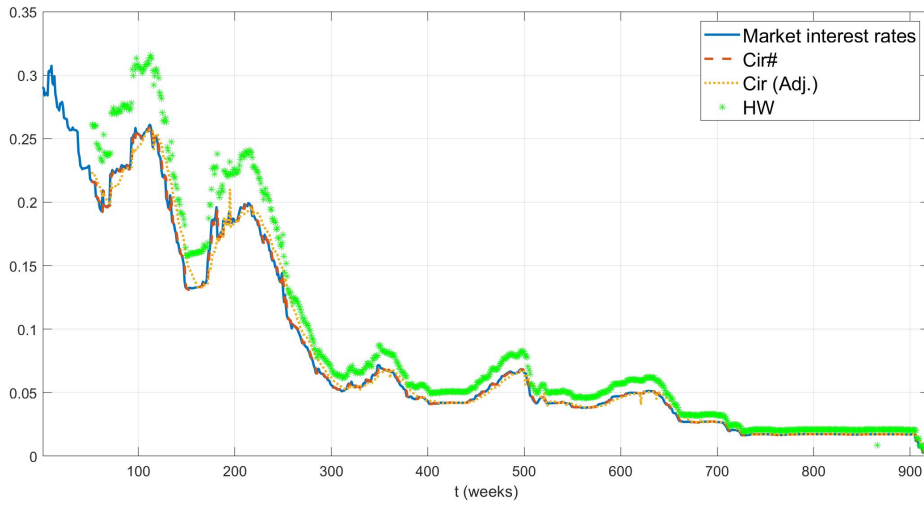


Figure 7-5: Out of sample forecasts of the $CIR\#$ versus CIR_{adj} and the single factor Hull and White model. Time series: Polish Zloty 3-month daily interest rates.

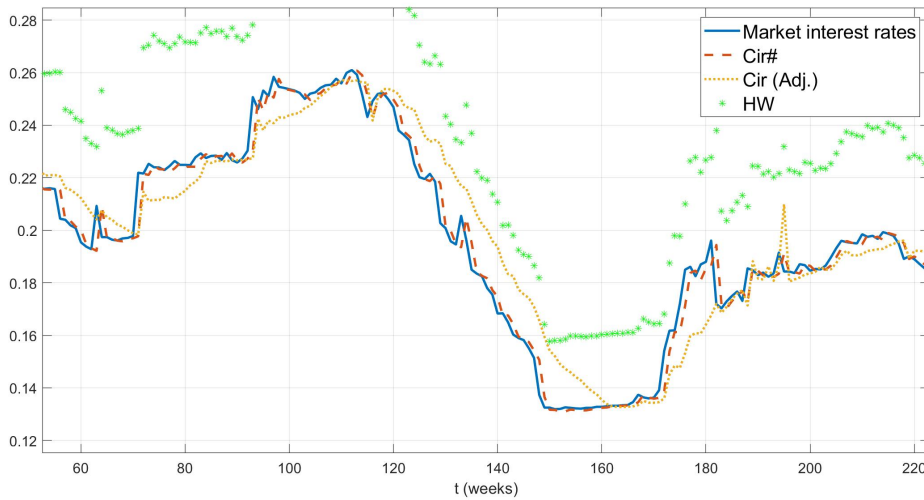


Figure 7-6: Zoomed-in figure: out of sample forecasts of the $CIR\#$ versus CIR_{adj} and the single factor Hull and White model. Time series: Polish Zloty 3-month interest rate, daily data.

Table 7.5 shows the results in terms of RMSE for the 3 models. As anticipated the CIR# has the lower value immediately followed by the CIR_adj. The Hull and White single factor model has the worse performance.

Table 7.3: RMSE for the three considered models - daily data

	<i>CIR#</i>	<i>CIR_{adj}</i>	Hull-White
RMSE	0.070%	0.263%	2.130%

7.2.2 Results on weekly data

From the same dataset aforementioned we extracted weekly observations. Fig. 7-7 shows a comparison between out of sample forecasts of the $CIR_{\#}$, the CIR_{adj} and the Hull and White model.

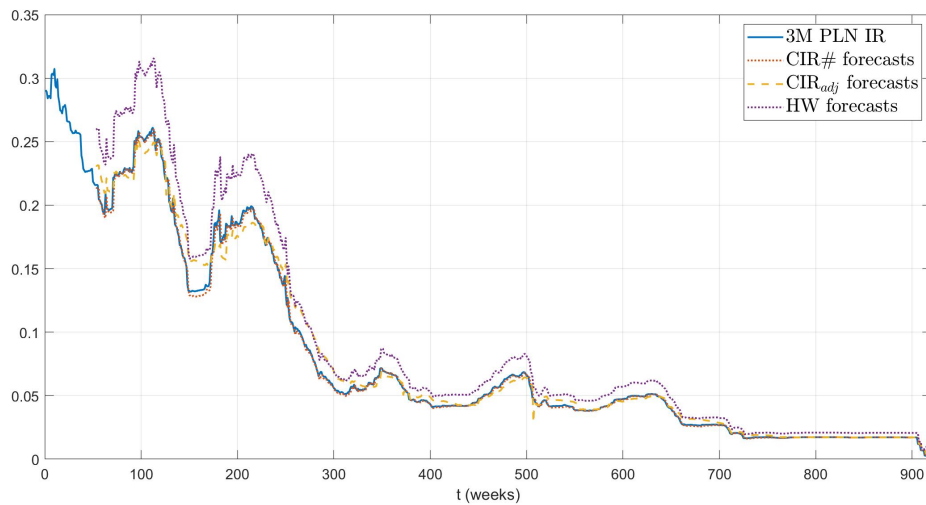


Figure 7-7: Out of sample forecasts of the $CIR_{\#}$ versus CIR_{adj} and the single factor Hull and White model. Time series: Polish Zloty 3-month interest rate, weekly data.

Tables 7.4, 7.5 and 7.6 report the IDX (see Eq. (6.3)), the RMSE and the MAPE for the three models, respectively. As in data, there are more volatile and less volatile periods, we divided the dataset into two parts so that the above-mentioned statistics describe how well a model performs in each period.

Table 7.4: IDX for the three considered models - weekly data

	IDX		
	<i>CIR#</i>	<i>CIR_{adj}</i>	Hull-White
All dataset	83.449%	65.046%	59.954%
First half	75.870%	52.900%	47.100%
Second half	91.183%	77.262%	72.622%

Table 7.5: RMSE for the three considered models - weekly data

	RMSE		
	<i>CIR#</i>	<i>CIR_{adj}</i>	Hull-White
All dataset	0.305%	0.741%	2.098%
First half	0.422%	1.018%	2.890%
Second half	0.090%	0.243%	0.666%

Table 7.6: MAPE for the three considered models - weekly data

	MAPE		
	<i>CIR#</i>	<i>CIR_{adj}</i>	Hull-White
All dataset	1.888%	6.472%	20.392%
First half	2.214%	7.322%	20.053%
Second half	1.562%	5.621%	20.732%

Conclusions

In this Thesis, we walked through the basics of interest rates, from the role played by central banks to the factors determining their fluctuations. Then we have described the mathematical framework in which interest rates models are derived. After having provided an inventory of interest rates models we focussed on three popular single factor models i.e. Vasicek, CIR and Hull-White models.

That introduced us to our original contribution in the field that we have called CIR# because it is an adaptation of the model developed by Cox, Ingersoll & Ross in 1985 [46].

Goal and scientific hypotheses

As mentioned in the introduction the goal of this Thesis is to provide a new accessible methodology to forecast future interest rates where all the improvements are obtained within the CIR framework in order to preserve the single-factor simplicity and the analytical tractability of the original model.

The goal has been achieved thanks to a suitable partition of data where the CIR parameters have been calibrated by replacing the Wiener process in the random term of the CIR model with normally distributed standardized residuals (which are the

proceeds of an “optimal” ARIMA model suitably chosen in our procedure). The proposed procedure captures all the statistically significant time changes in the volatility of interest rates, thus giving an account of jumps and related market dynamics.

The scientific hypothesis is that the so-called CIR# outperforms other single factor models and that the new approach proves particularly useful in describing the term structure of interest rates post 2007 financial crisis. In fact, as shown through the Thesis, the CIR# is superior to other single-factor models and overcomes the inability of modelling negative/near-to-zero values and the issue of the built-in mechanism of dampening volatility when rates are low. Moreover, it provides an alternative to Monte Carlo for deriving the expected value of interest rates as the suggested discretization scheme returns the same results without the need of simulating 100,000 paths.

Apart from the scientific confirmations on both goal and hypothesis achieved during those years of work on the Thesis [123, 124, 125, 121], the proposed model has been adopted by a number of financial institutions (e.g. Naumov et al. (2021) [118]).

Pros and cons of the CIR# model

Like any other model, the CIR# has pros and cons. We already mentioned some of the pros in terms of forecasting capability, parsimony, analytical tractability, etc.

Furthermore, the model does not suffer the limitations of the Hull-White and the CIR++ models that cannot describe twists of the term structure of interest rates in which the short-maturity and long-maturity yields move in opposite directions Russo et al. (2019) [141]. This is because they can only produce an increasing curve, a decreasing curve, and a curve with a small hump.

The CIR#, also, is not affected by the limitation that that changes over infinitesimal time periods of any two interest rates are perfectly correlated. The reason lies in the fact that the CIR# is not a short rate model and, therefore, it is not true that unexpected changes are proportional to the shock to the short rate. The CIR# is, instead, a forecasting model for any given rate of the yield curve. In addition, the model produces, robust and reproducible forecasts without any arbitrariness [118].

The cons of the CIR# model derive from the very same fact that is a single factor model. Two-factor models can generate additional yield curve shapes and movements. Furthermore, two-factor models are featured by non-perfect correlations between different interest rate dependent variables. Instead, for a single factor model, it is not possible to describe correlation structure between different objects/rates. That means the CIR# model cannot provide a fit of both the cross-section and time-series dynamics.

Finally, single factor models provide closed-form pricing formulas for zero-coupon bond options, caps and floors but not for European swaptions and European coupon bond options. This is an additional limitation as "market practices are moving towards the use of swaptions more than caps and floors, as they contain information on the correlation between different maturities of the interest rates curve" [141].

Implications for hedging

First of all, we need to distinguish between pricing accuracy and hedging performance. In fact, a single factor model such as the CIR# (as demonstrated by us) or the LIBOR market model (as demonstrated Gupta et al. (2005) [81]) may produce good pricing accuracy. Contrarily, hedging performance has to be measured in terms of hedging errors i.e. in terms of the dynamic performance of the model.

As mentioned, for short rate single factor models a change in the instantaneous spot rate implies a change of all the entire yield curve. That means, for example, the need to change the basket of vanilla options that are a good hedge for a Bermudan option. In addition, as short rate models only have one driving factor, they imply a perfect positive correlation among forward rates.

Those issues partially affect the CIR# model. In addition, Gupta et al. (2005) [81] assert that "for hedging performance, introducing a second stochastic factor is more important than fitting the skew of the underlying distribution. This constitutes evidence against claims in the literature that correctly specified and calibrated one-factor models could replace multi-factor models for consistent pricing and hedging of interest rate contingent claims".

The drawback is that the optimization problem for a two factor model may be not convex, not stable in the parameters, slow and may lead to some overfitting because of the larger number of parameters to calibrate [141].

Implications for economic policy

As mentioned in Chapter 1, central banks need to control interest rates for the effectiveness of inflation targeting, the ability to correctly model and predict them is essential. While the adopted models are comprehensive and provide a full sketch of policy changes, with up to 1,000 equations they might be difficult to handle. In this respect, a single equation and risk factor model such as the CIR# could provide a quick answer when needed.

Implications for financial institutions

For financial institutions that need to price fixed income instruments, the CIR# provides a suitable choice. For example, VTB capital mentioned that "due to RUONIA's lack of an OIS term structure, it is impossible to build an arbitrage-free strategy to compare floaters with bullets. Using other curves, such as MosPrime, IRS or swaps on CBR's key rate, for forecasting the future RUONIA trajectory exposes the analyst to the basis with RUONIA, which has been historically unstable. Such approach also suffers from subjective assumptions, which makes the estimates of z-spreads poorly comparable". Instead, "an enhanced CIR model produces robust and reproducible RUONIA forecasts without any arbitrariness, giving common ground upon which to estimate spot and historical z-spreads" Naumov et al. (2021) [118].

Future research

What we discussed above leads us to the next research. A possible extension could be the addition of a second factor similar to the G2++ by Brigo and Mercurio [28]. For such an extension, which we call CIR2#, it could be interesting to compute the sensitivities to a change in the interest rate to test the hedging performance.

Another possible direction of future research could be a comparison between CIR2# and the G2++, not only in terms of hedging and pricing but also in terms of the ability to capture the relevant shape and movement of the yield curve. This is in terms of both cross sectional correlations and time-series dynamics.

We believe that the G2++ is a good benchmark because, as proved by Brigo and Mercurio (2006) [28], it is the general case of the two factors Hull and White model and, thanks to the normal distribution of the underlying short rate, it is usable

for deriving explicit formulas for a number of financial instruments such as a zero-coupon bond, European option on a zero-coupon bond, cap/floor, caplet/floorlet, etc. The resulting formulas allow easy calibration of correlation-based products such as swaptions and the model is arbitrage free (as the current interest-rate term structure is used as input so the results are according to the current term structure).

Appendix A

Dataset

A.1 EUR and USD dataset

The dataset records both monthly and weekly EUR and USD interest rates with maturities 1/360A, 30/360A, 60/360A, ..., 360/360A and 1Y, ..., 50Y (i.e. at 1 day (overnight), 30 days, 60 days, ..., 360 days and 1 Year, ..., 50 Years) available from IBA ¹ [90]. For our convenience we have partitioned the data in two: money market (Partition I) and short- to long-term interest rates (Partition II). All together we are considering 63 maturities.

A.1.1 EUR and USD monthly dataset

¹ICE Benchmark Administration, Data from 31 December 2010 to 18 November 2016.

Table A.1: Monthly EUR interest Rates: the Dataset

	Partition I				Partition II			
Date	Maturity				1Y	2Y	...	50Y
	1/360A	30/360A	...	360/360A				
31.12.2010	0.606	0.788	...	1.507	1.311	1.557	...	3.306
31.01.2011	1.231	0.895	...	1.644	1.582	2.012	...	3.482
⋮	⋮	⋮	...	⋮	⋮	⋮	...	⋮
29.07.2016	-0.397	-0.371	...	-0.049	-0.201	-0.215	...	0.632

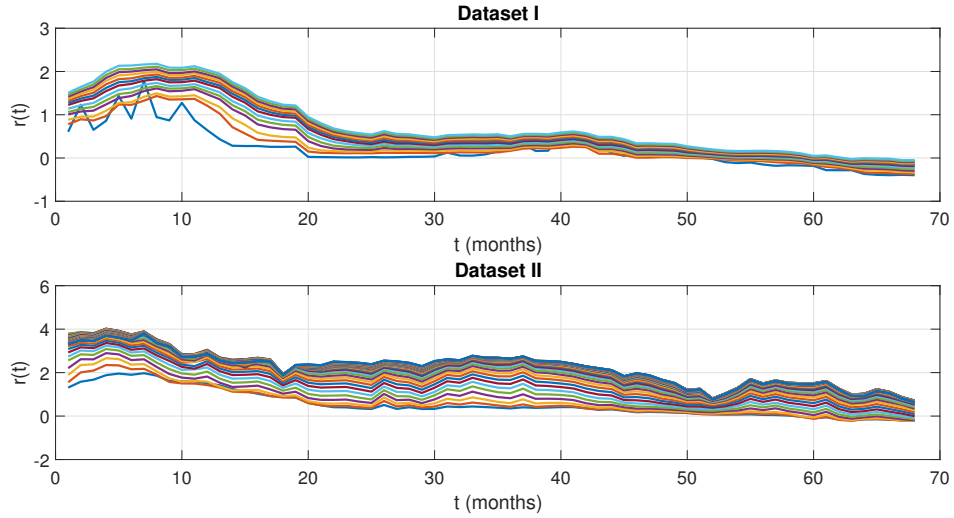


Figure A-1: Partition I and II: monthly observed EUR interest rates

A.1.2 EUR and USD weekly dataset

In Table A.2), each column lists a sample of $n = 308$ weekly observed EUR interest rates with a set maturity; each row shows interest rates on different maturities observed at a fixed date.

The plots in Figure A-2 represent the columns of Dataset I and II, so they are different from the yield curves (term structure) by plotting the rows. From Dataset

Table A.2: Weekly EUR interest Rates: the Dataset

	Partition I				Dataset II			
Date	Maturity				1Y	2Y	...	50Y
	1/360A	30/360A	...	360/360A				
31.12.2010	0.606	0.782	...	1.507	1.311	1.557	...	3.306
07.01.2011	0.341	0.759	...	1.505	1.345	1.603	...	3.229
⋮	⋮	⋮	...	⋮	⋮	⋮	...	⋮
18.11.2016	-0.410	-0.373	...	-0.077	-0.195	-0.139	...	1.120

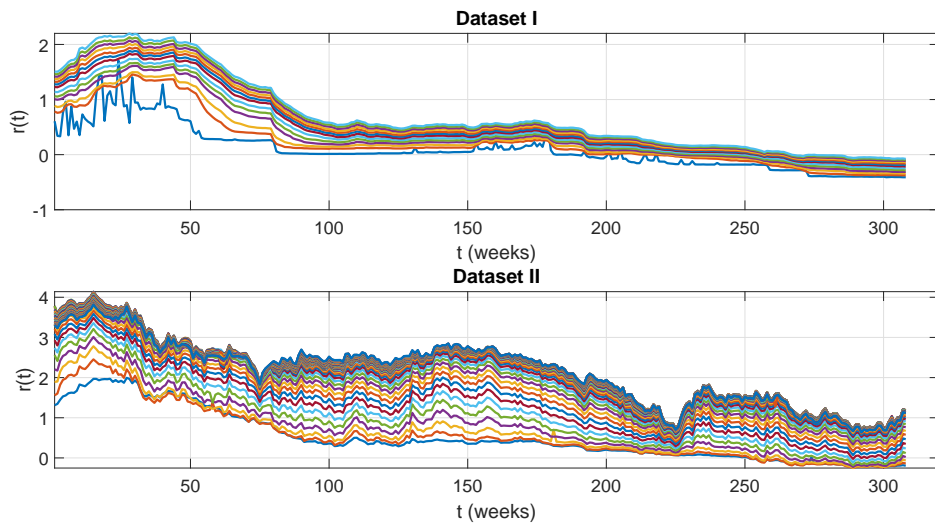


Figure A-2: Partition I and II: Dataset with weekly observed EUR interest rates

It is evident that the short-term rates become permanently negative after 2014 (as from March 2015). However, sample data from Dataset II also show a downward trend.

A.2 EUR, USD, JPY and CHF LIBOR - Real data and testing data

Our data consists of London Inter-bank Offered Rate (LIBOR) time series retrieved from Bloomberg and test data built by us for the said purpose. LIBOR is the average interest-rate calculated from quotes submitted by the leading banks in London. LIBOR in the past was known as British Bankers' Association (BBA) Libor.

Real time series

Real data consists of weekly interest rates from 31 December, 2009 to 31 January, 2020 as retrieved from Bloomberg at the "LIBOR Index Page BBAM <GO>" and described in Table A.3.

Table A.3: Bloomberg tickers for money market interest rates

Code	Description	Bloomberg Ticker	Tenor
EUR1	EUR Overnight	EE00O/N Curncy	N
EUR2	EUR 1 Month	EE0001M Curncy	1M
EUR3	EUR 2 Month	EE0002M Curncy	2M
EUR4	EUR 3 Month	EE0003M Curncy	3M
EUR5	EUR 6 Month	EE0006M Curncy	6M
EUR6	EUR 12 Month	EE0012M Curncy	12M
USD1	USD Overnight	US00O/N Curncy	N
USD2	USD 1 Month	US0001M Curncy	1M
USD3	USD 2 Month	US0002M Curncy	2M
USD4	USD 3 Month	US0003M Curncy	3M
USD5	USD 6 Month	US0006M Curncy	6M
USD6	USD 12 Month	US0012M Curncy	12M
JPY1	JPY Spot Next	JY00S/N Curncy	N
JPY2	JPY 1 Month	JY0001M Curncy	1M
JPY3	JPY 2 Month	JY0002M Curncy	2M
JPY4	JPY 3 Month	JY0003M Curncy	3M
JPY5	JPY 6 Month	JY0006M Curncy	6M
JPY6	JPY 12 Month	JY0012M Curncy	12M
CHF1	CHF Overnight	SF00S/N Curncy	N
CHF2	CHF 1 Month	SF0001W Curncy	1M
CHF3	CHF 2 Month	SF0001M Curncy	2M
CHF4	CHF 3 Month	SF0003M Curncy	3M
CHF5	CHF 6 Month	SF0006M Curncy	6M
CHF6	CHF 12 Month	SF0012M Curncy	12M

Test data

Test data are composed by the EUR Overnight, a copy of the EUR Overnight, the out-of-sample forecast of the EUR Overnight, a random time series, the EUR Overnight plus the random time series above-mentioned and the changed sign of the EUR Overnight as detailed in Table A.4.

Table A.4: Identifiers and description of test data

#	Test data	Description
1	RealEUR1	EE00O/N Curncy
2	Random	Randomly generated time series
3	NoiseEUR1	RealEUR1 + Random
4	NegEUR1	Negative RealEUR1
5	CopyEUR1	Copy of RealEUR1
6	ForEUR1	Out-of-sample forecast of RealEUR1

A.3 Polish Zloty (PLN) data

Real market data consists of Warsaw Interbank Offered Rates from 1995-01-02 to 2021-02-05, as displayed in Table A.5.

Table A.5: Polish Interest Rates

Code	Tenor
WIBOR ON	Overnight
WIBOR 1W	1 Week
WIBOR 1M	1 Month
WIBOR 3M	3 Months
WIBOR 6M	6 Months
WIBOR 1Y	1 Year

Source: www.money.pl [160].

Contents

Introduction	i
I Goal, original contribution and hypotheses	ii
II Structure of the Thesis	iii
1 Interest rates and the role of central banks	1
1.1 The yield curve	1
1.1.1 Par and zero-coupon yield curve	2
1.1.2 Forward yield curve	3
1.1.3 Normal yield curve	4
1.1.4 Flat and humped yield curve	4
1.1.5 Inverted yield curve	4
1.1.6 Relation between the yield curve and business cycle	5
1.1.7 Estimation of yields: The Nelson-Siegel and Svensson models	9
1.2 The role of central banks	11
1.2.1 Operation of payment system	12
1.2.2 Lender of last resort	13
1.2.3 The USA Federal Reserve System (FRS)	13
1.2.4 The European Central Bank (ECB)	14

1.2.5	The Bank of Japan (BOJ)	14
1.2.6	The Schweizerische Nationalbank (SNB)	15
1.2.7	Monetary policy	16
1.2.8	Unconventional monetary policy	19
1.2.9	Importance of interest rates models for central banks	21
1.2.10	Supervision and regulation	22
1.3	Factors determining real interest rates	24
1.3.1	Natural and potential growth rates	24
1.3.2	Demographic factors	26
1.3.3	Saving glut	28
1.3.4	Diverging trends of returns on risky and risk-free assets	30
1.3.5	Implications of low rates and monetary policy issues	32
2	Stochastic processes and short rate models	35
2.1	No arbitrage and risk-neutral probability measure	37
2.2	Short rates process	40
2.3	Term structure of interest rates models	41
2.3.1	Single factor interest rates models	41
2.3.2	Multi factor interest rates models	42
3	The CIR, Vasicek and the Hull-White models	45
3.1	The CIR model	45
3.2	The Vasicek model	48
3.3	The one-factor Hull-White model	50
4	The CIR# model: a new approach to forecast market interest rates	53
4.1	Introduction	53

4.2	Literature	55
4.3	The CIR# model	57
4.4	Numerical implementation and empirical analysis	59
4.4.1	STEP 1: ANOVA test and market data translation	59
4.4.2	STEP 2. Sub-optimal ARIMA models	63
4.4.3	STEP 3. Calibration of CIR parameters	65
4.4.4	The change points detection problem	72
4.5	Forecast of future interest rates	73
4.5.1	CIR# forecasts versus CIR forecasts	75
4.5.2	Qualitative analysis related to Table 4.2	80
4.5.3	CIR parameter estimates	85
4.6	Conclusions	86

5 Forecasting interest rates through Vasicek and CIR models: a partitioning approach **89**

5.1	Introduction	89
5.2	The Model: procedure and accuracy	91
5.2.1	Step 1- Dataset partition	91
5.2.2	Step 2 - Shift in interest rates	95
5.2.3	Step 3 - Calibration	96
5.2.4	Step 4 - Forecasting	97
5.2.5	Accuracy	98
5.3	Empirical results	98
5.3.1	Forecasting expected interest rates	106
5.4	Conclusions	109

6	The CIR# model: real data versus test data	111
6.1	Introduction	111
6.2	Results	113
6.2.1	Forecasting accuracy	113
6.2.2	Forecasting results over the whole dataset	115
6.2.3	Forecasting results in turbulent periods	119
6.2.4	Correlations between forecasts and real data	122
6.3	Testing and validation	125
6.3.1	Results on test data	125
6.4	Conclusions	129
7	The predictive power of the CIR# model: An empirical analysis on Polish Zloty interest rates	131
7.1	Results on Polish interest rates (all tenors)	131
7.2	Results on 3-month Polish Zloty	136
7.2.1	Results on daily data	136
7.2.2	Results on weekly data	139
	Conclusions	141
	Goal and scientific hypotheses	141
	Pros and cons of the CIR# model	142
	Implications for hedging	143
	Implications for economic policy	144
	Implications for financial institutions	145
	Future research	145

A Dataset	147
A.1 EUR and USD dataset	147
A.1.1 EUR and USD monthly dataset	147
A.1.2 EUR and USD weekly dataset	148
A.2 EUR, USD, JPY and CHF LIBOR - Real data and testing data . . .	150
A.3 Polish Zloty (PLN) data	153

List of Figures

- 1-1 Snapshots of USA Treasury yield curves for different dates. Yield lines describe: red = flat and humped; orange = inverted at the short-end; blue = normal; green = steep. Sources FRED and [158]. 3
- 1-2 USA Treasury yield curve spreads. In blue 1 year T-bill versus 10 year T-bond. In red 3 month T-bill versus 10 year T-bond. Gray stripes indicate recessions. Sources [66, 64, 65]. 5
- 1-3 Percent (monthly average) probability of USA recession, twelve months ahead of the term spread [63]. Sources: Board of Governors of the Federal Reserve; National Bureau of Economic Research. The shaded areas indicate periods designated as recessions by the National Bureau of Economic Research (NBER). 7
- 1-4 The Bundesbank’s daily estimates for NSS parameters. Source Bundesbank and Gilli et al. (2010) [74]). 11
- 1-5 Timeline of The Bank of Japan (BOJ). Source Shizume (2018) [145]). 15
- 1-6 Models adopted by European central banks. Source [61]. 22
- 1-7 Potential output growth and long-term growth expectations. Sources: Bureau of Economic Analysis, European Commission and Consensus Economics [98]. 25

1-8	Euro area labour productivity by sector: real gross value added per person employed. Sources: European Commission AMECO database and ECB staff calculations [98].	26
1-9	Old-age dependency ratios: historical data (solid line) and projections (dashed line). Sources: World Bank, Eurostat, OECD and ECB staff calculations [98].	27
1-10	Share of national income earned by households in the top 1 percent income bracket. Sources: World Inequality Database [98].	28
1-11	Ten-year Euro area sovereign bond yield to OIS spread. Sources: Bloomberg and ECB staff calculations [98].	31
1-12	Share of short-term government debt with AAA rating relative to GDP. Source: ECB [98].	32
4-1	a). Boxplots with notches around the median (red line). Notches of boxes A-1, A-2, A-8 do not overlap each other and with the other groups, this offers evidence of a statistically significant difference between the medians. Notches of boxes A-3,...,A-7 overlap, indicating they may be from the same or similar populations. b). Multiple comparison test of the means. The plot displays the mean estimates of each group with 95% intervals around them. The intervals of groups A-2,...,A-8 are highlighted in red and the comparison interval of the group A-1 is in blue. The lack of intersection between intervals indicates that the corresponding group means are significantly different from each other.	62

4-2	Qualitative statistical analysis related to the group 9–16. Top line: ARIMA (1, 1, 2) standardized residuals versus Johnson’s transformed residuals (<i>left</i>); Q-Q normal plot for the ARIMA(1, 1, 2) standardized residuals (<i>right</i>). Middle line: AC plot (<i>left</i>) and PAC plot(<i>right</i>). Bottom line: market interest rates versus ARIMA (1, 1, 2) fitted values (<i>left</i>); comparison between the empirical distribution function of the ARIMA (1, 1, 2) standardized residuals, before and after the Johnson’s transformation, and the cumulative distribution function (CDF) of the standard normal distribution (<i>right</i>).	71
4-3	Monthly EUR interest rates with T=1 day (overnight) maturity vs CIR fitted rates	72
4-4	Forecast of the next-month interest rate based on a historical rolling window of size $m = 8$ market data: monthly EUR interest rates with maturity T=1 day (overnight) versus predicted next-month interest rates.	74
4-5	Forecast of the next-month interest rate based on a historical rolling window of size $m = 8$ market data: monthly USD interest rates with maturity T=1 day (overnight) versus predicted next-month interest rates.	75
4-6	CIR# versus CIR: forecast of future next-month interest rates. Monthly EUR interest rates with overnight maturity (<i>green line</i>); future next-month interest rates predicted by the CIR# model based on a rolling window of $m = 8$ market data (<i>magenta dashed line</i>); future next-month interest rates predicted by the classical CIR model based on a rolling window of $m = 14$ market data (<i>blue dashed line</i>).	76

4-7	CIR# versus CIR: forecast of future next-month interest rates. Monthly USD interest rates with overnight maturity (<i>green line</i>); future next-month interest rates predicted by the CIR# model based on a rolling window of $m = 8$ market data (<i>magenta dashed line</i>); future next-month interest rates predicted by the classical CIR model based on a rolling window of $m = 14$ market data (<i>blue dashed line</i>).	77
4-8	Statistics for EUR dataset: $R^2_{CIR\#}$ versus R^2_{CIR} , computed on a rolling window of size $m = 14$	78
4-9	Statistics for EUR dataset: $RMSE_{CIR\#}$ versus $RMSE_{CIR}$, computed on a rolling window of size $m = 14$	78
4-10	Statistics for USD dataset: $R^2_{CIR\#}$ versus R^2_{CIR} , computed on a rolling window of size $m = 14$	79
4-11	Statistics for USD dataset: $RMSE_{CIR\#}$ versus $RMSE_{CIR}$, computed on a rolling window of size $m = 14$	79
4-12	Qualitative statistical analysis related to the sub-group 1–8. Top line: ARIMA (2, 0, 1) standardized residuals versus Johnson’s transformed residuals (<i>left</i>); Q-Q normal plot for the ARIMA (2, 0, 1) standardized residuals (<i>right</i>). Middle line: AC (<i>left</i>) and PAC (<i>right</i>) plots. Bottom line: real interest rates versus ARIMA (2, 0, 1) fitted values (<i>left</i>); comparison of the standard normal cumulative distribution function (CDF) with the empirical CDF of ARIMA (2, 0, 1) standardized residuals and of Johnson’s transformed residuals (<i>right</i>).	80

4-13	<p>Qualitative statistical analysis related to the sub-group 17–32. Top line: ARIMA (1, 0, 3) standardized residuals versus Johnson’s transformed residuals (<i>left</i>); Q-Q normal plot for the ARIMA (1, 0, 3) standardized residuals (<i>right</i>). Middle line: AC (<i>left</i>) and PAC (<i>right</i>) plots. Bottom line: real interest rates versus ARIMA (1, 0, 3) fitted values (<i>left</i>); comparison of the standard normal cumulative distribution function (CDF) with the empirical CDF of ARIMA (1, 0, 3) standardized residuals and of Johnson’s transformed residuals (<i>right</i>).</p>	81
4-14	<p>Qualitative statistical analysis related to the sub-group 33–48. Top line: ARIMA (3, 0, 1) standardized residuals versus Johnson’s transformed residuals (<i>left</i>); Q-Q normal plot for the ARIMA (3, 0, 1) standardized residuals (<i>right</i>). Middle line: AC (<i>left</i>) and PAC (<i>right</i>) plots. Bottom line: real interest rates versus ARIMA (3, 0, 1) fitted values (<i>left</i>); comparison of the standard normal cumulative distribution function (CDF) with the empirical CDF of ARIMA (3, 0, 1) standardized residuals and of Johnson’s transformed residuals (<i>right</i>).</p>	82
4-15	<p>Qualitative statistical analysis related to the sub-group 49–56. Top line: ARIMA (3, 1, 2) standardized residuals versus Johnson’s transformed residuals (<i>left</i>); Q-Q normal plot for the ARIMA (3, 1, 2) standardized residuals (<i>right</i>). Middle line: AC (<i>left</i>) and PAC (<i>right</i>) plots. Bottom line: real interest rates versus ARIMA (3, 1, 2) fitted values (<i>left</i>); comparison of the standard normal cumulative function (CDF) with the empirical CDF of ARIMA (3, 1, 2) standardized residuals and of Johnson’s transformed residuals (<i>right</i>).</p>	83

4-16	Qualitative statistical analysis related to the sub-group 57–68. Top line: ARIMA (2, 1, 1) standardized residuals versus Johnson’s transformed residuals (<i>left</i>); Q-Q normal plot for the ARIMA (2, 1, 1) standardized residuals (<i>right</i>). Middle line: AC (<i>left</i>) and PAC (<i>right</i>) plots. Bottom line: real interest rates versus ARIMA (2, 1, 1) fitted values (<i>left</i>); comparison of the standard normal cumulative distribution function (CDF) with the empirical CDF of ARIMA (2, 1, 1) standardized residuals and of Johnson’s transformed residuals (<i>right</i>).	84
4-17	Plots of the functions $S_j(k)$ for each group/sub-group	85
5-1	Estimated expected interest rates: CIR model (blue line) and Vasicek model (magenta line) versus $n = 308$ weekly observed EUR interest rates (green line) with maturity $T = 30Y$ from Dataset II in Table A.2.	99
5-2	Estimated expected interest rates (blue line) versus market rates (green line) after segmentation with the Normal distribution for a data sample of $n = 308$ weekly EUR interest rates with maturity $T = 30Y$ from Dataset II in Table A.2.	101
5-3	Estimated expected interest rates (blue line) versus market rates (green line) after segmentation with non-central Chi-square distribution for a data sample of $n = 308$ weekly EUR interest rates with maturity $T = 30Y$ from Dataset II in Table A.2.	103
5-4	Estimated expected interest rates (blue line) versus market rates (green line) after segmentation with Normal distribution for a data sample of $n = 308$ weekly EUR interest rates with maturity $T = 30/360A$ from Dataset I in Table A.2.	104

5-5	Estimated expected interest rates (blue line) vs market rates (green line) after segmentation with non-central Chi-square distribution for a data sample of $n = 308$ weekly EUR interest rates with maturity $T = 30/360A$ from Dataset I in Table A.2.	106
5-6	Forecast of expected next-week interest rates based on a rolling window of variable size: sequence of $n = 308$ weekly EUR interest rates with maturity $T=30Y$ (green line); CIR forecasted expected interest rates (blue dashed line); Vasicek forecasted expected interest rates (red dashed line); EWMA predicted values (yellow dashed line). . . .	108
5-7	Error analysis in the forecast procedure of future next-week expected interest rates across 63 maturities. RMSE values computed by the proposed numerical procedure based on a rolling window of variable size: CIR model (blu line), Vasicek model (red line). RMSE values computed by the EWMA model (yellow line) based on a rolling window of fixed size $m = 52$ weeks. The vertical black line differentiates samples of Dataset I from samples of Dataset II in Table A.2.	109
6-1	Multiple comparisons for the overnight interest rate occurrences across currencies versus their corresponding forecasts.	115
6-2	Bland-Altman plot. Multiple comparisons for the overnight interest rates occurrences across currencies versus their corresponding forecasts. Maximum number of outliers are 0.885%.	119
6-3	Multiple comparisons for the overnight interest rates across currencies. Vertical lines identify cluster of volatilities partitioning the sample data in subgroups.	121

6-4	EUR overnight and test data. Euclidean distance and dendrogram based on complete clustering criterion.	126
6-5	EUR overnight and test data. Manhattan distance and dendrogram based on Ward's criterion.	127
6-6	EUR overnight and test data. Minkowski distance and dendrogram based on Ward's criterion.	128
7-1	Multiple comparisons for the Polish interest rates occurrences tenors versus their corresponding forecasts.	132
7-2	Real market data - Polish Zloty (PLN) interest rates.	133
7-3	CIR# forecasts for the Overnight - Polish Zloty (PLN)- versus the baseline models.	134
7-4	Polish Zloty 3-month daily interest rates	136
7-5	Out of sample forecasts of the $CIR\#$ versus CIR_{adj} and the single factor Hull and White model. Time series: Polish Zloty 3-month daily interest rates.	137
7-6	Zoomed-in figure: out of sample forecasts of the $CIR\#$ versus CIR_{adj} and the single factor Hull and White model. Time series: Polish Zloty 3-month interest rate, daily data.	137
7-7	Out of sample forecasts of the $CIR\#$ versus CIR_{adj} and the single factor Hull and White model. Time series: Polish Zloty 3-month interest rate, weekly data.	139
A-1	Partition I and II: monthly observed EUR interest rates	148
A-2	Partition I and II: Dataset with weekly observed EUR interest rates	149

List of Tables

1.1	Recessions following yield curve inversion (all values in months unless noted)	6
1.2	Tools of Monetary Policy	16
2.1	Alternative Specifications of the Spot Interest Rate Process of Single-Factor Models	43
2.2	Alternative Specifications of the Spot Interest Rate Process of Multi-Factor Models	44
4.1	The ANOVA Table shows the between-groups (Groups) and the within-groups (Error) variation. "SS" is the sum of squares and "df" means degrees of freedom associated to SS. MS indicates the mean squared error, i.e. the estimate of the error variance. The value of the F-statistic is given by the ratio of the mean squared errors.	61
4.2	Outputs from the ARIMA-CIR algorithm for the 68 monthly EUR interest rates on overnight maturity	69
4.3	CIR parameter estimates based on 68 monthly observed 1-day (overnight) EUR interest rates	85
5.1	"Forward" procedure	93

5.2	Optimal parameter estimates and the corresponding RMSE ε for the Vasicek and CIR model. Data sample: $n = 68$ monthly observed interest rates with maturity $T = 30Y$ from Dataset II in Table A.2.	99
5.3	Partition by a Normal distribution: error analysis of a sample of $n = 308$ weekly EUR interest rates with maturity $T = 30Y$ from the Dataset II in Table A.2.	101
5.4	Partition by a non-central Chi-square distribution: error analysis of a sample of $n = 308$ weekly EUR interest rates with maturity $T = 30Y$ from Dataset II in Table A.2.	102
5.5	Partition by a Normal distribution: error analysis of a sample of $n = 308$ weekly EUR interest rates with maturity $T = 30/360A$ from Dataset I in Table A.2.	104
5.6	Partition by a non-central Chi-square distribution: error analysis of a sample of $n = 308$ weekly EUR interest rates with maturity $T = 30/360A$ from Dataset I in Table A.2.	105
6.1	Averaged NRMSE and IDX for the dataset in Table A.3.	117
6.2	Averaged NRMSE and IDX for the dataset in Table A.3.	117
6.3	NRMSE for different models, tenors and currencies	117
6.4	IDX for different models, tenors and currencies	118
6.5	NRMSE and IDX in turbulent periods for the CIR#, CIR _{adj} and EWMA over overnight maturities and different currencies	120
6.6	EUR Kendall correlations	122
6.7	EUR Kendall p-values	122
6.8	USD Kendall correlations	123
6.9	USD Kendall p-values	123

6.10	JPY Kendall correlations	123
6.11	JPY Kendall p-values	124
6.12	CHF Kendall correlations	124
6.13	CHF Kendall p-values	124
7.1	Forecasting accuracy: $CIR_{\#}$ vs. CIR_{adj} , EWMA and HW	135
7.2	Tukey's Honestly Significant Difference: $CIR_{\#}$, CIR_{adj} , and HW vs. real data	135
7.3	RMSE for the three considered models - daily data	138
7.4	IDX for the three considered models - weekly data	140
7.5	RMSE for the three considered models - weekly data	140
7.6	MAPE for the three considered models - weekly data	140
A.1	Monthly EUR interest Rates: the Dataset	148
A.2	Weekly EUR interest Rates: the Dataset	149
A.3	Bloomberg tickers for money market interest rates	151
A.4	Identifiers and description of test data	152
A.5	Polish Interest Rates	153

Bibliography

- [1] R. P. ADAMS AND D. J. MACKAY, *Bayesian online changepoint detection*, arXiv:0710.3742, (2007).
- [2] Y. AÏT-SAHALIA, *Nonparametric pricing of interest rate derivative securities*, *Econometrica: Journal of the Econometric Society*, (1996), pp. 527–560.
- [3] D. G. ALTMAN AND J. M. BLAND, *Measurement in medicine: the analysis of method comparison studies*, *Journal of the Royal Statistical Society: Series D (The Statistician)*, 32 (1983), pp. 307–317.
- [4] M. ANDERSSON, B. SZÖRFI, M. TOTH, N. ZORELL, ET AL., *Potential output in the post-crisis period*, *Economic Bulletin Articles*, 7 (2018).
- [5] S. ARLOT AND A. CELISSE, *Segmentation of the mean of heteroscedastic data via cross-validation*, *Statistics and Computing*, 21 (2011), pp. 613–632.
- [6] K. BACK, *Yield curve models: A mathematical review*, Irwin Professional Publishing, 1997.
- [7] J. BAI AND P. PERRON, *Computation and analysis of multiple structural change models*, *Journal of Applied Econometrics*, 18 (2003), pp. 1–22.
- [8] R. BALDWIN AND C. TEULINGS, *Secular stagnation: facts, causes and cures*, 2014.
- [9] D. S. BATES, *Jumps and stochastic volatility: Exchange rate processes implicit in deutsche mark options*, *The Review of Financial Studies*, 9 (1996), pp. 69–107.
- [10] J. A. BATTEN AND N. WAGNER, *Derivatives Securities Pricing and Modelling*, Emerald Group Publishing, 2012, pp. 3–14.

- [11] I. BATYRSHIN, *Constructing time series shape association measures: Minkowski distance and data standardization*, in 2013 BRICS Congress on Computational Intelligence and 11th Brazilian Congress on Computational Intelligence, IEEE, 2013, pp. 204–212.
- [12] B. BERNANKE, *The Global saving glut and the US Current Account Deficit*, 2005.
- [13] B. S. BERNANKE, C. C. BERTAUT, L. DEMARCO, AND S. B. KAMIN, *International capital flows and the return to safe assets in the united states, 2003-2007*, FRB International Finance Discussion Paper, (2011).
- [14] J. M. BERROSPIDE, *Bank liquidity hoarding and the financial crisis: An empirical evaluation*, (2012).
- [15] B. M. BIBBY, M. JACOBSEN, AND M. SØRENSEN, *Estimating functions for discretely sampled diffusion-type models*, in Handbook of Financial Econometrics: Tools and Techniques, Y. Aït-Sahalia and L. P. Hansen, eds., vol. 1, North-Holland, Oxford, 2010, pp. 203–268.
- [16] —, *Estimating functions for discretely sampled diffusion-type models*, in Handbook of Financial Econometrics: Tools and Techniques, Y. Aït-Sahalia and L. P. Hansen, eds., vol. 1, North-Holland, Oxford, 2010, pp. 203–268.
- [17] M. BIELECKI, M. BRZOZA-BRZEZINA, M. KOLASA, ET AL., *Demographics, monetary policy, and the zero lower bound*, National Bank of Poland Education & Publishing Department, 2018.
- [18] J. M. BLAND AND D. ALTMAN, *Statistical methods for assessing agreement between two methods of clinical measurement*, The Lancet, 327 (1986), pp. 307–310.
- [19] D. J. BOLDER AND D. STRÉLISKI, *Yield curve modelling at the bank of canada*, Available at SSRN 1082845, (1999).
- [20] G. E. P. BOX, G. M. JENKINS, G. C. REINSEL, AND G. M. LJUNG, *Time Series Analysis: Forecasting and Control*, Wiley Series in Probability and Statistics, Wiley, 5th ed., 2015.
- [21] C. BRAND, L. FERRANTE, AND A. HUBERT, *From cash-to securities-driven euro area repo markets: the role of financial stress and safe asset scarcity*, (2019).

- [22] M. J. BRENNAN AND E. S. SCHWARTZ, *A continuous time approach to the pricing of bonds*, Journal of Banking & Finance, 3 (1979), pp. 133–155.
- [23] E. S. BREZIS AND J. CARIOLLE, *Financial sector regulation and the revolving door in us commercial banks*, in State, Institutions and Democracy, Springer, 2017, pp. 53–76.
- [24] D. BRIGO AND N. EL-BACHIR, *Credit derivatives pricing with a smile-extended jump stochastic intensity model*, ICMA Centre Discussion Papers in Finance DP2006-13. Available at SSRN 950208, (2006).
- [25] D. BRIGO AND F. MERCURIO, *The CIR++ model and other deterministic-shift extensions of short rate models*, in Proceedings of the 4th Columbia-JAFEE conference for mathematical finance and financial engineering, 2000, pp. 563–584.
- [26] —, *A deterministic-shift extension of analytically-tractable and time-homogeneous short rate models*, Finance and Stochastics, 5 (2001), pp. 369–388.
- [27] —, *Interest rate models-theory and practice: with smile, inflation and credit*, Springer-Verlag, Berlin, Heidelberg, 2006.
- [28] D. BRIGO AND F. MERCURIO, *Interest rate models: theory and practice: with smile, inflation, and credit*, Springer, 2006.
- [29] R. H. BROWN AND S. M. SCHAEFER, *Interest rate volatility and the shape of the term structure*, Philosophical Transactions of the Royal Society of London. Series A: Physical and Engineering Sciences, 347 (1994), pp. 563–576.
- [30] S. J. BROWN AND P. H. DYBVIG, *The empirical implications of the cox, ingersoll, ross theory of the term structure of interest rates*, The Journal of Finance, 41 (1986), pp. 617–630.
- [31] J. B. BULLARD ET AL., *"the monetary policy implications of a low r-star: An update," joint dnb/ecb workshop on the natural rate of interest, de nederlandse bank, amsterdam, netherlands*, tech. rep., 2019.
- [32] L. BUTLER, *Recession? A market view*, FRBSF Economic Letter, (1978).
- [33] G. CAMBA-MÉNDEZ, M. FORSELLS, ET AL., *The recent slowdown in euro area output growth reflects both cyclical and temporary factors*, Economic Bulletin Boxes, 4 (2018).

- [34] A. CANALE, R. M. MININNI, AND A. RHANDI, *Analytic approach to solve a degenerate parabolic PDE for the Heston model*, *Mathematical Methods in the Applied Sciences*, 40 (1985), pp. 4982–4992.
- [35] ———, *Analytic approach to solve a degenerate parabolic PDE for the Heston model*, *Mathematical Methods in the Applied Sciences*, 40 (2017), pp. 4982–4992.
- [36] R. A. CARMONA AND M. R. TEHRANCHI, *Interest rate models: an infinite dimensional stochastic analysis perspective*, Springer-Verlag: Berlin, Heidelberg, 2006.
- [37] C. CARVALHO, A. FERRERO, AND F. NECHIO, *Demographics and real interest rates: Inspecting the mechanism*, *European Economic Review*, 88 (2016), pp. 208–226.
- [38] K. C. CHAN, G. A. KAROLYI, F. A. LONGSTAFF, AND A. B. SANDERS, *An empirical comparison of alternative models of the short-term interest rate*, *The journal of finance*, 47 (1992), pp. 1209–1227.
- [39] L. CHEN, *Stochastic Mean and Stochastic Volatility: A Three-Factor Model of the Term Structure of Interest Rates and Its Applications and Its Applications in Derivatives Pricing and Risk Management*, Cambridge, MA :Blackwell Publishers, 1996.
- [40] ———, *Interest rate dynamics, derivatives pricing, and risk management*, vol. 435, Springer Science & Business Media, 2012.
- [41] R. H. CLARIDA ET AL., *Monetary policy, price stability, and equilibrium bond yields: Success and consequences: a speech at the high-level conference on global risk, uncertainty, and volatility, co-sponsored by the bank for international settlements, the board of governors of..., november 12, 2019*, tech. rep., 2019.
- [42] G. COENEN, C. MONTES-GALDÓN, AND F. SMETS, *Effects of state-dependent forward guidance, large-scale asset purchases and fiscal stimulus in a low-interest-rate environment*, (2020).
- [43] G. M. CONSTANTINIDES, *A theory of the nominal term structure of interest rates*, *The Review of Financial Studies*, 5 (1992), pp. 531–552.

- [44] G. COURTADON, *A more accurate finite difference approximation for the valuation of options*, Journal of Financial and Quantitative Analysis, (1982), pp. 697–703.
- [45] J. C. COX, J. E. INGERSOLL, AND S. A. ROSS, *An analysis of variable rate loan contracts*, The Journal of Finance, 35 (1980), pp. 389–403.
- [46] J. C. COX, J. E. INGERSOLL, AND S. A. ROSS, *A theory of the term structure of interest rates*, Econometrica, 53 (1985), pp. 385–407.
- [47] E. DEHAAN, S. KEDIA, K. KOH, AND S. RAJGOPAL, *The revolving door and the SEC’s enforcement outcomes: Initial evidence from civil litigation*, Journal of Accounting and Economics, 60 (2015), pp. 65–96.
- [48] M. DEL NEGRO, D. GIANNONE, M. P. GIANNONI, AND A. TAMBALOTTI, *Safety, liquidity, and the natural rate of interest*, Brookings Papers on Economic Activity, (2017), pp. 235–316.
- [49] ———, *Global trends in interest rates*, Journal of International Economics, 118 (2019), pp. 248–262.
- [50] R. DESANTIAGO, J.-P. FOUQUE, AND K. SOLNA, *Bond markets with stochastic volatility*, Emerald Group Publishing, 2008, pp. 215–242.
- [51] F. X. DIEBOLD AND C. LI, *Forecasting the term structure of government bond yields*, Journal of econometrics, 130 (2006), pp. 337–364.
- [52] L. U. DOTHAN, *On the term structure of interest rates*, Journal of Financial Economics, 6 (1978), pp. 59–69.
- [53] D. DUFFIE, *Credit risk modeling with affine processes*, Journal of Banking & Finance, 29 (2005), pp. 2751–2802.
- [54] D. DUFFIE AND R. KAN, *A yield-factor model of interest rates*, Mathematical finance, 6 (1996), pp. 379–406.
- [55] ECB, *What are minimum reserve requirements?*, Aug. 2016.
- [56] [EIB], *EIB Investment Report 2019/2020: accelerating Europe’s transformation*, tech. rep., nov 2019.
- [57] A. ESTRELLA AND G. A. HARDOUVELIS, *The term structure as a predictor of real economic activity*, The journal of Finance, 46 (1991), pp. 555–576.

- [58] A. ESTRELLA AND F. S. MISHKIN, *Predicting US recessions: Financial variables as leading indicators*, Review of Economics and Statistics, 80 (1998), pp. 45–61.
- [59] EUROPEAN CENTRAL BANK, *Overview of the euro short-term rate (€STR)*. https://www.ecb.europa.eu/stats/financial_markets_and_interest_rates/euro_short-term_rate/html/eurostr_overview.en.html, 2020. Accessed: 2020-08-08.
- [60] B. EVERITT, S. LANDAU, AND M. LEESE, *Cluster Analysis*, Oxford University Press: New York, 2001.
- [61] G. FAGAN AND J. MORGAN, *Econometric models of the Euro-area central banks*, Edward Elgar Publishing, 2006.
- [62] S. FALLAH, A. R. NAJAFI, AND F. MEHRDOUST, *A fractional version of the Cox Ingersoll Ross interest rate model and pricing double barrier option with Hurst index H* , Communications in Statistics - Theory and Methods, 48 (2019), pp. 2254–2266.
- [63] FEDERAL RESERVE BANK OF NEW YORK, *The yield curve as a leading indicator*, 2020. [Online; accessed 9-August-2020].
- [64] FEDERAL RESERVE BANK OF ST. LOUIS, *Board of Governors of the Federal Reserve System (US), 1-Year Treasury Constant Maturity Rate [GS1]*, retrieved from FRED, 2020. [Online; accessed 24-August-2020].
- [65] —, *Board of Governors of the Federal Reserve System (US), 10-Year Treasury Constant Maturity Rate [GS10]*, retrieved from FRED, 2020. [Online; accessed 24-August-2020].
- [66] —, *Board of Governors of the Federal Reserve System (US), 3-Month Treasury Bill: Secondary Market Rate [TB3MS]*, retrieved from FRED, 2020. [Online; accessed 24-August-2020].
- [67] W. FELLER, *Two singular diffusion problems*, Annals of Mathematics, 54 (1951), pp. 173–182.
- [68] W. E. FERSON, *The Empirical Implications of the Cox, Ingersoll, Ross Theory of the Term Structure of Interest Rates: Discussion*, The Journal of Finance, 41 (1986), pp. 630–632.

- [69] H. G. FONG AND O. A. VASICEK, *Interest rate volatility as a stochastic factor*, Gifford Fong Associates, (1991).
- [70] F. T. FURLONG ET AL., *The yield curve and recessions*, FRBSF Economic Letter, (1989).
- [71] E. GAGNON, B. K. JOHANNSEN, AND D. LOPEZ-SALIDO, *Understanding the new normal: the role of demographics*, (2016).
- [72] G. GEORGEV, J. JUNG, H. B. KAZEMI, AND M. MAHDAVI, *Revealing the market price of risk from the short-term rate process*, *Studies in Economics and Finance*, 20 (2002), pp. 19–38.
- [73] M. R. GIBBONS AND K. RAMASWAMY, *A test of the Cox, Ingersoll, and Ross model of the term structure*, *The Review of Financial Studies*, 6 (1993), pp. 619–658.
- [74] M. GILLI, S. GROSSE, AND E. SCHUMANN, *Calibrating the Nelson-Siegel-Svensson model*, Available at SSRN 1676747, (2010).
- [75] M. GILLI AND P. WINKER, *Heuristic optimization methods in econometrics*, Wiley Online Library, 2009, pp. 81–119.
- [76] L. GIORDANO AND G. SICILIANO, *Real-world and risk-neutral probabilities in the regulation on the transparency of structured products*, Tech. Rep. 74, Consob, aug 2013.
- [77] R. GIUSTI AND G. E. BATISTA, *An empirical comparison of dissimilarity measures for time series classification*, in 2013 Brazilian Conference on Intelligent Systems, IEEE, 2013, pp. 82–88.
- [78] P. GOMME, B. RAVIKUMAR, AND P. RUPERT, *The return to capital and the business cycle*, *Review of Economic Dynamics*, 14 (2011), pp. 262–278.
- [79] D. GRANT AND G. VORA, *The Hull and White model of the short rate: an alternative analytical representation*, *Journal of Financial Research*, 25 (2002), pp. 463–476.
- [80] A. GREENSPAN, *Testimony of Alan Greenspan*, April 2010.
- [81] A. GUPTA AND M. G. SUBRAHMANYAM, *Pricing and hedging interest rate options: Evidence from cap-floor markets*, *Journal of Banking & Finance*, 29 (2005), pp. 701–733.

- [82] R. S. HACKER AND A. HATEMI-J, *Tests for causality between integrated variables using asymptotic and bootstrap distributions: theory and application*, Applied Economics, 38 (2006), pp. 1489–1500.
- [83] A. H. HANSEN, *Economic progress and declining population growth*, The American economic review, 29 (1939), pp. 1–15.
- [84] C. R. HARVEY, *Recovering expectations of consumption growth from an equilibrium model of the term structure of interest rates*, 1986. Ph.D. thesis.
- [85] C. R. HARVEY, *The real term structure and consumption growth*, Journal of Financial Economics, 22 (1988), pp. 305–333.
- [86] M. HEFTER AND A. HERZWURM, *Strong convergence rates for Cox-Ingersoll-Ross processes - Full parameter range*, Journal of Mathematical Analysis and Applications, 459 (2018), pp. 1079–1101.
- [87] S. L. HESTON, *A closed-form solution for options with stochastic volatility with applications to bond and currency options*, The Review of Financial Studies, 6 (1993), pp. 327–343.
- [88] Y. HOCHBERG AND A. C. TAMHANE, *Multiple Comparison Procedures*, John Wiley & Sons, 1989.
- [89] J. HULL AND A. WHITE, *Pricing interest-rate-derivative securities*, The review of financial studies, 3 (1990), pp. 573–592.
- [90] IBA, *Data vendor codes*. ICE Benchmark Administration (IBA), 2020. https://www.theice.com/publicdocs/IBA_Quote_Vendor_Codes.xlsx.
- [91] M. JEANBLANC, M. YOR, AND M. CHESNEY, *Mathematical Methods for Financial Markets*, Springer: London, 2009.
- [92] N. L. JOHNSON, *Systems of frequency curves generated by methods of translation*, Biometrika, 36 (1949), pp. 149–176.
- [93] D. L. JONES, *The Johnson curve toolbox for Matlab: analysis of non-normal data using the Johnson system of distributions*. <https://it.mathworks.com/matlabcentral/fileexchange/46123-johnson-curve-toolbox>, 2014.
- [94] R. A. KESSEL, *The cyclical behavior of the term structure of interest rates*, in The Cyclical Behavior of the Term Structure of Interest Rates, NBER, 1965, pp. 12–0.

- [95] K. KLADIVKO, *Maximum likelihood estimation of the Cox-Ingersoll-Ross process: the matlab implementation*. <https://it.mathworks.com/matlabcentral/fileexchange/37297-maximum-likelihood-estimation-of-the-cox-ingersoll-ross-process-the-matlab-implementation>, 2007.
- [96] R. KOO, *Balance sheet recession is the reason for secular stagnation*, in *Secular stagnation: facts, causes and cures*, C. Teulings and R. Baldwin, eds., CEPR Press London, 2014.
- [97] T. O. KVALSETH, *Cautionary note about R^2* , *The American Statistician*, 39 (1985), pp. 279–285.
- [98] P. R. LANE, *Determinants of the real interest rate*. https://www.ecb.europa.eu/press/key/date/2019/html/ecb.sp191128_1~de8e7283e6.en.html, 2019.
- [99] T. C. LANGETIEG, *A multivariate model of the term structure*, *The Journal of Finance*, 35 (1980), pp. 71–97.
- [100] R. D. LAURENT, *An interest rate-based indicator of monetary policy*, *Economic Perspectives*, (1988), pp. 3–14.
- [101] R. D. LAURENT ET AL., *Testing the spread*, *Federal Reserve Bank of Chicago Economic Perspectives*, 13 (1989), pp. 22–34.
- [102] M. LAVIELLE, *Using penalized contrasts for the change-point problem*, *Signal processing*, 85 (2005), pp. 1501–1510.
- [103] M. LAVIELLE AND G. TEYSSIERE, *Detection of multiple change-points in multivariate time series*, *Lithuanian Mathematical Journal*, 46 (2006), pp. 287–306.
- [104] A. LEANDRO AND J. ZETTELMEYER, *The search for a Euro area safe asset*, (2018).
- [105] N. LISACK, R. SAJEDI, AND G. THWAITES, *Demographic trends and the real interest rate*, (2017).
- [106] O. LIU AND C. F. BAUM, *An alternative strategy for estimation of a nonlinear model of the term structure of interest rates*, *Working Papers in Economics*, (1994), p. 359.

- [107] F. A. LONGSTAFF AND E. S. SCHWARTZ, *Interest rate volatility and the term structure: A two-factor general equilibrium model*, The Journal of Finance, 47 (1992), pp. 1259–1282.
- [108] T. A. MARSH AND E. R. ROSENFELD, *Stochastic processes for interest rates and equilibrium bond prices*, The Journal of Finance, 38 (1983), pp. 635–646.
- [109] G. A. MEDVEDEV, *Yield Curves and Forward Curves for Diffusion Models of Short Rates*, Springer International Publishing, 2019.
- [110] R. C. MERTON, *Theory of rational option pricing*, The Bell Journal of economics and management science, (1973), pp. 141–183.
- [111] G. MILSHTEIN, *A method of second-order accuracy integration of stochastic differential equations*, Theory of Probability and Its Applications, 23 (1979), pp. 396–401.
- [112] Y. MISHURA AND A. YURCHENKO-TYTARENKO, *Fractional Cox Ingersoll Ross process with non zero mean*, Modern Stochastics: Theory and Applications, 5 (2018), pp. 99–111.
- [113] W. C. MITCHELL, *Business cycles*, vol. 3, University of California Press, 1913.
- [114] S. MOLLAH, *Financial crisis: is there a need for paradigm shift?*, Studies in Economics and Finance, 27 (2010).
- [115] M. MORENO AND F. PLATANIA, *A cyclical square-root model for the term structure of interest rates*, European journal of operational research, 241 (2015), pp. 109–121.
- [116] A. R. NAJAFI AND F. MEHRDOUST, *Bond pricing under mixed generalized CIR model with mixed wishart volatility process*, J. Comput. Appl. Math., 319 (2017), pp. 108–116.
- [117] A. R. NAJAFI, F. MEHRDOUST, AND S. SHIRINPOUR, *Pricing american put option on zero-coupon bond under fractional CIR model with transaction cost*, Communications in Statistics - Simulation and Computation, 0 (2017), pp. 1–7.
- [118] V. NAUMOV AND M. KOROVIN, *Floaters Z-spread to RUONIA: avoiding unnecessary arbitrariness*, July 2021.
- [119] C. R. NELSON AND A. F. SIEGEL, *Parsimonious modeling of yield curves*, Journal of business, (1987), pp. 473–489.

- [120] S. NERI AND A. GERALI, *Natural rates across the Atlantic*, Journal of Macroeconomics, 62 (2019), p. 103019.
- [121] G. ORLANDO AND M. BUFALO, *Interest rates forecasting: between Hull and White and the CIR#*. *How to make a single factor model work*, Journal of Forecasting, (2021).
- [122] G. ORLANDO, R. M. MININNI, AND M. BUFALO, *A new approach to CIR short-term rates modelling*, in New Methods in Fixed Income Modeling - Fixed Income Modeling, M. Mili, R. Medina Samaniego, and d. P. Filippo, eds., Springer International (USA), 2018, pp. 35–44.
- [123] —, *Interest rates calibration with a CIR model*, The Journal of Risk Finance, 20 (2019), pp. 370–387.
- [124] —, *A new approach to forecast market interest rates through the CIR model*, Studies in Economics and Finance, doi: 10.1108/SEF-03-2019-0116, (2019).
- [125] —, *Forecasting interest rates through Vasicek and CIR models: a partitioning approach*, Journal of Forecasting, doi: 10.1002/for.2642, (2020).
- [126] G. ORLANDO AND G. TAGLIALATELA, *A review on implied volatility calculation*, Journal of Computational and Applied Mathematics, 320 (2017), pp. 202–220.
- [127] G. ORLANDO AND G. ZIMATORE, *RQA correlations on real business cycles time series*, in Proc. Conf. Perspect. Nonlinear Dyn, 2016, pp. 35–41.
- [128] —, *Recurrence quantification analysis of business cycles*, Chaos, Solitons & Fractals, 110 (2018), pp. 82–94.
- [129] A. PAPETTI, *Demographics and the natural real interest rate: historical and projected paths for the euro area*, (2019).
- [130] M. POLETTI LAURINI AND L. K. HOTTA, *Gmc-gel estimation of stochastic volatility models*, Communications in Statistics - Simulation and Computation, 46 (2017), pp. 6828–6844.
- [131] P. S. POLLARD, *A look inside two central banks: the european central bank and the federal reserve*, Federal Reserve Bank of St. Louis Review, 85 (2003).
- [132] S. M. POTTER AND F. SMETS, *Unconventional monetary policy tools: a cross-country analysis*. <https://www.bis.org/publ/cgfs63.pdf>, 2019.

- [133] Ł. RACHEL AND L. H. SUMMERS, *On secular stagnation in the industrialized world*, tech. rep., National Bureau of Economic Research, 2019.
- [134] A. RANNENBERG, *Inequality, the risk of secular stagnation and the increase in household debt*, tech. rep., NBB Working Paper, 2019.
- [135] R. REBONATO, *Interest-rate option models: understanding, analysing and using models for exotic interest-rate options*, Wiley, 1996.
- [136] S. F. RICHARD, *An arbitrage model of the term structure of interest rates*, Journal of Financial Economics, 6 (1978), pp. 33–57.
- [137] RIK, *Bland-Altman Plot*. MATLAB Central File Exchange, 2020. Retrieved June 30, 2020.
- [138] D. ROBERTS, A. SARKAR, O. SHACHAR, ET AL., *Bank liquidity creation, systemic risk, and Basel liquidity regulations*, Federal Reserve Bank of New York Staff Reports, (2019).
- [139] L. ROGERS, *Gaussian errors*, Risk, 9 (1996), pp. 42–45.
- [140] G. RUDEBUSCH AND M. BAUER, *Interest rates under falling stars*, Federal Reserve Bank of San Francisco, 2017.
- [141] V. RUSSO AND G. TORRI, *Calibration of one-factor and two-factor hull–white models using swaptions*, Computational Management Science, 16 (2019), pp. 275–295.
- [142] M. SAKBANI, *The global recession: Analysis, evaluation, and implications of the policy response and some reform proposals*, Studies in Economics and Finance, 27 (2010), pp. 91–109.
- [143] J. M. SÁNCHEZ, E. YURDAGUL, ET AL., *Why are corporations holding so much cash?*, The Regional Economist, 21 (2013), pp. 4–8.
- [144] A. S. SHIRKHORSHIDI, S. AGHABOZORGI, AND T. Y. WAH, *A comparison study on similarity and dissimilarity measures in clustering continuous data*, PloS one, 10 (2015), p. e0144059.
- [145] M. SHIZUME, *A History of the Bank of Japan, 1882–2016*, 328 (2018), pp. 328–360.

- [146] R. STANTON, *A nonparametric model of term structure dynamics and the market price of interest rate risk*, The Journal of Finance, 52 (1997), pp. 1973–2002.
- [147] J. H. STOCK AND M. W. WATSON, *How did leading indicator forecasts perform during the 2001 recession?*, FRB Richmond Economic Quarterly, 89 (2003), pp. 71–90.
- [148] R. STORN AND K. PRICE, *Differential evolution—a simple and efficient heuristic for global optimization over continuous spaces*, Journal of global optimization, 11 (1997), pp. 341–359.
- [149] L. H. SUMMERS, *Reflections on the 'new secular stagnation hypothesis'*, in Secular stagnation: facts, causes and cures, C. Teulings and R. Baldwin, eds., CEPR Press London, 2014, pp. 2–42.
- [150] M. SUNDARESAN, *Consumption and equilibrium interest rates in stochastic production economies*, the Journal of Finance, 39 (1984), pp. 77–92.
- [151] S. M. SUNDARESAN, *Continuous-time methods in finance: A review and an assessment*, The Journal of Finance, 55 (2000), pp. 1569–1622.
- [152] L. E. SVENSSON, *Estimating and interpreting forward interest rates: Sweden 1992-1994*, tech. rep., National bureau of economic research, 1994.
- [153] THE SCHWEIZERISCHE NATIONALBANK (SNB), *Goals and responsibilities of the snb*, 2021. [Online; accessed 9-August-2021].
- [154] U.S.A. DEPARTMENT OF THE TREASURY, *Troubled Assets Relief Program (TARP)*. <https://home.treasury.gov/data/troubled-assets-relief-program>, 2021. Accessed: 2021-08-08.
- [155] O. VASICEK, *An equilibrium characterization of the term structure*, Journal of financial economics, 5 (1977), pp. 177–188.
- [156] J. H. WARD JR, *Hierarchical grouping to optimize an objective function*, Journal of the American statistical association, 58 (1963), pp. 236–244.
- [157] G. WARNES AND AL., *R Enhanced Heat Map - gplots package*. <https://www.rdocumentation.org/packages/gplots/versions/3.0.4/topics/heatmap.2>, 2020. Accessed: 2020-07-10.
- [158] WIKIPEDIA, *U.S. treasury yield curves for different dates.*, 2020. [Online; accessed 9-August-2020].

- [159] —, *Yield curve*, 2020. [Online; accessed 9-August-2020].
- [160] WWW.MONEY.PL, *Warsaw Interbank Offered Rates (WIBOR)*, 2021. [Online; accessed 9-March-2021].
- [161] S. ZEYTUN AND A. GUPTA, *A comparative study of the Vasicek and the CIR model of the short rate*, Tech. Rep. 124, Fraunhofer (ITWM), 2007.
- [162] L. ZHU, *Limit theorems for a Cox-Ingersoll-Ross process with Hawkes jumps*, *Journal of Applied Probability*, 51 (2014), pp. 699–712.